THE UNIVERSITY OF MICHIGAN

INDUSTRY PROGRAM OF THE COLLEGE OF ENGINEERING

TWO-PHASE COCURRENT FLOW IN PACKED BEDS

Robert P. Larkins

A dissertation submitted in partial fulfillment
of the requirements for the degree of
Doctor of Philosophy in the
University of Michigan
1959

May, 1959

IP-369

Doctoral Committee:

Professor Robert R. White, Chairman
Professor Lloyd E. Brownell
Associate Professor Ben Dushnik
Assistant Professor Kenneth F. Gordon
Professor Victor L. Streeter

ACKNOWLEDGMENTS

The author wishes to express his appreciation to the following individuals and organizations for their contributions to the research which was the basis of this dissertation:

Professor R. R. White, chairman of the doctoral committee, for his wise counsel, for his interest and encouragement, and for his wholehearted and prompt cooperation on every occasion.

The other members of the doctoral committee for their advice and encouragement.

The Humble Oil and Refining Company for partial financial support of the research and for their contribution of data on hydrocarbon systems.

The Dow Chemical Company for their donation of ethylene glycol.

Dr. G. R. L. Shepherd and Mr. D. W. Jeffrey (Humble Oil and Refining Company) for their personal interest, advice, and data.

The Industry Program of the College of Engineering for the preparation of the dissertation.

Consumers Power Company for their fellowship during the academic years 1956-57, 1957-58, and 1958-59.

TABLE OF CONTENTS

TABLE OF CONTENTS (CONT'D)

LIST OF TABLES

LIST OF FIGURES

NOMENCLATURE

A	Area, cross-sectional area of pipe, or that area through which the flow occurs.
D	Inside diameter of pipe containing packing.
D_p	Characteristic diameter of packing materials.
f	Friction factor.
g_c	Conversion factor, 32.17 poundals per pound in English units.
G	Mass velocity [(lb mass)/(sec)(sq ft) or (lb mass)/(min)(sq ft)].
L	Length of linear dimension.
M	Molecular weight.
m,m'	Exponent dependent on packing material.
n,n'	Exponent dependent on packing material.
P	Pressure [(lb force)/(sq ft) or (lb force)/(sq in)], absolute.
P'	Pressure, gauge.
$\frac{\Delta P}{\Delta L}$	Pressure drop per unit length due to friction (psi/ft or lb/sq ft/ft).
R	Fraction of void volume occupied by a phase, saturation.
Re	Modified Reynolds number, $(G\ D_p)/(\mu)(1-\epsilon)$.
S	Surface area of packing per unit volume (sq ft/cu ft).
s	Exponent dependent on mode of flow.
T	Temperature (°R or °F).
u	Superficial velocity in open column (ft/sec).

Greek Letters

δ	Total energy to overcome friction, (-dP/dL) for horizontal flow, or (-dP/dL) + ρ for vertical flow.
ϵ	Fraction voids in packing (void volume/unit volume of column).

Greek Letters (Continued)

μ	Coefficient of viscosity (cp or consistent units).
ρ	Density (mass per unit volume).
φ_ℓ	$\sqrt{\delta_{\ell g}/\delta_\ell}$.
φ_g	$\sqrt{\delta_{\ell g}/\delta_g}$.
χ	$\sqrt{\delta_\ell/\delta_g}$.

Subscripts

corr	Designating that a pressure drop has been corrected for density of the flowing mixture of fluids, $(-dP/dL) + \rho_m = \delta = (-dP/dL)_{corr}$.
g	Designating the gas phase. This subscript on δ indicates the value of δ calculated from single-phase correlation for the gas flowing alone in the bed at the same temperature and pressure as the two-phase case.
ℓ	Designating the liquid phase. This subscript on δ indicates the value of δ calculated from a single-phase correlation for the liquid flowing alone in the bed at the same temperature and pressure as the two-phase case.
ℓg	Designating liquid and gas phases flowing simultaneously and cocurrently.
m	Designating the flowing mixture of gas and liquid.

I. INTRODUCTION

A. Purpose of Investigation

Reaction vessels involving two-phase flow of liquid and gas through catalyst beds are assuming increased importance in the chemical and petroleum industries. The design of such reactors requires a knowledge of cocurrent two-phase flow in order to predict the pressures, pressure drops, and liquid-to-gas ratios in the catalyst bed.

The treatment of lube oil with hydrogen over a catalyst bed has become an important process in the petroleum industry and is an outstanding example of a trickle bed reaction. Hydrogen gas and lube oil are passed downward over a long catalyst bed at extreme conditions approximating 700°F and 700 pounds pressure. The reaction vessels which are perhaps a foot in thickness, are probably the largest pieces of high pressure equipment used in the petroleum industry. Many other reactions involving the cocurrent flow of liquid and gas over a catalyst are in current use.

The simultaneous flow of liquids and gases has been studied for two important cases, but no investigation has been made to develop a correlation for cocurrent flow in packed beds. The case of two-phase cocurrent flow in porous media has been studied to solve problems in oil reservoir production and in filter cake calculation. In addition, the case of two-phase countercurrent flow of liquid and gas over a packed bed has been investigated to determine the capacity and pressure drop for absorbers and other packed equipment.

The purpose of this investigation is to obtain data for the two-phase cocurrent flow of liquid and gas in packed beds and to

establish a suitable correlation for the prediction of the pressure drop and the fraction of the void volume occupied by the liquid, termed the liquid saturation. The term "two-phase flow" in this dissertation will refer to the flow of liquid and gas unless otherwise stated.

B. Statement of the Problem

Sufficient data are to be taken to determine the important variables in two-phase flow in packed beds and to develop design methods suitable for the solution of the design problem which may be stated in the following manner.

The porosity of a packed bed, the downward flow rates of liquid and gas, and the viscosities and densities of the liquid and gas are given. The calculation of the rate of change of pressure with distance and the fraction of the void volume occupied by liquid, i.e., the liquid saturation, is required. If the density of the gas is given as a function of the pressure and the entrance or exit conditions are known, the computation of the pressure drop over the packed section and the average liquid saturation is required.

C. Summary

The following paragraphs will outline the material in the various sections of the dissertation. For the reader with limited time or a primary interest in the use of the results, the following sections and subsections are recommended: Introduction, Subsections B through J under Correlation of Experimental Data, Sample Problem, and Conclusions.

Section II is a review of the literature relating to pressure drop measurements and correlations for single-phase flow in packed beds

and for two-phase flow in open pipes, in porous media, and countercurrently in packed beds. Measurements of liquid saturation are reported for the two-phase mechanisms. The single-phase correlations are a basis for the two-phase calculations, and the correlations for two-phase flow in open channels serve to suggest the important parameters in packed beds.

Section III is a description of the flow of fluids through the experimental equipment, the sizes and capacities of the components of the equipment, and the instruments used in making the experimental measurements. The operating procedures used in making the experimental runs, and the actual measurements recorded, are detailed in this section.

Section IV is concerned with the systems which were investigated, the properties of the fluids and packings used, the flow patterns observed, and the explanation of the tabulated processed data. The first processing of the raw data is explained, and the role of the run code as an index to the data and as a description of the individual run is detailed.

Section V is the most important portion of the dissertation and presents the final correlation of the experimental data. The correlation relationships are derived from the established relationships for single-phase flow. The correlation parameters rest upon a knowledge of the pressure drop for the single-phase systems, and correlations are accordingly obtained for the single-phase data taken on the systems investigated. The calculation of the correlation parameters is explained, and plots are presented showing the calculated points against the parameters suggested by the derivation. The scope and accuracy of the correlation is discussed, and equations are presented which represent the

data. The saturation data are shown to support the assumptions upon which the derivation is based. The effect of foaming on pressure drop, and the similarity between correlations obtained for packed beds and open channels are discussed. The application of the correlations to problems involving the flow of two immiscible liquid phases, or two immiscible liquid phases and a gas phase, is discussed at the close of this section.

Section VI concerns itself with a number of data obtained from another experimenter which support the proposed correlation when foaming is not encountered. Additional data on foaming systems are presented, and a form of instability peculiar to foaming systems is described.

Section VII concludes the dissertation with observations drawn from the experiences of the author and the symmetrical form of the final correlation. The extension of the correlation to two immiscible liquids is not advised, but its use with two immiscible liquid phases and a gas phase is discussed. The extension or revision of the correlation to predict the behavior of upflow and horizontal flow systems is discussed in connection with suggestions for further investigation in the area of two-phase flow in packed beds.

II. REVIEW OF LITERATURE RELATED TO TWO-PHASE FLOW

In the absence of data for two-phase cocurrent flow in packed beds, this section is devoted to a review of pressure drop data and correlations falling into two areas of interest. The first area of interest includes correlations for single-phase flow in packed beds and for two-phase cocurrent flow in open channels which have importance in the development of the correlation for two-phase cocurrent flow in packed beds. The second area of interest includes information on two-phase cocurrent flow in porous media and two-phase countercurrent flow in packed beds since these are the problems in two-phase flow which have been previously investigated.

A. Single-Phase Flow in Packed Beds

Experiments on flow in packed beds followed extensive work on the determination and correlation of pressure drop in open pipes. These data in pipes have been widely correlated on the basis of a dimensionless friction factor, a roughness of the pipe, and the Reynolds number. If the open pipe is considered to be a packed bed with 100 per cent voids, it is reasonable to look for a correlation of data in porous media which reduces to the friction factor plot for 100 per cent voids.

Brownell and Katz[5] have presented a correlation incorporating the data of earlier investigations and based upon a modified Reynolds number and a modified friction factor defined by

$$Re = \frac{D_p u \rho}{\mu \epsilon^m} \qquad (1)$$

and

$$f = \frac{2g_c D_p \Delta P \epsilon^n}{\Delta L u^2 \rho} \tag{2}$$

in which

D_p = Diameter of the particles,

u = Superficial velocity,

ϵ = Porosity of the beds, fraction voids,

ΔP = Pressure drop due to friction, and

ΔL = Length over which ΔP is measured.

A family of friction factor versus Reynolds number plots is presented with roughness as a parameter. The values of the exponents, m and n, are to be obtained from a plot as a function of (ψ/ϵ), where ψ is the sphericity and is defined as the ratio of the surface area of a sphere, having the same volume as the particle, to the surface area of the particle. Tabulated values for roughness are given for representative packing materials. An excellent review of the earlier literature related to pressure drop in porous media is to be found in the introduction of Reference 5.

A second paper by Brownell, Dombrowski, and Dickey[8] redefined the Reynolds number by

$$R = \frac{D_p u \rho F_{Re}}{\mu} \tag{3}$$

and the friction factor by

$$f = \frac{2g_c D_p \Delta P}{\Delta L u^2 \rho F_f} \tag{4}$$

where F_{Re} is given graphically as a function of the porosity and sphericity of the particles, and F_f is given graphically as a function of the

same variables. The roughness of the particles is concluded to be neglibible and is eliminated as a variable. The data then fall on a single friction factor versus Reynolds number plot which is identical with that for flow in smooth pipes. A subsequent work by Brownell, Gami, Miller, and Nekarvis[9] suggests a general correlation for flow through porous media covering porosities from 0 to 100 per cent as well as the systems of free settling, fluidized solids, packed beds, and open channels, on a single plot of the modified friction factor as defined by Equation (4) versus the modified Reynolds number as defined by Equation (3).

Another approach to the problem of single-phase flow in packed beds does not draw upon the relationships developed for flow in open channels. Morcom[28] plotted data by an equation of the form

$$\frac{1}{u}\frac{\Delta P}{\Delta L} = a + \rho b u \qquad (5)$$

where the constants, a and b, hold for a single packing and flowing fluid and u is the superficial linear velocity. For low flow rates the second term is negligible, and Equation (5) becomes the classical Darcy equation for laminar flow in porous media. Ergun and Orning[13] have also demonstrated the validity of Equation (5), which states that for a given packing material and flowing fluid the pressure drop is proportional to the first power of velocity for low flow rates, and to the second power of velocity at high flow rates.

Equation (5) establishes the effect of flow rate on pressure drop, and the condition for viscous flow as stated by the Poiseuille equation and by Darcy's law requires that the factor a be proportional

to viscosity, as is seen by allowing u to approach zero. The expression for pressure drop now becomes

$$\frac{\Delta P}{\Delta L} = c\mu u + b\rho u^2 \tag{6}$$

The first term of Equation (6) represents the viscous energy losses and the second term represents the kinetic energy losses.

Important variables in the determination of pressure drop are the porosity, ϵ, and the particle diameter, D_p. Leva and Grummer[21] found that the pressure drop is proportional to $(1-\epsilon)^2/\epsilon^3$ at low flow rates, and to $(1-\epsilon)/\epsilon^3$ at high flow rates. The general expression obtained by Ergun and Orning[13] was

$$g_c\left(\frac{\Delta P}{\Delta L}\right) = 2\alpha\mu S_V^2 u \frac{(1-\epsilon)^2}{\epsilon^3} + \frac{\beta}{8} G u S_V \frac{(1-\epsilon)}{\epsilon^3} \tag{7}$$

where α and β are constants, and S_V is the surface of solids per unit volume of the solids. It is customary to use a characteristic dimension of the particle in such a manner as to define S_V. The dimension generally used is the diameter of the sphere having the specific surface S_V, and the expressions for the volume and surface of a sphere lead to the equation

$$D_p = \frac{6}{S_V} = \frac{6(1-\epsilon)}{S} \tag{8}$$

where S is the surface per unit packed volume and is related to S_V by

$$S = (1-\epsilon)S_V. \tag{9}$$

Substituting Equation (8) into Equation (7) gives the expression

$$g_c\left(\frac{\Delta P}{\Delta L}\right) = k_1 \frac{(1-\epsilon)^2}{\epsilon^3} \frac{\mu u}{D_p^2} + k_2 \frac{(1-\epsilon)}{\epsilon^3} \frac{Gu}{D_p} \tag{10}$$

which has been presented by Ergun.[14] Ergun has evaluated the constants in Equation (10) for granular beds and other small diameter packing materials, and has arrived at the final equation

$$-g_c\left(\frac{\Delta P}{\Delta L}\right) = 150\,\frac{(1-\epsilon)^2}{\epsilon^3}\,\frac{\mu u}{D_p^2} + 1.75\,\frac{(1-\epsilon)}{\epsilon^3}\,\frac{Gu}{D_p}\,. \qquad (11)$$

Equation (11) can be arranged in a more convenient form by the definition of the modified Reynolds number

$$Re = \frac{GD_p}{\mu(1-\epsilon)} = \frac{D_p u \rho}{\mu(1-\epsilon)} \qquad (12)$$

and by its substitution into Equation (11). With some rearrangement the following expression is obtained:

$$-\frac{\Delta P}{\Delta L} = \frac{Re(150 + 1.75\,Re)}{\frac{g_c \rho D_p^3}{\mu^2}\left(\frac{\epsilon}{1-\epsilon}\right)^3}\,. \qquad (13)$$

The two types of correlations which have been discussed in detail are reported to have an accuracy of approximately plus or minus 50 per cent. The deviations are to be expected in the light of an investigation by Martin[25] which reports a 50 per cent difference in pressure drop for two methods of stacking the same spheres to obtain identical porosities. These observations indicate that the method of packing the bed is an important factor even though the porosities are identical.

B. Two-Phase Flow in Open Channels

There has been a substantial interest in pressure drop data for two-phase flow in open pipes for as long as engineers have been

designing equipment to vaporize liquids or to condense vapors inside of tubes. An extensive bibliography of the early investigations may be found in Reference 26.

The first important correlation for two-phase flow in open channels was proposed by Martinelli, Boelter, Taylor, Thomsen, and Morrin[26], and was based upon previously reported data as well as data obtained in horizontal pipes of one inch diameter and smaller. Martinelli, Putnam, and Lockhart[27] extended the base of the proposed correlation with additional data in the viscous region. The final paper in the series by Lockhart and Martinelli[24] presents the completed correlation in terms of a single curve for each of the four flow mechanisms observed. These mechanisms are as follows:

1. Turbulent flow in the gas phase - turbulent flow in the liquid phase.
2. Turbulent flow in the gas phase - viscous flow in the liquid phase.
3. Viscous flow in the gas phase - turbulent flow in the liquid phase.
4. Viscous flow in the gas phase - viscous flow in the liquid phase.

Martinelli and Lockhart[24] have defined

$$\varphi_g = \sqrt{\left(\frac{\Delta P}{\Delta L}\right)_{lg} \div \left(\frac{\Delta P}{\Delta L}\right)_g} \tag{14}$$

$$\varphi_l = \sqrt{\left(\frac{\Delta P}{\Delta L}\right)_{lg} \div \left(\frac{\Delta P}{\Delta L}\right)_l} \tag{15}$$

$$\chi = \sqrt{\left(\frac{\Delta P}{\Delta L}\right)_l \div \left(\frac{\Delta P}{\Delta L}\right)_g} \tag{16}$$

where $(\frac{\Delta P}{\Delta L})_{lg}$ is the pressure drop observed for the simultaneous flow of liquid and gas in a pipe, $(\frac{\Delta P}{\Delta L})_{l}$ is the pressure drop observed for the flow of the liquid phase alone in the same pipe at the same conditions, and $(\frac{\Delta P}{\Delta L})_{g}$ is the pressure drop observed for the flow of the gas phase alone in the same pipe at the same conditions. The two parameters, φ_g and φ_l, were found to be functions of the independent variable X for each flow mechanism, and may either be calculated from a single-phase correlation or obtained from experimental observations. The liquid saturation in the pipe was found to be a function of X alone, and the same function of X for all flow mechanisms.

Bergelin[3] has made three important observations about the flow of gas-liquid mixtures:

1. For a given gas flow rate, the addition of small amounts of liquid may increase the pressure drop from 2 to 50 times.

2. At high gas velocities, the orientation of the tube is not important.

3. At high velocities, the liquid phase imparts a roughness effect to the wall.

The prediction of two-phase pressure drop from the correlation of Lockhart and Martinelli[24] results in errors of less than plus or minus 40 per cent provided the correct flow mechanism is assumed. Rough criteria for the transition from one mechanism to another have been given, but the need for clarification of these criteria is apparent. The use of both φ_g and φ_l in correlating the data is not necessary since Equation (16) may be combined with Equation (15) to obtain

$$\varphi_g = \varphi_l X. \tag{17}$$

Since X is the only independent variable, either φ_g or φ_l defines the correlation completely.

An improved correlation for two-phase flow in pipes proposed by Chenoweth and Martin[10] suggests the calculation of the single-phase pressure drop based on the total mass rate which is assumed to have the viscosity of the liquid phase. Though some improvement in accuracy was obtained, no correlation of liquid saturation was presented and theoretical justification of the correlation parameters is considerably weaker than for the correlation of Lockhart and Martinelli.[24] The main contribution of the improved correlation is the presentation of a method for handling fittings of various types and of considerable data for fittings.

C. Two-Phase Flow in Porous Media

While the term porous media may be used to refer to configurations of all particle sizes and porosities, the general practice is to use the term in reference to small particle sizes and low porosities. The particles are small enough that capillary forces are quite significant and the flow of the liquid phase is usually laminar. The term "packed beds" generally refers to larger particle sizes in which the capillary effects on flow are small. The production of oil from beds of rock or sand, and filtration of various materials, are the two major problems of importance in the area of two-phase flow in porous media.

Wyckoff[34] studied the flow of gas-liquid mixtures through sands and found that the relative permeability is a function of the liquid saturation, the fraction of the void volume occupied by liquid. Relative permeability is defined as the actual quantity of flow of a given phase divided by the quantity of flow of that phase under the

same driving force when that phase fills the voids, i.e., single-phase flow. Leverett[23] confirmed that relative permeability was a function of liquid saturation for a given system, and also showed that the relative permeability is independent of viscosity. It is interesting to note the similarity between the relative permeability and the parameter, φ_g, as defined by Equation (14) for two-phase flow in pipes and to note that φ_g is a function of liquid saturation, since φ_g and the liquid saturation are both functions of X alone. Hassler[17] has established the same relationship for gas-liquid mixtures flowing through sandstone and has further established with Brunner and Deahl[18] the importance of capillary forces for flow in porous media.

Brownell and Katz[6] have presented a correlation for two-phase flow in porous media. Each fluid is treated as a single-phase which is modified by the effect of the other fluid. Consideration of the capillary forces and the structure of the porous media are used to estimate the portion of the void volume which is active in flow. Another relation is developed to express the wetted sphericity of the small particles. The correlations suggested[5] for single-phase flow are then applied to the gas phase using the wetted sphericity and wetted porosity to determine the Reynolds number and friction factor corrections. New correction factors for Reynolds number and friction factor are applied to the wetting fluid which depend upon the effective saturation, the fraction of the active void volume occupied by liquid, and the size of the particles. With the pressure drop correlations thus modified, the pressure drop can be calculated when the gas and liquid rates are known by assuming the effective saturation and calculating the pressure drop

for each phase. If the pressure drops are equal, the correct assumption was made. If the pressure drops are not equal, other assumptions must be made. Brownell and Katz[7] have discussed the application of the two-phase correlation to the filtration problem which requires integration through the filter cake and with respect to time.

D. Two-Phase Flow in Packed Beds

Previous investigations into two-phase flow in packed beds are restricted to the countercurrent case normally encountered in an absorber with liquid flowing downward and the gas phase upward. Various investigators[11,12,15] have reported that the liquid saturation is independent of the gas rate for low gas rates. Hence, the correlation developed for flow in porous media by Brownell and Katz[6] may be expected to hold for both cocurrent and countercurrent flow in packed beds so long as the gas rate has negligible effect on the fraction of the void volume which is active in flow. Furnas and Bellinger[15] report that the amount of liquid in the packed bed can be expressed by

$$H = C\, L^{s} \tag{18}$$

where H is the amount of liquid in the column per cubic foot of packing, and the constants, C and s, are dependent upon the packing and the properties of the liquid. This expression is clearly independent of the gas rate. Elgin and Jesser[12] verified Equation (18) by experiments considering liquids running in empty columns.

The main consideration in studies of countercurrent towers has been that of capacity, or the determination of the gas rate which will result in flooding of the tower. If the pressure drop is plotted versus gas rate for a constant liquid rate, two changes in slope will

be observed. The first change in slope is termed the loading point, and the second change in slope is called the flooding or spilling point since the liquid saturation builds up rapidly at this point. Bain and Hougen[1] have used pressure drop plots to obtain data on the loading and flooding points of packed columns. Other investigators[31-33] have obtained data on various systems of liquids and gases, and a theoretical treatment of the flooding velocities in packed columns has been presented by Bertetti[4]. A recent series of articles by Leva[22] has reviewed the literature in this area, and has presented revised correlations to predict two-phase countercurrent flow in packed beds.

The distribution of liquid in a packed column has been investigated by Baker, Chilton, and Vernon[2] who found that uniform distribution in a large tower persists when obtained. There still exists wide disagreement on the degree of uniformity in towers of various sizes.

Piret, Mann, and Wall[31] was the only reference found for cocurrent flow in packed beds. The data for four runs indicated that pressure drops for a given liquid rate and with a gas velocity of 0.46 feet per second were different by a factor of two for the countercurrent and cocurrent systems. The cocurrent pressure drop was observed to be the lower drop.

III. EXPERIMENTAL EQUIPMENT AND MEASUREMENTS

A. Description of Flow and Equipment

Figure 1 is a photograph of the experimental equipment used to obtain the pressure drop and liquid saturation data reported in this dissertation. At the right of the photograph is the control panel, and at the left are the test section and liquid reservoir. The control panel is divided into two sections. The right section of the panel is composed of the controls and flow meters for the liquid and gas streams. The left section of the panel is composed of the pressure instruments and the manifolding system used to connect them to various pressure taps.

Figure 2 is a photograph of the test section showing the four pressure taps, the quick-closing valves used to obtain the liquid saturation data, and the system of weights and pulleys used to close the valves. Figure 3 is a schematic diagram of the equipment, and a comparison with Figure 1 will help to identify the various pieces of equipment in the photograph.

In order to facilitate the description of the equipment, the system will be considered in operation. The cycle for the liquid phase begins in a 200-gallon reservoir which is located beneath the test section, and which serves as a platform in making observations of the test section. The liquid is picked up by a five horsepower, two-stage, turbine pump manufactured by the Aurora Pump Company. The pump is capable of delivering a maximum of 37.5 gpm of water at 1750 rpm. A rate of 20 gpm is obtained against a head of 470 feet of water. A portion of the liquid leaving the pump is returned to the liquid reservoir and the remaining portion passes into the liquid rotameter system.

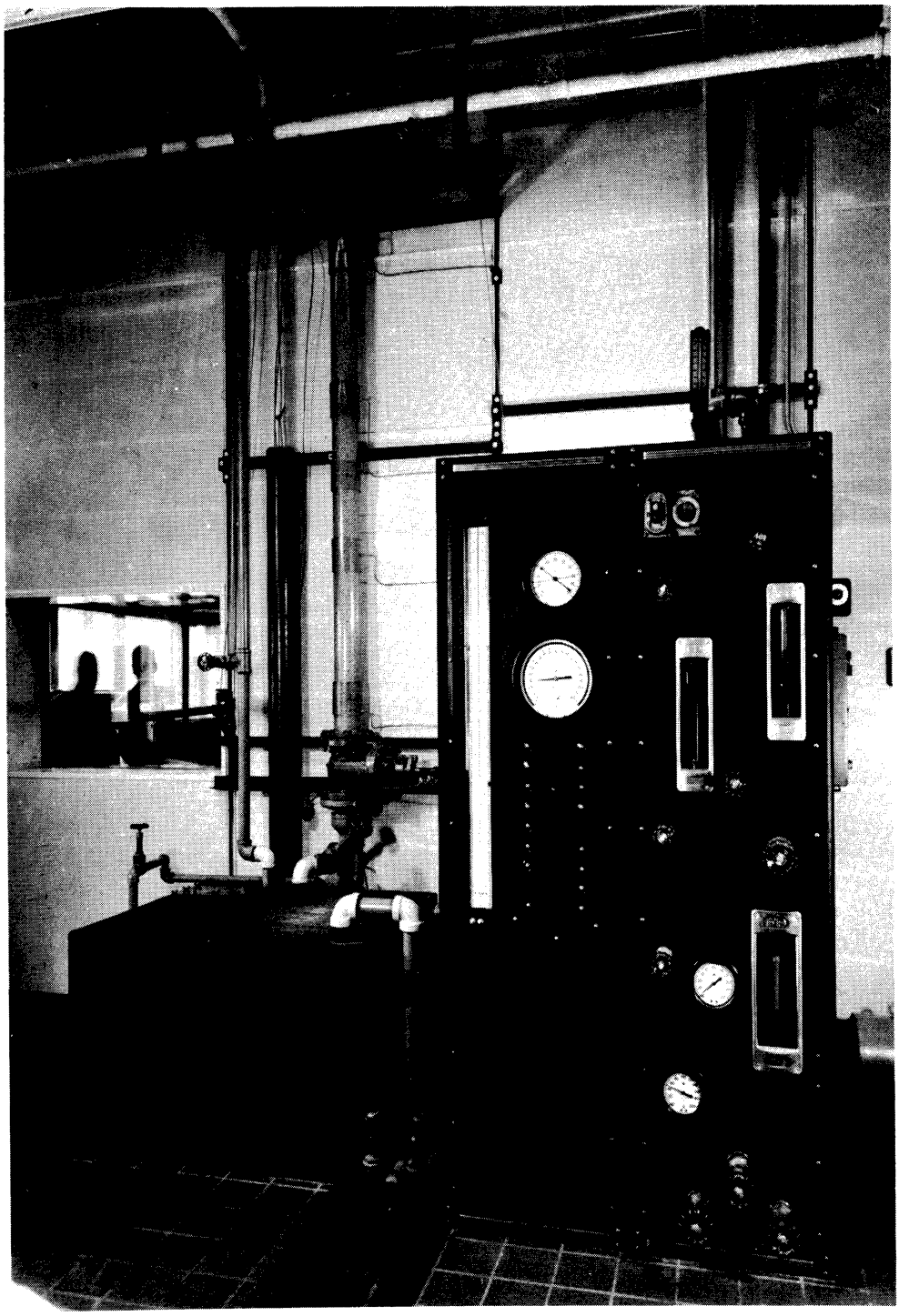

Figure 1. Photograph Showing Experimental Equipment

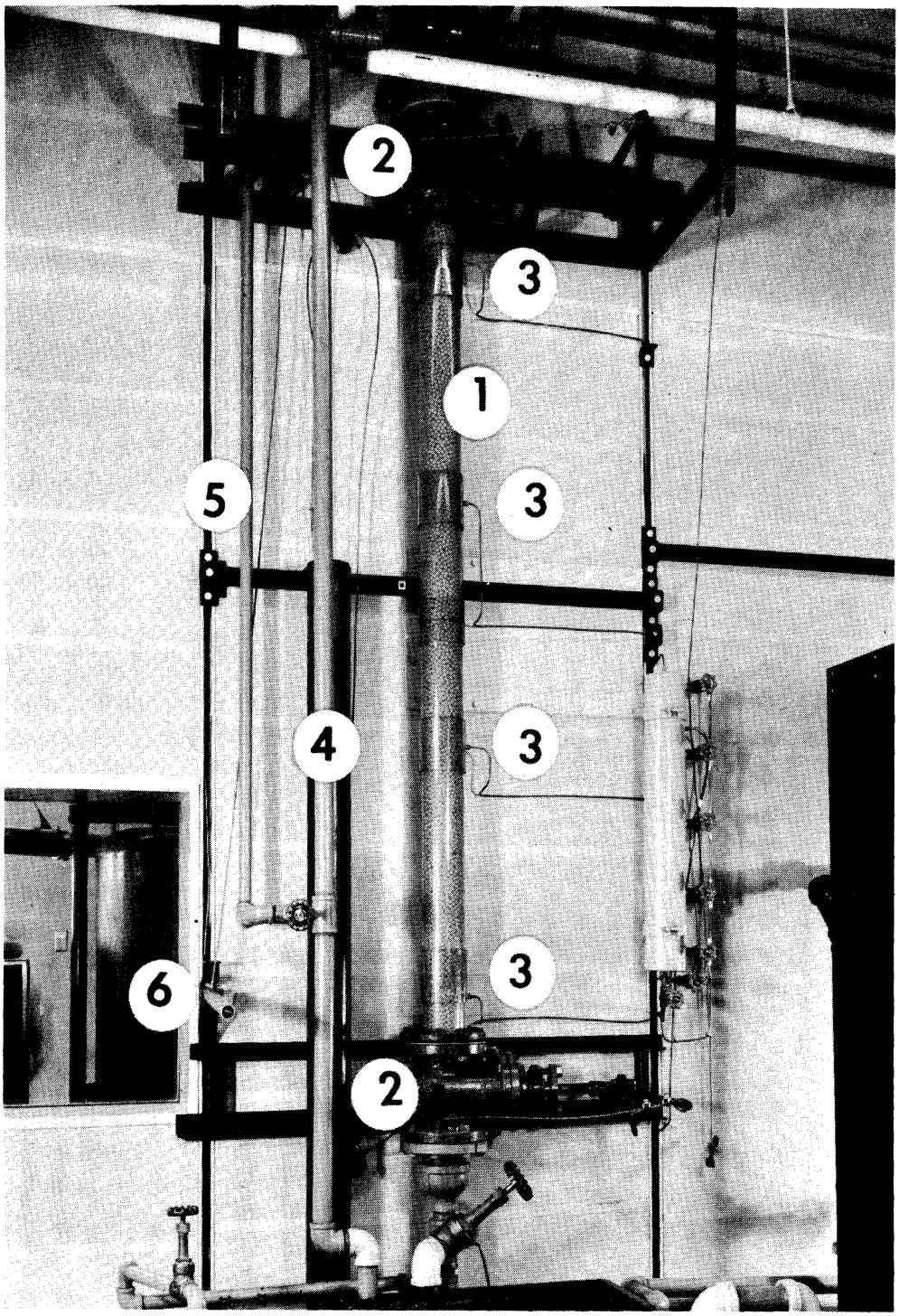

Figure 2. Photograph Showing Test Section

1. Test Section
2. Quick-Closing Valve
3. Pressure Tap
4. Case for Falling Weight - 4-Inch Pipe
5. Drain for Surge Drum
6. Trigger for Valve Closing System

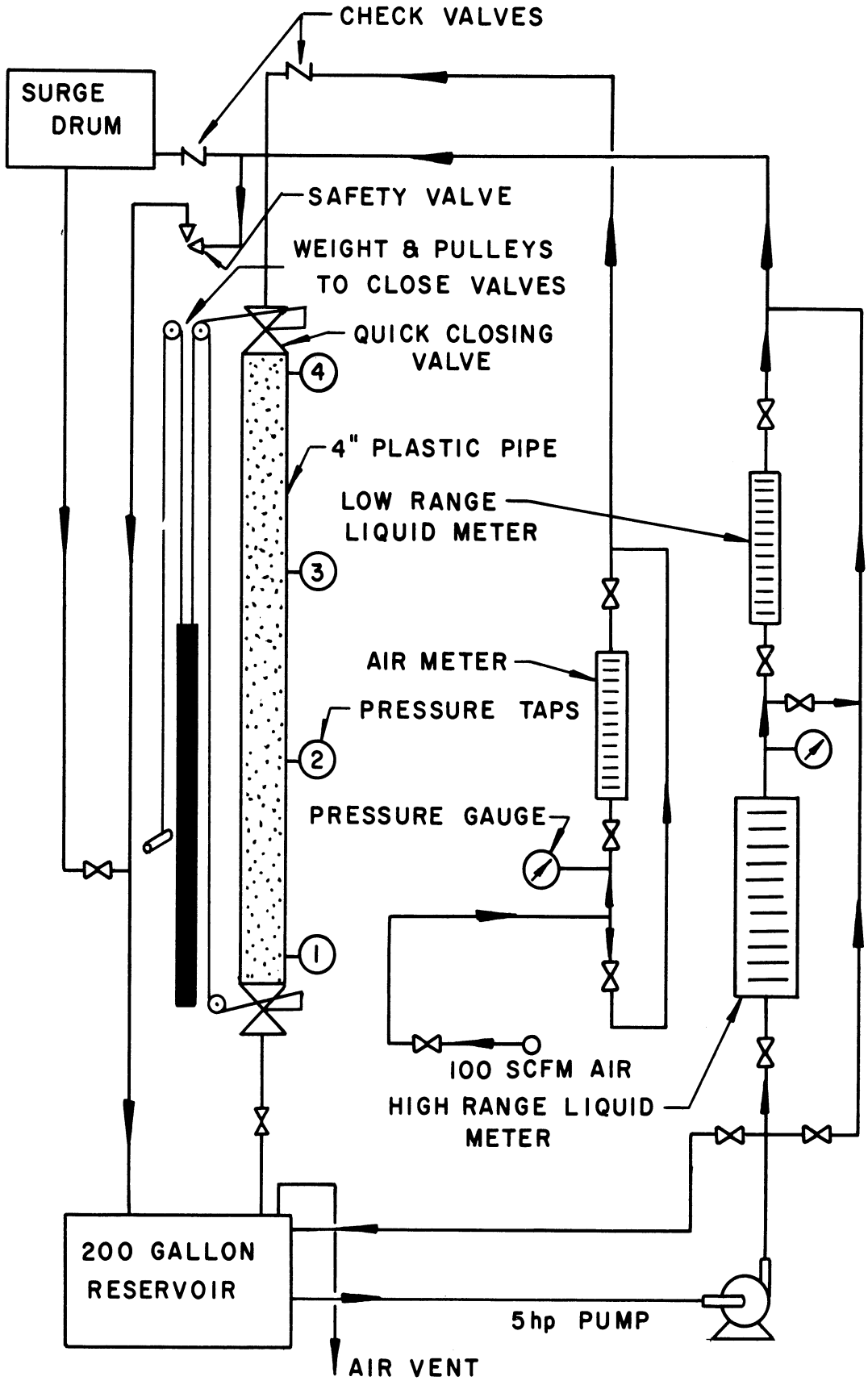

Figure 3. Schematic Diagram of Experimental Equipment

A large rotameter, having a maximum capacity of 29.0 gpm, is connected in series with a smaller rotameter, having a maximum capacity of 10.4 gpm. By-pass lines are provided so that the entire liquid stream can be taken through both meters in series, the larger meter alone, or neither of the meters. The pressure of liquid in the larger rotameter is monitored with a pressure gauge.

After leaving the rotameter system, the liquid passes into a 2-inch cross above the test section. In normal operation the liquid passes into a short section of 4-inch piping, through a 4-inch quick-closing valve, and into the test section. When the quick-closing valves are actuated, the liquid passes through a check valve into a small surge drum to avoid a water hammer. When the drum pressure builds up to 110 psig, the safety valve opens and the liquid is by-passed into the reservoir. The surge drum is pressurized with an air cushion before each run which holds the check valve shut until the quick-closing valves are actuated. After passing through the packed test section, the liquid flows through a second quick-closing valve and into the liquid reservoir which ends the liquid cycle.

Air is obtained from a building supply at 90 psig and a maximum rate of 140 SCFM. The air comes from a large receiver and any pulsation from the reciprocating machines is well damped. The air rate is measured in a rotameter having a capacity of 134 SCFM at 90 psig and 70°F. A thermocouple and a pressure gauge on the air rotameter make it possible to calculate the flow rate for any experimental condition. Upon leaving the rotameter, the air passes through a check valve and into the 2-inch cross above the test section where the liquid and gas phases are mixed.

The check valve in the air line prevents the flow of liquid into the air system when no air is flowing. After mixing with the liquid stream, the mixed phases pass through the quick-closing valves and test section before entering the liquid reservoir. A vent is provided to carry the air to the sewer after separation from the liquid. When the quick-closing valves are shut, the alternate paths for the air are the same as for the liquid.

The measurement of liquid saturation depends upon the trapping of the fluids within the packed test section between the two quick-closing valves. The accuracy of the measurements depends upon the amount of unpacked column between the quick-closing valves and upon the rapidity and uniformity with which the valves are closed. In order to reduce the unpacked volume, cups and screens were introduced into each of the 4-inch quick-closing valves on the column side. This arrangement allows for uniform packing to within one-half inch of the valve gates. The system of weights and cables was so arranged that a single weight closed both valves, assuring that they closed simultaneously. The weight was lifted and allowed to accelerate for about three feet before acting upon the valve handles, and the time required to close the valves is calculated to be less than 1/10 of a second from the time the valve gates begin to move. A rubber cushion absorbed the major portion of the shock at the end of the weight's travel.

The test column was made of a transparent section of 4-inch diameter Busada 210 Butyrate plastic pipe, manufactured by the Busada Supply Company, Inc., of New York. The maximum recommended working pressure for the material is 107 psig at 70°F. Four pressure taps were

placed along the test section with the normal drilling and tapping operations. The remaining piping of the equipment was done in standard materials. Most liquid lines were nominally 1-1/2 inches, and most air lines were one inch. Instrument lines were of 3/16-inch copper tubing.

B. Description of Instrumentation

The rates of liquid and gas were measured by rotameters. The large liquid meter was a Fischer & Porter model 10A1735 rotameter, and used a size 8 tube and an NSVP-87 float to measure a maximum of 29.0 gpm of water at full scale. At high viscosities an NSVP float is unstable, and the head of the float was reversed to obtain a SVP-87 float, which is stable at high viscosities, that yielded a maximum capacity of 21.2 gpm of water or 19.92 gpm of ethylene glycol. The smaller liquid meter was a Fischer & Porter model 10A1735 rotameter, and used a size 6 tube and an SVP-67 float to yield a maximum capacity of 7.60 gpm of water or 7.15 gpm of ethylene glycol. The air meter was a Fischer & Porter model 10A1735 rotameter using a size B6 tube and two floats, BNSVT-63 and BSVT-64. The capacity of the air meter at full scale may be expressed as

$$\text{Full Scale Rate (SCFM)} = C\sqrt{P/T} \qquad (19)$$

where P and T are the absolute temperature and pressure of the air and the constant, C, has a value of 161.0 for the BSVT-64 float, and 302.0 for the BNSVT-63 float. The manufacturer of the rotameters guarantees an error of less than 2 per cent at full scale, increasing to as much as 20 per cent at 10 per cent of full scale. The three new rotameters were checked against one another by connecting them in series

and passing water through the system. Data from the overlapping portions of the three scales were consistent, and calibration revealed maximum deviations of 10 per cent for low scale readings.

Temperatures were measured by copper-constantan thermocouples of the immersion type. The thermocouples were mounted in 1.5-inch lengths of 1/4-inch stainless steel tubing and mounted through the pipe walls at the desired points. A commercial temperature indicator was used to obtain the temperature readings. Temperatures were measured in the air rotameter outlet and at the bottom of the packed test section.

Pressure and pressure drop measurements were made with instruments indicated in Figure 4. Two other pressure gauges were used to measure the discharge pressure of the liquid pump and the metering pressure of the air in the rotameter. The manifolding system shown in Figure 4 was designed to apply the set of pressure and pressure difference instruments across any desired pair of taps on the packed test section. The set of pressure instruments consists of two pressure gauges and two manometers. For accurate determination of the pressure at a point in the system, an Ashcroft laboratory test gauge was provided with a range of 0 to 100 psig and an error of less than 0.25 per cent of full scale. An Ashcroft duplex pressure gauge with a range of 0 to 100 psig could be applied across both of the pressure taps being monitored, to determine which of the manometers should be opened to the system. A dual, well-type manometer manufactured by the Meriam Instrument Company with a 40-inch range and a maximum operating pressure of 350 psig, completed the set of instruments. One manometer tube was filled with mercury having a specific gravity of 13.57 at 50°F compared

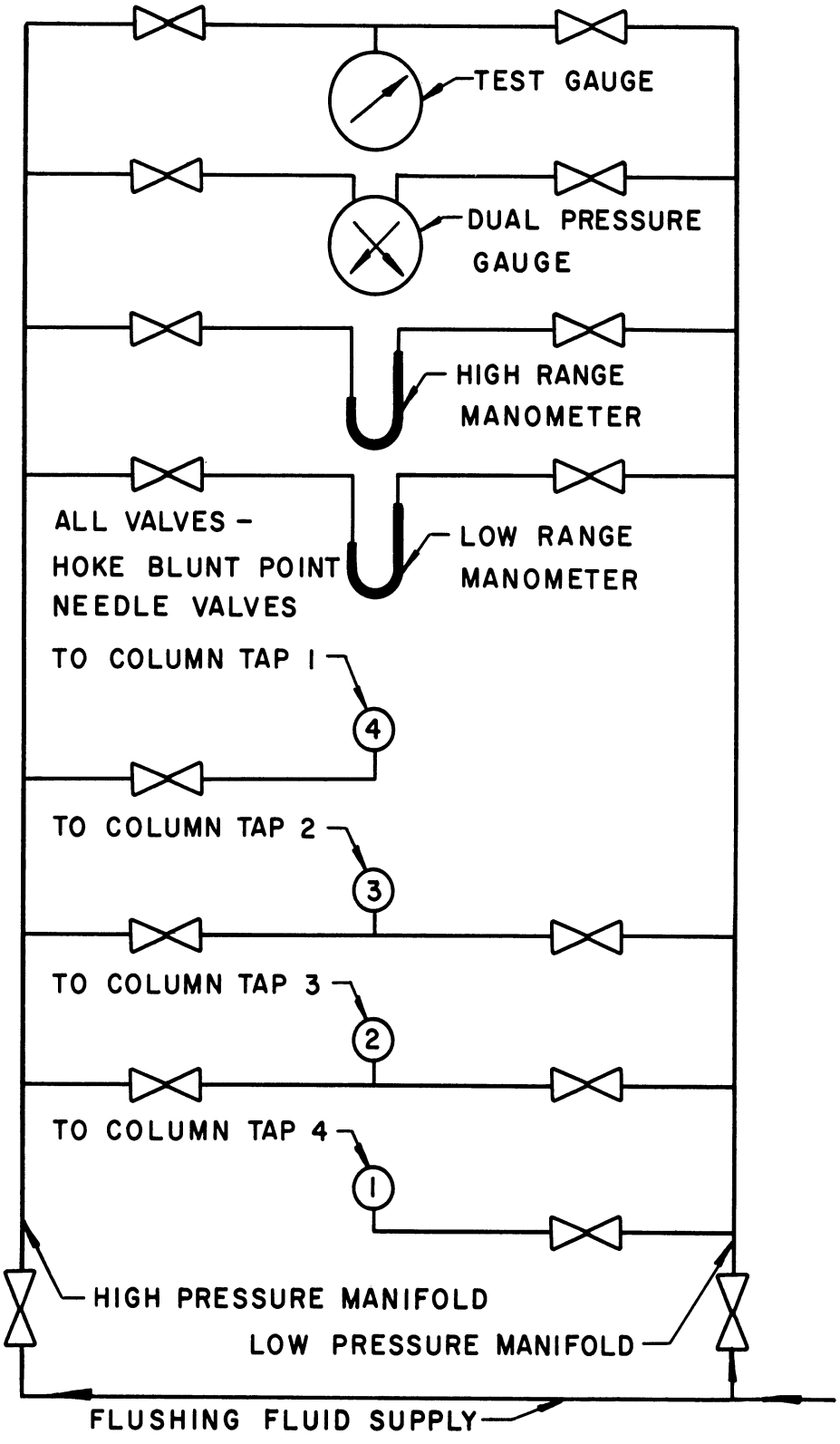

Figure 4. Diagram of Pressure Instrumentation

to water at 4 °C, and the other tube was filled with Meriam fluid D-8325 with a specific gravity of 1.75 at 55 °F compared to water at 4 °C.

Instrument lines were always filled with liquid, and flushing liquid was available to each of the manifolds from the pump discharge to assure that the lines were full of liquid before each measurement. Instrument lines of 3/16-inch copper tubing were used to reduce aspiration of the liquid from the lines at the column taps. With water on top of the manometer fluids, the high range manometer scale factor was 0.4535 psi/inch, and the low range manometer factor was 0.0272 psi/inch. With ethylene glycol in the instrument lines, the high range manometer factor was 0.4500 psi/inch. Reading the manometers to .2 of the smallest scale division indicates an error of less than 0.0091 psi for the high range manometer and less than 0.00054 psi for the low range manometer. The dimensions of the empty test section which are required to correct the manometer reading for unequal leg lengths are shown in Figure 5.

The numbered circles on Figure 4 correspond to the numbered pressure taps on Figure 3. The high pressure manifold was always open to the pressure tap having the higher pressure, and the low pressure manifold to the other. Tap 4 was always at the highest pressure, and could only be open to the high pressure manifold. Similarly, Tap 1 could only be connected to the low pressure manifold. Taps 2 and 3 may have either the higher or lower pressure of a pair of taps. When operated, one pressure tap was connected to each manifold, and the dual gauge was open to both manifolds. The test gauge can be connected to either manifold and thus, to any pressure tap. Either the high or low range manometer could be opened to the manifolds to measure the difference in pressure between any pair of column taps.

Inside diameter of column	= 4.03 in.
Cross sectional area	= 0.08854 ft^2.
Volume of empty test section	= 0.643 ft^3.
Distance between valve disks = Length of packed section, e	= 87.21 in.
Distance between top taps, a	= 23.88 in.
Distance between center taps, b	= 23.94 in.
Distance between bottom taps, c	= 24.25 in.
Distance from bottom tap to bottom valve disc, d	= 7.63 in.

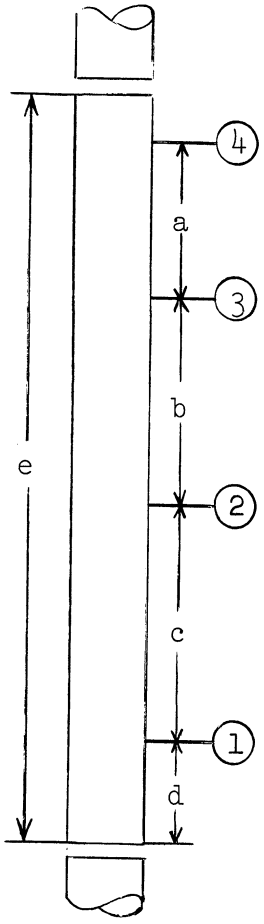

Figure 5. Specifications for Empty Test Section

C. Description of Operating Procedures

Before starting the flow of liquid or gas, the pump by-pass line to the liquid reservoir was opened, the drain valve on the surge drum was closed, and the quick-closing valves were shut. After closing the by-pass and the inlet valves for the large liquid rotameter, the surge drum was pressurized with air to a pressure about 20 psig higher than the top column pressure expected during the run. Opening the quick-closing valves released the pressure on the system and left the surge drum pressurized. The inlet valve to the liquid rotameter was opened and the pump by-pass was gradually closed until the desired liquid rate and metering pressure were obtained by suitable adjustments to the valves in the rotameter system. The air rate was selected by opening the inlet and outlet valves to the air meter until the desired float level and metering pressure were obtained.

The system was allowed to come to equilibrium, after final adjustments to the rates of liquid and gas, before the measurements were obtained for each run. When the measurements had been obtained from the pressure instruments, rotameters, and thermocouples, the liquid saturation was determined. A trigger was pulled to release the weight which actuated the quick-closing valves, and an instant later the drain valve on the surge drum was opened to prevent the release of the safety valve. The pump by-pass was opened and the air valves were closed to shut down the equipment. The test section was allowed to drain, and the height of liquid in the section was measured to complete the run.

For safety, it was imperative that the surge drum be pressurized with air before each run, and that the valve-closing system

be checked to see that the valves were closing simultaneously. Should the top valve fail to close with or before the bottom valve, the test section would fail before the surge drum drain could be opened if high rates were being investigated.

D. Description of Measurements Obtained

When the equipment had come to steady state at the desired liquid and gas rates, measurements were made of rates, pressures, pressure drops, liquid saturation, and temperatures. The measurements obtained are indicated in Figure 6 by a sample data sheet.

The measurement of liquid rate consisted of noting the per cent of maximum flow indicated on the rotameter being used and noting the capacity of the meter at full scale for the liquid being metered. The rate in gallons per minute was obtained by multiplication of these two quantities. The measurement of the air rate requires the recording of the per cent of maximum flow, the float being used, the temperature of the air being metered, and the pressure of the air. The rate in standard cubic feet per minute was obtained by the application of Equation (19).

The measurements of pressure were begun with all manifold valves closed. Tap 4 was opened to the high pressure manifold, and Tap 3 to the low pressure manifold. The test gauge was opened to the high pressure manifold to measure the top column pressure, and then to the low pressure manifold to obtain the pressure at Tap 3. The duplex gauge was opened to both manifolds to determine which of the manometers should be opened. A manometer was then opened to both manifolds, and the difference in pressure between Taps 4 and 3 was recorded. The valve to

Run Number					
Liquid Rate % of max. flow					
Max. flow, gpm					
Rate, gpm					
Air Rate % of max. flow					
Float (L,H)					
Temp., °F					
Pres., psig					
Rate, SCFM					
Pressure Drop 4(top)Pres.,psig					
3 Pres., psig					
2 Pres., psig					
1(btm)Pres.,psig					
4-3 Pres.Dif.,psi					
4-2 Pres.Dif.,psi					
4-1 Pres.Dif.,psi					
Column Temp., °F					
Holdup Measurement Description					
Liq. Height, in.					
Col. Pres., psig					
Holdup, cu.ft.					

Column _____ Packing _____ % Voids _____

Liquid _____ Viscosity _____

Figure 6. Sample Data Sheet

Tap 3 was closed, and Tap 2 was opened to the low pressure manifold in order to record the pressure at Tap 2, and the difference in pressure between Taps 4 and 2. Finally, the valve to Tap 2 was closed and Tap 1 was opened to obtain the bottom column pressure, and the difference in pressure between Taps 4 and 1. The temperature at the bottom of the column was then recorded as the temperature of the fluids in the test section. In some cases, the pressure difference was greater than the range of either manometer, and the indicated differences were obtained from the test gauge readings.

The measurement of liquid saturation was started with a brief comment on the type of flow pattern observed before the quick-closing valves were shut. After the test section was allowed to drain, the liquid height above the bottom flange was recorded along with the pressure in the section. The pressure was compared with the average of the top and bottom column pressures recorded previously to determine whether or not the quick-closing valves operated properly. The holdup was calculated by multiplying the fraction of the packed length occupied by liquid times the void volume of the test section.

The size of the column, the liquid phase, the packing material, the viscosity of the liquid phase at some temperature, and the fraction voids were recorded at the bottom of each data sheet. The fraction voids for each packing used was obtained by introducing measured volumes of water into the test section and measuring the rise in liquid level. Values were obtained and averaged for large and small rises in liquid level.

IV. EXPERIMENTAL SYSTEMS AND DATA

A. Flowing Fluids and Their Properties

The systems of fluids and packings selected for this investigation of two-phase pressure drop and liquid saturation in packed beds were chosen to provide a wide range of the variables used in the correlation of the data. The systems investigated were as follows:

1. Air and water on 3/8-inch Raschig Rings.
2. Air and a mildly foaming methylcellulose solution (2.5 wt.%) on 3/8-inch Raschig Rings.
3. Air and ethylene glycol on 3/8-inch Raschig Rings.
4. Air and ethylene glycol on 3/8-inch spheres.
5. Air and water on 3/8-inch spheres.
6. Air and water on 1/8-inch cylinders.
7. Air and foaming methylcellulose solution (0.5 wt.%) on 1/8-inch cylinders.
8. Air and foaming soap solution (0.0326 wt.%) on 1/8-inch cylinders.

Single-phase pressure drop measurements were also made for each combination of a single fluid and packing.

The properties of fluids used in the experiments are summarized in Table I. A portion of the properties listed in the table were obtained from the literature, and the remaining portion were measured in the Sohma Precision Laboratory of the University of Michigan.

Water solutions of methycellulose and soap were prepared in the liquid reservoir, since the volume of water in the reservoir was easily calculated as a result of the rectangular base and vertical sides of the tank. The solids to be dissolved were weighed out on a small laboratory scale. Methylcellulose was obtained under the trade

TABLE I

PROPERTIES OF FLOWING FLUIDS

Fluid	Concentration Wt.%	Density #/ft^3	Viscosity in Centipoise Temp. °F	cp.	Source
Water	--	62.4 @ 0°C	50	1.307	(29)
			60	1.126	
			70	0.975	
			80	0.860	
			90	0.765	
Ethylene Glycol	--	69.5 @ 0°C	73	17.6	(20)
			77	16.3	
			82	14.8	
			86	13.8	
			90	12.8	
			95	11.9	
Air	--	0.0808 @ 0°C 1 atm	50	0.0185	(30)
			60	0.0187	
			70	0.0190	
			80	0.0192	
			90	0.0196	
Methocel Solution	2.5	62.4 @ 0°C	70	14.6	Lab. Data
			74	13.3	
			78	12.2	
			82	11.5	
			84	11.1	
			89	10.0	
Methocel Solution	0.5	62.4 @ 0°C	54	2.97	Lab. Data
			63	2.45	
			74	2.02	
Soap Solution	0.033	62.4	71	0.965 Same as Water	Lab. Data

name Methocel from the Dow Chemical Company, and was of the 25 centipoise type indicating a viscosity of 25 centipoise for a 2 wt.% solution in water at 68°F. In order to reduce the foaming of the methylcellulose solution, 1000 ppm of lauryl alcohol was added to the 2.5 wt.% solution used on 3/8-inch Raschig Rings. No defoamer was added to the 0.50 wt.% solution since it was desired to study the effect of foaming on pressure drop. The foaming soap solution was prepared from a commercial granulated laundry soap.

The densities of water and ethylene glycol were obtained from the literature, and the densities of the water solutions were measured by determining the weight of a known volume of sample. The densities of the water solutions were found to be those of water at the same temperatures, to the accuracy shown in Table I.

The viscosities of air were obtained from Perry[29], and those of water were obtained from Perry[30]. Data on ethylene glycol were obtained from Hodgman.[20] The viscosities of methylcellulose and soap solutions were determined in Ostwald viscosimeters calibrated by the National Bureau of Standards and maintained in the Sohma Precision Laboratory. The viscosity of the weak soap solution was found to be the same as that of water for the temperatures measured.

B. Packing Materials and Their Properties

The properties of the packing materials used are summarized in Table II. Figure 7 is a photograph showing the shape and relative sizes of the materials.

The properties of the 3/8-inch ceramic Raschig Rings were supplied by the manufacturer, and the porosity of the material was

TABLE II

PROPERTIES OF PACKING MATERIALS

Packing Material	Nominal Size (in.)	Effective Diameter (ft.)	Specific Surface ft^3/ft^2	Fraction Voids
Raschig Rings	3/8	0.01945	148	0.520
Spheres	3/8	0.03125	122	0.362
Cylinders	1/8	0.0104	371	0.357

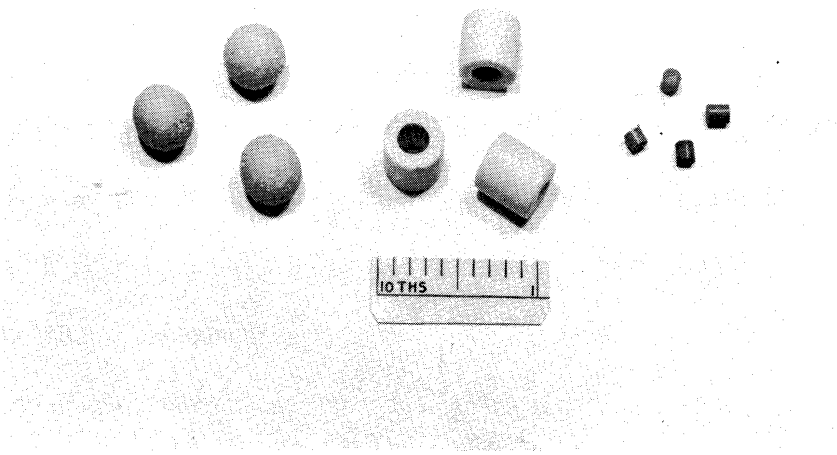

Figure 7. Photograph Showing Packing Materials

carefully checked after placing it in the test section. All of the materials were packed by settling the particles through water while tapping the test section with a rubber hammer. This method of packing the column successfully prevented further settling of the materials during the course of the experiments. The porosities of the materials were measured by introducing a measured quantity of water into the vertical, packed column and measuring the rise in the liquid level. After introducing the water, the test section was pressurized with air to see that the water level was not depressed due to air bubbles trapped within the packing. The measurement of porosity obtained in this manner checked the value given by the manufacturer for 3/8-inch Raschig Rings. The reported value of specific surface was assumed to be correct since no accurate method of measuring the exterior surface area of the material was available. A calculation based upon the careful measurement of several particles agreed with the reported value.

The 3/8-inch spheres were made of a chemical stoneware material and, as may be observed in Figure 7, were not quite spherical. The porosity of the material was measured with the method described above, and the diameter reported for the spheres was observed to be the average of the longest and shortest dimensions of the particles. In the absence of measurements of the specific surface, the particles were assumed to be spherical, and the specific surface was calculated from Equation (8), which gives the aerodynamic surface area per unit volume.

The catalyst cylinders investigated were 1/8-inch in diameter and 1/8-inch in length. The porosity of the material was measured, and the specific surface was calculated from Equation (8) using 1/8-inch

as the effective diameter, which is correct for spheres and cylinders whose length and diameter are equal. The cylinders were quite uniform in size and shape.

C. Description and Coding of Observed Flow Patterns

Two basic types of flow patterns were observed during the course of the experiments, and they have been termed the "homogeneous mode" and the "slugging mode." The term homogeneous flow will refer to a mode which is uniform throughout the length of the test section, and which is unchanging at a given point with respect to time. The term slug flow will refer to a mode which is composed of alternate portions of more dense and less dense mixtures traveling down the column, resulting in cyclic variations in the observation which is made at a given point in the column. A modification of the two basic flow patterns will be referred to as the "transition mode" to indicate that a section of the test column is operating in the homogeneous mode, and another section in the slugging mode.

In order to describe the variations observed in the flow pattern, a low liquid rate and a high liquid rate will be discussed as the air rate is varied from zero to the maximum value possible. With liquid filling the column, a low and constant liquid rate is established in the packed bed. There is sufficient resistance at the bottom of the test section to keep the column full of liquid. As air is introduced to the column at a very low rate, the liquid saturation is seen to decrease sharply. The formerly clear liquid phase becomes milky or opaque, and small bubbles of air can be seen in the liquid on close observation. As the air rate is increased, while holding the liquid

rate constant, the pressure drop continues to increase and the liquid saturation to decrease. The air bubbles increase in size and soon occupy the major portion of the void volume while the liquid phase takes a path over the particles of the packing material. At first the liquid layer on the packing particles is relatively thick, but it decreases as the air rate is increased. The flow patterns encountered up to this point are all of the homogeneous mode. At some point, however, the flow pattern becomes non-uniform with homogeneous flow at the top of the column and slugging flow at the bottom of the column. As the air rate is further increased, the fully developed slugging flow appears. The slugs appear to be flat plugs of high density material flowing down the column. When they first appear, they might be about four inches thick and two feet apart. As the air rate is further increased, the slugs become closer and closer together and thinner at the same time. The limit is reached with the slugs blurring together with one another, and the pattern reduces to a "poorly defined quiver." Even though the slugs appear well defined when viewed from a distance, close examination reveals only a small increase in the density of the flowing mixture. There is no jump or abrupt change of slope in the plot of pressure drop versus air rate for any of the transitions mentioned. If the amount of liquid flowing next to the surface of the packing material is observed during the increase of air rate, it is seen to decrease steadily until at the limiting air rate, there is a very thin film of liquid on the packing and the voids are filled with a heavy mist.

At very low liquid rates, the slugging mode is not observed and the limiting air rates produce a homogeneous mode of flow in which

the liquid is carried through as a mist, with very little liquid clinging to the surface of the packing material.

As the liquid rate is increased to higher constant rates, the same modes of flow are observed with the shift from all liquid, to transition mode, to the slugging mode, and finally into the limiting blur as the slugs become closer together. There is, however, a shift in the rate of flow of air at which each mode is observed. As the liquid rate becomes higher, the blurred pattern is observed at lower air rates and the liquid saturation is higher during the homogeneous mode of flow. At a very high liquid rate, the slugging mode is different in nature. As the air is introduced at the very high liquid rate, the liquid becomes milky, but the liquid saturation does not drop sharply. The liquid saturation remains quite high as the air is increased even when a tunneling of the air is observed. Pockets of air about a foot long seem to pass through the interior of the packing without an observable drop in the liquid saturation outside the pockets. At the limiting air rate a uniform, dense mixture of liquid dispersed in air is observed.

A close examination of the test section reveals instability on at least two scales. In addition to the instability evidenced by the slugging mode of flow, a small scale instability of the magnitude of the particles was observed. An attempt was made to measure the frequency of the two instabilities. The small scale effect was investigated with the aid of a stroboscope which was used as a standard of comparison. The measurements were very rough, but values between 17 and 33 cycles per second were observed. The frequency of this small scale disturbance

seemed to lie within the above range for all of the runs showing the slugging mode of flow. The small scale disturbance was not observed in the homogeneous mode. The frequency of the large scale instability can be estimated from the spacing of the slugs and the pore velocity of the air. The frequencies of the large scale disturbance vary from zero for the homogeneous mode, to very high values as the slugs become close together.

In reporting the data on the mode of flow, a code was used to designate four types of patterns as follows: homogeneous, transition, slugs, and close slugs or blur. In addition, the estimated spacing of the slugs has been recorded.

D. Description of Tabulated Processed Data

For a fixed geometry and fluid system, the independent variables which affect pressure drop and liquid saturation are the flow rates of each fluid and the temperature and pressure levels. The temperature level was the ambient value and was not controlled. Of the three independent variables, flow rates were varied widely, and pressure levels were varied over a more limited range.

The flow rates were varied at different levels in a two-by-two matrix of liquid and gas rates, as typified by the pattern shown in Figure 8.

The original data recorded in the form shown in Figure 6 was transcribed on IBM cards and processed with an IBM 650 computer as described in Appendix II. The large number of digits reported in the processed data and in the tabulated results, are the result of computer processing and do not indicate the accuracy of the data. The accuracy

Liquid Rate - % of Maximum

Air Rate - % of Maximum	3.58	14.3	23.3	35.0	55.0	78.0	100.0
0.0	X	X	X	X	X	X	X
15.0	X	X		X		X	
30.0	X		X		X		X
45.0	X	X		X		X	
60.0			X		X		X
80.0	X	X		X		X	

Figure 8. Chart Showing Typical Data Sampling

of the observations ranges from plus or minus 10 per cent for the rotameters to 0.5 per cent for some manometer readings. The accuracy of the calculated numbers may be considered to be between 3 and 10 per cent. A sample of the processed data is shown in Table III. The runs shown are for water and air on 3/8-inch Raschig Rings.

The first column of Table III is a run code which contains information about the type of flow as well as a run number. The second column is the liquid rate in gallons per minute and is obtained directly from the original data cards. The third column of Table III is the liquid mass rate, and was obtained by multiplying the liquid rate times the density in pounds per gallon, and dividing by the open cross sectional area of the test column.

The fourth column of Table III, the air rate in standard cubic feet per minute, was obtained through the use of Equation (19) which yields the capacity of the air meter at the temperature and pressure recorded in the original data and using the recorded float. The capacity of the meter was then multiplied by the scale reading recorded in the original data to obtain the air rate in standard cubic feet per minute. Column five was obtained by multiplying the volume rate times the density of air at standard conditions and dividing by the area of the open test column, yielding the mass rate of air in pounds per minute per square foot.

The sixth and seventh columns of Table III record the average pressure and the pressure drop between the top two pressure taps in the test section. The average pressure was obtained from the pressures indicated on the data sheets for the ends of the top section. The

TABLE III

SAMPLE PROCESSED DATA FOR WATER ON 3/8-INCH RASCHIG RINGS

	Liquid Rate		Air Rate		Top Section		Middle Section		Bottom Section				
Run Code	gpm	#/(ft^2 - min)	SCFM	#/(ft^2 - min)	Avg. Pres. psig	Pres. Drop psi/ft	Avg. Pres. psig	Pres. Drop psi/ft	Avg. Pres. psig	Pres. Drop psi/ft	Column Temperature °F	Liquid Viscosity cp	Liquid Saturation %
32113120	17.400	1638.401	46.1492	39.7806	32.96000	5.06634	23.01000	4.92279	11.92500	6.11144	66.0	1.035	21.257
33113060	17.400	1638.401	61.6022	53.1011	38.20000	5.42822	27.00000	5.81511	14.10000	7.02692	67.5	1.012	20.359
34113040	17.400	1638.401	79.2741	68.3342	43.55000	5.98110	31.35000	6.26629	16.80000	8.21456	68.5	.998	19.760
35114000	17.400	1638.401	93.0390	80.1996	47.55000	6.38319	34.50000	6.71746	18.75000	8.95684	70.0	.975	19.161
36111000	20.300	1911.468	11.6393	10.0331	20.72000	3.29714	14.22000	3.22839	7.05000	3.90934	74.0	.925	48.203
37112240	20.300	1911.468	25.3785	21.8763	27.56000	4.26216	19.13500	4.19590	9.77500	5.12173	75.0	.913	33.532
38112120	20.300	1911.468	35.2894	30.4194	32.20000	4.82509	22.55000	4.86264	11.75000	5.88875	75.5	.908	29.341
39113050	20.300	1911.468	47.3618	40.8259	37.00000	5.42822	26.10000	5.51433	13.80000	6.73000	76.0	.901	27.544
40113030	20.300	1911.468	61.8995	53.3573	42.83500	5.99618	30.58500	6.30138	16.45000	7.76920	77.0	.890	24.850
41113020	20.300	1911.468	77.4539	66.7653	48.20000	6.53397	34.75000	6.96811	18.90000	8.80839	78.0	.880	21.856
42114000	20.300	1911.468	94.2125	81.2111	53.49000	7.04664	38.84000	7.65991	21.55000	9.55067	78.0	.880	20.658
43111000	23.200	2184.535	16.0696	13.8520	29.42000	4.40289	20.41000	4.64206	10.24000	5.48297	60.0	1.126	43.712
44112000	23.200	2184.535	28.5327	24.5952	35.57000	5.55890	24.52000	5.53438	12.50000	6.43309	61.5	1.103	36.227
45113060	23.200	2184.535	40.0881	34.5559	40.91000	6.12183	28.71000	6.12592	15.15000	7.37331	63.0	1.080	29.041
46113040	23.200	2184.535	52.7174	45.4424	46.54500	6.68978	32.89500	7.01323	17.45000	8.36302	64.0	1.064	25.748
47113030	23.200	2184.535	71.8506	61.9352	53.75000	7.38841	38.50000	7.92059	20.80000	9.69912	66.0	1.035	24.550
48114000	23.200	2184.535	86.3775	74.4574	57.95000	7.99155	42.00000	8.02085	23.20000	10.68883	67.0	1.020	23.952
49114000	23.200	2184.535	96.6754	83.3342	61.30000	8.34338	44.75000	8.27150	25.10000	11.28266	68.0	1.005	24.251
50111000	26.100	2457.602	13.8410	11.9309	30.35500	4.87032	20.60500	4.91778	10.05000	5.59184	73.5	.930	49.401
51112000	26.100	2457.602	26.4911	22.8354	38.07000	5.86047	26.42000	5.83517	13.40000	7.12589	74.0	.925	38.323
52112001	26.100	2457.602	36.7283	31.6598	43.04000	6.49376	30.29000	6.30639	15.70000	8.21456	75.0	.913	31.437
53113081	26.100	2457.602	48.4819	41.7914	48.57500	7.16224	34.37500	7.09344	18.10000	9.10530	76.0	.900	27.844
54113040	26.100	2457.602	66.9815	57.7381	56.45500	7.98653	40.50500	8.02586	21.85000	10.54038	76.0	.900	27.544
55113023	26.100	2457.602	83.2792	71.7867	63.10000	8.74547	45.70000	8.72267	25.05000	11.82699	76.5	.896	26.347
56114003	26.100	2457.602	94.4460	81.4124	66.65000	9.19782	47.85000	9.67515	26.35000	11.72802	77.0	.891	23.952
57111001	29.000	2730.669	15.1737	13.0797	39.02500	6.40832	26.57500	6.09083	13.20000	7.22486	59.0	1.142	47.005
58111001	29.000	2730.669	25.0602	21.6019	45.46000	7.27784	31.16000	7.07840	15.80000	8.21456	61.0	1.110	39.820
59111002	29.000	2730.669	36.1593	31.1693	51.24000	8.00160	35.44000	7.86043	18.05000	9.45170	63.0	1.080	34.730
60112003	29.000	2730.669	49.3522	42.5416	57.50500	8.74045	40.25500	8.57730	20.95000	10.63935	65.0	1.050	28.742

pressure drop was obtained by dividing the difference in pressure between Taps 4 and 3 by the distance between Taps 4 and 3, in feet, as shown in Figure 5. Columns eight and nine were obtained in a similar manner for the middle section, as were columns ten and eleven for the bottom section of the packed column.

The column temperature was obtained from the data sheets without calculation, and the liquid viscosity was obtained from charts and punched in the original data cards using the bottom column temperature.

The last column of Table III is the liquid saturation in per cent. The saturation is obtained by dividing the liquid holdup in cubic feet reported on the original data sheets by the total void volume of the column. The total void volume is obtained by multiplying the fraction voids times the open column volume calculated from the dimensions given in Figure 5.

The tabulation of processed data is too lengthy to place in the main body of this paper, and the complete tabulation has been placed in Appendix III. Table IV will serve as an index to the tabulation of processed data, and will indicate the run numbers which are associated with the various systems investigated. Single-phase pressure drop measurements will be recognized by the zero rate of one fluid. Table V is a description of the run code itself and explains how the mode of flow, the spacing of the slugs, and the type of packing have been coded for each run. Thus, it will be seen that the only information not given about a run is the liquid phase, which must be determined from Table IV.

TABLE IV

RUN CODES CORRESPONDING TO EXPERIMENTAL SYSTEMS

Run Codes From	To	System
1111000	161111000	Air - Water on 3/8" Raschig Rings
162111000	188111000	Air - Methocel Solution (2.5%) on 3/8" Raschig Rings
190111000	216111000	Air - Ethylene Glycol on 3/8" Raschig Rings
217121000	251121000	Air - Ethylene Glycol on 3/8" Spheres
252121000	272123000	Air - Water on 3/8" Spheres
273131000	293133000	Air - Water on 1/8" Cylinders
294132000	297133000	Air - Methocel Solution (0.5%) on 1/8" Cylinders
301131000	307132000	Air - Soap Solution (0.033%) on 1/8" Cylinders

TABLE V

RUN CODE DESCRIPTION

Run Code - uuuuvwxyyz

Characters	Information		Code
uuuu	A four digit number designating an individual experimental run		uuuu
v	Column number	- 4" Plastic	1
w	Column packing	- 3/8" Raschig Rings	1
		3/8" Spheres	2
		1/8" Cylinders	3
x	Mode of flow	- Homogeneous mode	1
		Transition zone	2
		Slugging mode	3
		Close slugs (spacing 2" or less)	4
yy	Approximate spacing of slugs in inches	- Slugging mode	yy
		Homogeneous mode	00
		Transition zone	00
		Close slugs	00
z	Maximum swing in top pressure gauge - psi		z

V. CORRELATION OF EXPERIMENTAL DATA

A. Derivation of Correlation Relationships

The general energy balance in a flow system can be written as

$$\int V' dP + \frac{\Delta u^2}{2g_c} + \Delta Z + W_f + W_s = 0 \qquad (20)$$

where V' is the volume of the flowing mixture per pound, the second term is the increase in energy due to an increase in velocity, Z is the position coordinate measured vertically, W_f is the energy converted into heat by friction in foot-pounds per pound, and W_s is shaft work done on the surroundings. Since the shaft work is zero for downward two-phase flow, and since the change in velocity over a small distance is negligible, Equation (20) can be rewritten

$$\int (1/\rho) dP + \Delta Z = -W'_f \Delta Z \qquad (21)$$

where W'_f is the friction energy per unit length. Over a small downward interval in length, the density may be considered constant, and the upward distance, ΔZ, may be replaced by the downward distance, $-\Delta L$. Upon integration and rearrangement, Equation (21) becomes

$$-\frac{\Delta P}{\Delta L} + \rho = W'_f \rho. \qquad (22)$$

The right side of the above equation represents the total energy required to overcome friction per unit length downward through the packing. It is convenient to express the total friction energy by a single symbol, δ, which is defined by the following equation, and may have the

units of pounds per square foot per foot, or pounds per square inch per foot:

$$-\frac{\Delta P}{\Delta L} + \rho = \delta. \tag{23}$$

For horizontal flow, the density is dropped from the above expression since ΔZ would be zero in Equation (20). Equation (23) can be written with greater accuracy as

$$-\frac{dP}{dL} + \rho = \delta. \tag{24}$$

Data is taken in the form $\Delta P/\Delta L$ in order to determine a correlation for dP/dL which can be applied to the general case.

The two assumptions which will be made in the derivation of the correlation relationships are as follows:

1. The pressure drop for the gas phase is equal to that of the liquid phase, and both drops must be equal to the two-phase pressure drop, $\left(\frac{\Delta P}{\Delta L}\right)_{\ell g}$.
2. If ϵ is the fraction voids for the bed, and if R_ℓ and R_g are the fractions of void volume occupied by the liquid and the gas respectively, then $(R_\ell + R_g)$ is equal to unity, and ϵR_ℓ and ϵR_g are the effective porosities for the liquid and gas respectively.

The form of the Reynolds number defined by Equation (1) may be used to define Reynolds numbers for the liquid and gas phases as

$$Re_\ell = \frac{D_p u_\ell \rho_\ell}{\mu_\ell (\epsilon R_\ell)^n} \tag{25}$$

and

$$Re_g = \frac{D_p u_g \rho_g}{\mu_g (\epsilon R_g)^{n'}} \tag{26}$$

where the subscript ℓ designates values for the liquid phase, the subscript g designates values for the gas phase, and the exponents n and n' are constant for a given packing material and flow regime. The Fanning form of the friction factor, which differs only by a constant from the form in Equation (2), may be used to express the total frictional energy, $\delta_{\ell g}$, as defined by Equation (24). The two-phase pressure drop per unit length may be expressed on the basis of either the liquid or gas phase as

$$-\left(\frac{\Delta P}{\Delta L}\right)_{\ell g} = \frac{2f_\ell \rho_\ell u_\ell^2}{(\epsilon R_\ell)^m D_p g_c} + \rho_m \tag{27}$$

and

$$-\left(\frac{\Delta P}{\Delta L}\right)_{\ell g} = \frac{2f_g \rho_g u_g^2}{(\epsilon R_g)^{m'} D_p g_c} + \rho_m \tag{28}$$

where the subscript ℓg refers to the simultaneous flow of two phases and the subscript m refers to the property of the gas-liquid mixture. The assumption that the pressure drop for the gas is equal to that of the liquid is equivalent to the statement that $\delta_{\ell g}$ can be expressed in terms of the friction factor for either the liquid or the gas, as seen by the rearrangement of Equations (27) and (28) as follows:

$$\delta_{\ell g} = \frac{2f_\ell \rho_\ell u_\ell^2}{(\epsilon R_\ell)^m D_p g_c} = \frac{2f_g \rho_g u_g^2}{(\epsilon R_g)^{m'} D_p g_c} \quad . \tag{29}$$

The friction factors for the liquid and the gas may be expressed in the general Blasius form as suggested for two-phase flow in pipes by Lockhart and Martinelli.[24] Expressing the friction factors in the Blasius form yields

$$f_\ell = \frac{C_\ell}{(Re_\ell)^s} = \frac{C_\ell}{\left[\frac{D_p G_\ell}{\mu_\ell (\epsilon R_\ell)^n}\right]^s} \tag{30}$$

and

$$f_g = \frac{C_g}{(Re_g)^{s'}} = \frac{C_g}{\left[\frac{D_p G_g}{\mu_g (\epsilon R_g)^{n'}}\right]^{s'}} \tag{31}$$

where the constants C_ℓ and C_g, as well as the exponents s and s', are dependent on the packing and the mode of flow. Substituting Equations (30) and (31) into Equation (29) and separating into two expressions, results in the following equations:

$$\delta_{\ell g} = C_\ell \left[\frac{\mu_\ell (\epsilon R_\ell)^n}{D_p G_\ell}\right]^s \left[\frac{2\rho_\ell u_\ell^2}{(\epsilon R_\ell)^m D_p g_c}\right] \tag{32}$$

$$\delta_{\ell g} = C_g \left[\frac{\mu_g (\epsilon R_g)^{n'}}{D_p G_g}\right]^{s'} \left[\frac{2\rho_g u_g^2}{(\epsilon R_g)^{m'} D_p g_c}\right] \tag{33}$$

The collection of R_ℓ terms in Equation (32) results in the expression

$$\delta_{\ell g} = C_\ell \left[\frac{\mu_\ell \epsilon^n}{D_p G_\ell}\right]^s \left[\frac{2\rho_\ell u_\ell^2}{\epsilon^m D_p g_c}\right] R_\ell^{(ns-m)} \tag{34}$$

Comparison of the product of C_ℓ and the first bracket of Equation (34) with Equation (30) will show that the product is the friction factor for the liquid phase flowing alone in the bed, since the total porosity has replaced ϵR_ℓ. A comparison of the second bracket in Equation (34) with Equation (29) will show that the first three terms in Equation (34) represent the total friction energy loss for the liquid flowing in the total void volume. The term ϵR_ℓ has been replaced by ϵ in every case. The first three terms on the right side of Equation (34) can be replaced by a term which represents the single-phase friction loss for the liquid flowing alone in the bed at the conditions of the two-phase flow as follows:

$$\delta_{\ell g} = \delta_\ell R_\ell^{(ns-m)} \tag{35}$$

where δ_ℓ is the value observed for single-phase flow or obtained from a single-phase correlation. Similar steps lead to an analogous result for the gas phase as follows:

$$\delta_{\ell g} = \delta_g R_g^{(n's'-m')} \tag{36}$$

where δ_g is the value of friction loss observed for single-phase flow of the gas alone in the bed or calculated from a single-phase correlation.

The division of Equation (35) by δ_ℓ and Equation (36) by δ_g leads to the definition of φ_ℓ and φ_g as follows:

$$\varphi_\ell = \sqrt{\delta_{\ell g}/\delta_\ell} = R_\ell^{(sn-m)/2} \tag{37}$$

$$\varphi_g = \sqrt{\delta_{\ell g}/\delta_g} = R_g^{(s'n'-m')/2}. \tag{38}$$

Equations (37) and (38) state the important result that φ_ℓ and φ_g are only functions of the liquid saturation, as was expected from similar results for two-phase flow in open pipes and porous media. The results of single-phase investigations have shown that the exponents in Equations (25), (26), (30), and (31) are the same for liquids and gases; and therefore, s = s', n = n', and m = m'.

The variables R_ℓ and R_g are not suitable for independent variables since they are unknown in the design calculation. A suitable independent variable can be obtained by dividing Equations (37) and (38) and defining χ as

$$\chi = \sqrt{\frac{\delta_\ell}{\delta_g}} = \frac{R_g^{(s'n'-m')/2}}{R_\ell^{(sn-m)/2}} \quad . \tag{39}$$

Using the equality of primed and unprimed exponents along with the assumption that $(R_\ell + R_g)$ equals unity yields the final result that

$$\chi = \sqrt{\frac{\delta_\ell}{\delta_g}} = (R_\ell/1-R_\ell)^{(m-sn)/2} \quad . \tag{40}$$

The value of χ can be calculated from single-phase correlations and is quite suitable for the independent variable in a design calculation. Further it is observed that φ_ℓ, φ_g, and χ are all functions of the liquid saturation. Therefore, φ_ℓ and φ_g may be considered functions of χ alone. The liquid saturation has been eliminated as the independent variable, and becomes a function of χ.

The result of the derivation can be expressed in the following compact form:

$$\varphi_\ell = F_1(\chi) \tag{41}$$

$$\varphi_g = F_2(\chi) \tag{42}$$

$$R_\ell = F_3(\chi) \tag{43}$$

where F_1, F_2, and F_3 are functions to be determined. Examination of the definitions of φ_ℓ, φ_g, and X will reveal the following relationships:

$$\varphi_g = \varphi_\ell X \tag{44}$$

$$\varphi_\ell = \varphi_g / X \tag{45}$$

which means that Equations (41) and (42) are not independent and that only one of the functions, F_1 and F_2, need be determined.

Further examination of the definition of φ_g will show that the value becomes infinite as the gas rate goes to zero and becomes unity as the liquid rate goes to zero. In order to obtain a symmetric form for the correlation, the definitions of φ_g and X may be combined to obtain

$$\frac{\delta_{\ell g}}{\delta_\ell + \delta_g} = \frac{\varphi_g^2}{1 + X^2} = F_4(X) \tag{46}$$

where F_4 is a function which can be obtained from F_1 or F_2. The form expressed by Equation (46) has a distinct advantage since it is finite across the entire range from all liquid to all gas.

The correlation of data for two-phase cocurrent flow in packed beds requires the evaluation and confirmation of Equations (42), (43), and (46).

B. Correlation of Single-Phase Data

Confirmation of the relationships suggested by the derivation requires the evaluation of δ_ℓ and δ_g for the single-phase flow of each fluid. The observation of single-phase pressure drops at the conditions of each two-phase run would be very difficult experimentally. It was

much more satisfactory to take single-phase data and establish a correlation which could be used to calculate the desired values of δ_ℓ and δ_g.

Computer processing of the two-phase data made the algebraic equation suggested by Ergun[14] much more convenient than the graphical relationships presented by Brownell and Katz[5]. Equation (13) did not fit the experimental results within the plus or minus 50 per cent deviation claimed for the correlation, and greater accuracy was necessary to prevent errors in the single-phase prediction from being transmitted to the two-phase correlation. The form of Equation (13) was confirmed, but the two constants were found to vary with the packing material. Equation (13) can be rewritten in terms of two arbitrary constants, A and B,

$$\left(-\frac{dP}{dL}\right)\left(\frac{g_c \rho D_p^3}{\mu^2}\right)\left(\frac{\epsilon}{1-\epsilon}\right)^3 = Re(A + BRe) \,. \qquad (47)$$

In order to determine the constants in Equation (47), the left member of the equation was plotted against the Reynolds number as shown in Figure 9.

Curves were fitted to the data shown in Figure 9 for 3/8-inch Raschig Rings, 3/8-inch spheres, and 1/8-inch cylinders. The data for the cylinders were found to agree with the values reported by Ergun[14] for A and B, 150 and 1.75 respectively. The values of A and B for the various packing materials are indicated in Figure 9 in terms of the right member of Equation (47) as follows:

1. Re(266 + 2.33Re) for 3/8-inch Raschig Rings,
2. Re(118.2 + 1.0Re) for 3/8-inch spheres, and
3. Re(150 + 1.75Re) for 1/8-inch cylinders.

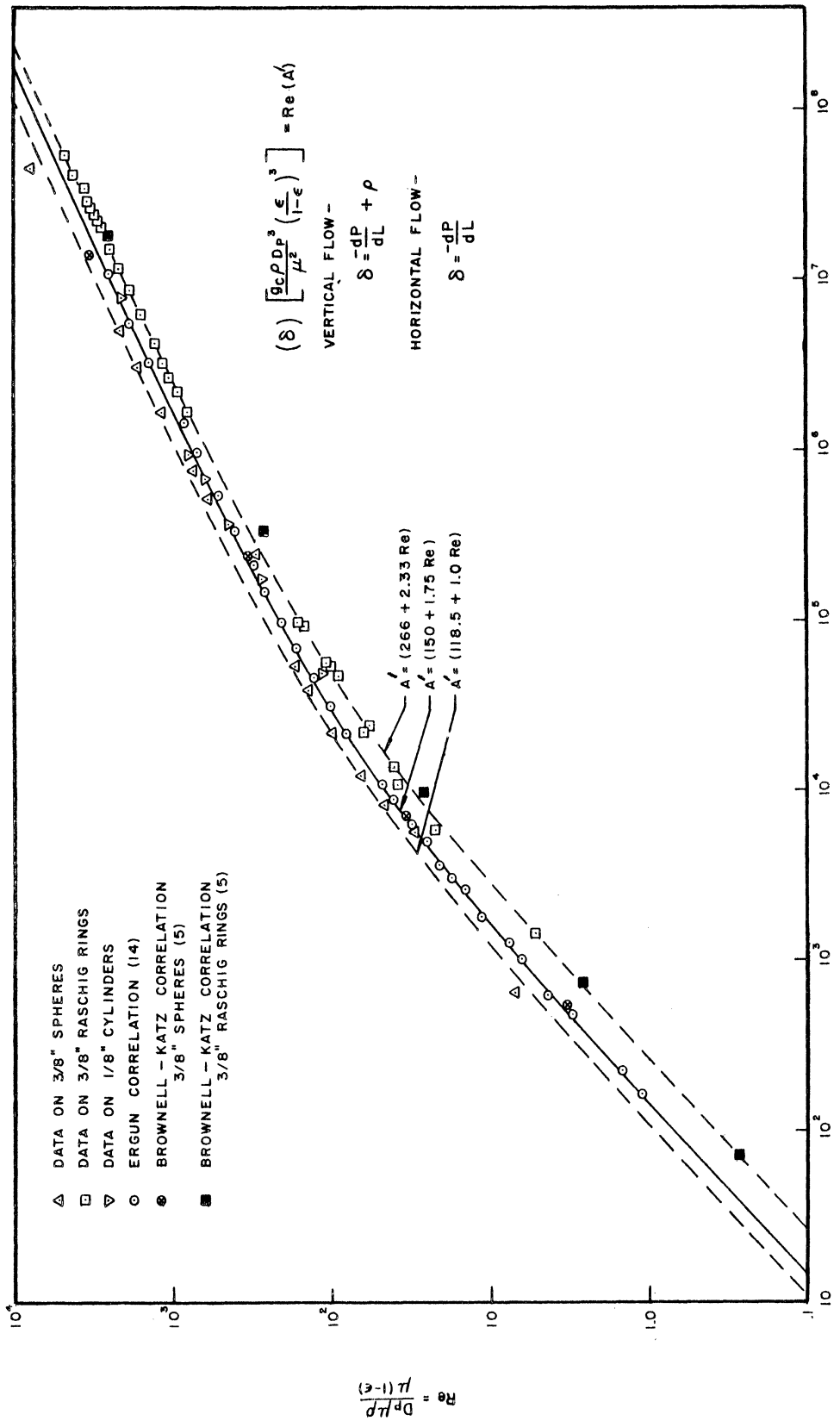

Figure 9. Single-Phase Pressure Drop in Packed Beds.

The expressions given above correlate the single-phase data within plus or minus 20 per cent. A possible entrance effect in the top section of the packed bed and a possible exit effect in the bottom section prompted the selection of the middle section of the column as a basis for the correlation of single-phase pressure drop. When all three sections are considered, the scatter of data is approximately 30 per cent.

Calculation of the single-phase data was done simultaneously with the two-phase data, and the calculated results are presented together in Appendix IV. The parameter $\frac{\delta_{lg}}{\delta_l + \delta_g}$ is presented in the calculated results, and it reduces to a comparison of the observed and calculated values for the single-phase cases. The single-phase runs are identified by a zero flow rate for one phase. A few of the single-phase runs for air at low rates are high as a result of flushing the instrument lines and wetting the bed. A few of the single-phase runs for liquid are high as a result of air bubbles which leaked into the system from the surge drum at low liquid rates. The points in which these effects were noticeable are excluded from the statements of deviation given above.

Examination of Figure 9 shows that Equation (11), presented by Ergun[14], predicts pressure drops which are low for Raschig Rings and high for spheres. The deviation of Equation (11) from the fitted curves ranges from 30 to 80 per cent for Raschig Rings, and from 20 to 40 percent for spheres, depending upon the Reynolds number. Figure 9 also presents a comparison of the correlation proposed by Brownell and Katz[5] with the observed data for Raschig Rings. The deviations for

this correlation are well within the experimental error; and the correlation appears to be more accurate than that of Ergun, although the form of the latter is excellent. The consideration of the sphericity of the particles allows the curves in Figure 9 to shift with the packing material in the correlation of Brownell and Katz[5], but such a shift is not possible with the Ergun[14] correlation as long as the constants of Equation (11) are considered independent of the packing.

C. Explanation of Tabulated Results

Table VI is a sample page of the tabulation of calculated results which forms the body of Appendix IV. The sample page of results is for the system of water and air on 3/8-inch Raschig Rings as is indicated by the index to run codes given in Table IV. Three lines of calculated results are obtained from each experimental run, representing the top, middle, and bottom sections of the packed column. The tabulation of results was prepared entirely by IBM machines as described in Appendix II.

The first column of Table VI is the run code, and each code appears on three lines. The second column indicates the section of the test column for which the calculations have been made. The combination of run code and column section gives an exact reference to the corresponding data in Table III or Appendix II.

The third and fourth columns of Table VI are the mass rates of the liquid and gas, and come directly from the tabulation of processed data without calculation. The mass rates are the same for all three column sections.

TABLE VI

SAMPLE CALCULATED RESULTS FOR WATER ON 3/8-INCH RASCHIG RINGS

Run Code	Column Section	Mass Rates: Liquid #/(ft² - min)	Mass Rates: Air #/(ft² - min)	Reynolds Number: Liquid	Reynolds Number: Air	$\delta_{\ell g}$	δ_ℓ	δ_g	Liquid Saturation %	X	Φ_ℓ	Φ_g	$\frac{\delta_{\ell g}}{\delta_\ell+\delta_g}$
40113030	MID	1911.468	53.3573	2156.827	2783.723	5.97403	1.50840	.31750	24.8502	2.1796	1.9900	4.3377	3.2718
40113030	BTM	1911.468	53.3573	2156.827	2783.723	7.44184	1.50840	.46157	24.8502	1.8077	2.2211	4.0153	3.7776
41113020	TOP	1911.468	66.7653	2181.336	3478.260	6.19358	1.50755	.35574	21.8562	2.0585	2.0269	4.1725	3.3239
41113020	MID	1911.468	66.7653	2181.336	3478.260	6.62772	1.50755	.45250	21.8562	1.8252	2.0967	3.8270	3.3813
41113020	BTM	1911.468	66.7653	2181.336	3478.260	8.46799	1.50755	.66596	21.8562	1.5045	2.3700	3.5658	3.8959
42114000	TOP	1911.468	81.2111	2181.336	4230.844	6.70103	1.50755	.48276	20.6586	1.7671	2.1083	3.7256	3.3668
42114000	MID	1911.468	81.2111	2181.336	4230.844	7.31430	1.50755	.61486	20.6586	1.5658	2.2026	3.4490	3.4462
42114000	BTM	1911.468	81.2111	2181.336	4230.844	9.20506	1.50755	.90813	20.6586	1.2884	2.4710	3.1837	3.8105
43111000	TOP	2184.535	13.8520	1948.314	740.756	4.15770	1.98076	.02357	43.7125	9.1654	1.4488	13.2789	2.0743
43111000	MID	2184.535	13.8520	1948.314	740.756	4.39688	1.98076	.02963	43.7125	8.1761	1.4898	12.1816	2.1870
43111000	BTM	2184.535	13.8520	1948.314	740.756	5.23778	1.98076	.04171	43.7125	6.8910	1.6261	11.2057	2.5897
44112000	TOP	2184.535	24.5952	1988.940	1312.354	5.28111	1.97852	.06162	36.2275	5.6662	1.6337	9.2573	2.5885
44112000	MID	2184.535	24.5952	1988.940	1312.354	5.25659	1.97852	.07898	36.2275	5.0048	1.6299	8.1578	2.5548
44112000	BTM	2184.535	24.5952	1988.940	1312.354	6.15530	1.97852	.11389	36.2275	4.1679	1.7638	7.3515	2.9417
45113060	TOP	2184.535	34.5559	2031.297	1839.781	5.81274	1.97628	.10775	29.0419	4.2826	1.7150	7.3447	2.7891
45113060	MID	2184.535	34.5559	2031.297	1839.781	5.81683	1.97628	.13803	29.0419	3.7838	1.7156	6.4915	2.7511
45113060	BTM	2184.535	34.5559	2031.297	1839.781	7.06422	1.97628	.20073	29.0419	3.1376	1.8906	5.9322	3.2448
46113040	TOP	2184.535	45.4424	2061.843	2415.835	6.36634	1.97472	.16715	25.7485	3.4371	1.7955	6.1714	2.9723
46113040	MID	2184.535	45.4424	2061.843	2415.835	6.68979	1.97472	.21509	25.7485	3.0299	1.8405	5.5768	3.0549
46113040	BTM	2184.535	45.4424	2061.843	2415.835	8.03958	1.97472	.31842	25.7485	2.4902	2.0177	5.0247	3.5059
47113030	TOP	2184.535	61.9352	2119.615	3283.015	7.05976	1.97190	.27555	24.5508	2.6750	1.8921	5.0615	3.1412
47113030	MID	2184.535	61.9352	2119.615	3283.015	7.59193	1.97190	.35455	24.5508	2.3583	1.9621	4.6274	3.2633
47113030	BTM	2184.535	61.9352	2119.615	3283.015	9.37047	1.97190	.53132	24.5508	1.9264	2.1799	4.1995	3.7433
48114000	TOP	2184.535	74.4574	2150.786	3941.029	7.66029	1.97044	.37383	23.9520	2.2958	1.9716	4.5267	3.2676
48114000	MID	2184.535	74.4574	2150.786	3941.029	7.68958	1.97044	.47899	23.9520	2.0282	1.9754	4.0067	3.1393
48114000	BTM	2184.535	74.4574	2150.786	3941.029	10.35757	1.97044	.71659	23.9520	1.6582	2.2926	3.8018	3.8546
49114000	TOP	2184.535	83.3342	2182.887	4404.465	8.01342	1.96898	.44716	24.2514	2.0984	2.0173	4.2332	3.3166
49114000	MID	2184.535	83.3342	2182.887	4404.465	7.94154	1.96898	.57164	24.2514	1.8559	2.0083	3.7272	3.1258
49114000	BTM	2184.535	83.3342	2182.887	4404.465	10.95270	1.96898	.85387	24.2514	1.5185	2.3585	3.5814	3.8800

The fifth and sixth columns of Table VI are the Reynolds numbers for the liquid and gas and are calculated from Equation (12), using the mass rates and viscosities of the fluids. The ratio of D_p to $(1 - \epsilon)$ is constant for a given packing, the values of the mass rates and the viscosity of the liquid are obtained from the tabulated data, and the viscosity of the air is obtained from the following equation given by Perry:(29)

$$\mu = 0.01709(T/460)^{.768} \tag{48}$$

in which T is the absolute temperature in degrees Rankine, and the viscosity is in centipoise.

The seventh column of Table VI is the corrected pressure drop per unit length as defined by Equation (23), or

$$\delta_{\ell g} = - \left(\frac{\Delta P}{\Delta L}\right)_{\ell g} + \rho_m \tag{49}$$

where ρ_m is the density of the flowing mixture at the average pressure in the column section. The value of $\frac{\Delta P}{\Delta L}$ is corrected for the unequal manometer legs before Equation (49) is applied. Since the unequal leg acts over the length ΔL, ρ_ℓ in psi per foot must be subtracted from the observed pressure drop. The density of the flowing mixture is calculated from

$$\rho_m = \rho_\ell R_\ell + \rho_g R_g = \rho_\ell R_\ell + \rho_g (1 - R_\ell). \tag{50}$$

The density of the liquid is assumed to be constant and equal to the value given in Table I, the value of R_ℓ is obtained from the tabulation of processed data, and the density of air is obtained from the ideal gas law, which is valid within the range of these experiments. The

expression used for air density is

$$\rho_g = \frac{PM}{RT} = 2.708 \left(\frac{P}{T + 460}\right) \tag{51}$$

where P is the absolute pressure, T is in Fahrenheit, R is the gas law constant, and the units of density are pounds per cubic foot. In order for the units of $\delta_{\ell g}$ to be in psi per foot, ρ_m which is in pounds per cubic foot must be divided by 144 before it is used in Equation (49).

The eighth column of Table VI is the friction loss for the liquid flowing alone, δ_ℓ, and is obtained from Equation (47) since this equation is for horizontal flow and -(dP/dL) is equal to δ_ℓ. The constants in Equation (47) are selected for the particular packing from those shown in Figure 9. The density of the liquid is again taken from Table I.

The ninth column of Table VI is the friction loss for the gas flowing alone, δ_g, and is also calculated from Equation (47) using the density function of Equation (51). The pressure at which the density is evaluated is the average pressure in the column section. The average pressure in each section of the column is tabulated in the processed data. The use of the average pressure in this calculation needs some justification. For a given mass rate, packing material, and viscosity, the Reynolds number is constant, and Equation (47) can be simplified to

$$-\frac{dP}{dL} = \frac{C}{P} \tag{52}$$

where C is a constant. Separation of variables and integration leads to

$$-\int_1^2 P\, dP = C \int_1^2 dL = -\left(\frac{1}{2}\right)(P_2^2 - P_1^2) = C(L_2 - L_1) \tag{53}$$

which can be rewritten

$$\left[\frac{-(P_2 + P_1)}{2}\right] (P_2 - P_1) = C(L_2 - L_1). \tag{54}$$

Finally

$$-\left(\frac{\Delta P}{\Delta L}\right) = -\left[\frac{P_2 - P_1}{L_2 - L_1}\right] = \frac{2C}{P_2 + P_1} = \frac{C}{P_{average}} \tag{55}$$

verifies that the use of the average pressure at the ends of an interval correctly approximates the average rate of pressure drop across the interval.

The tenth column of Table VI is the liquid saturation in per cent, and is obtained directly from the data tabulation.

Columns eleven, twelve, thirteen, and fourteen of Table VI are the correlation parameters which are calculated directly from $\delta_{\ell g}$, δ_{ℓ}, and δ_{g} according to Equations (39), (37), (38), and (46), respectively. Since the computer will not divide by zero, infinite values are designated in the tabulated results by the value 999.9999. The accuracy of the calculated results lies between 3 and 20 per cent as a result of errors in instruments and meters.

D. Presentation of Correlated Data

Figure 10 is a plot of the calculated results obtained from data on 3/8-inch Raschig Rings. The calculated values of φ_g and R_ℓ are shown plotted against X. The liquids used were water, Methocel solution, and ethylene glycol. The run codes included in Figure 10 are between 1111000 and 216111000, or runs between 1 and 216. The points in Figure 10 have been coded to identify the mode of flow for each of the runs plotted. The straight line represents the locus of points for which

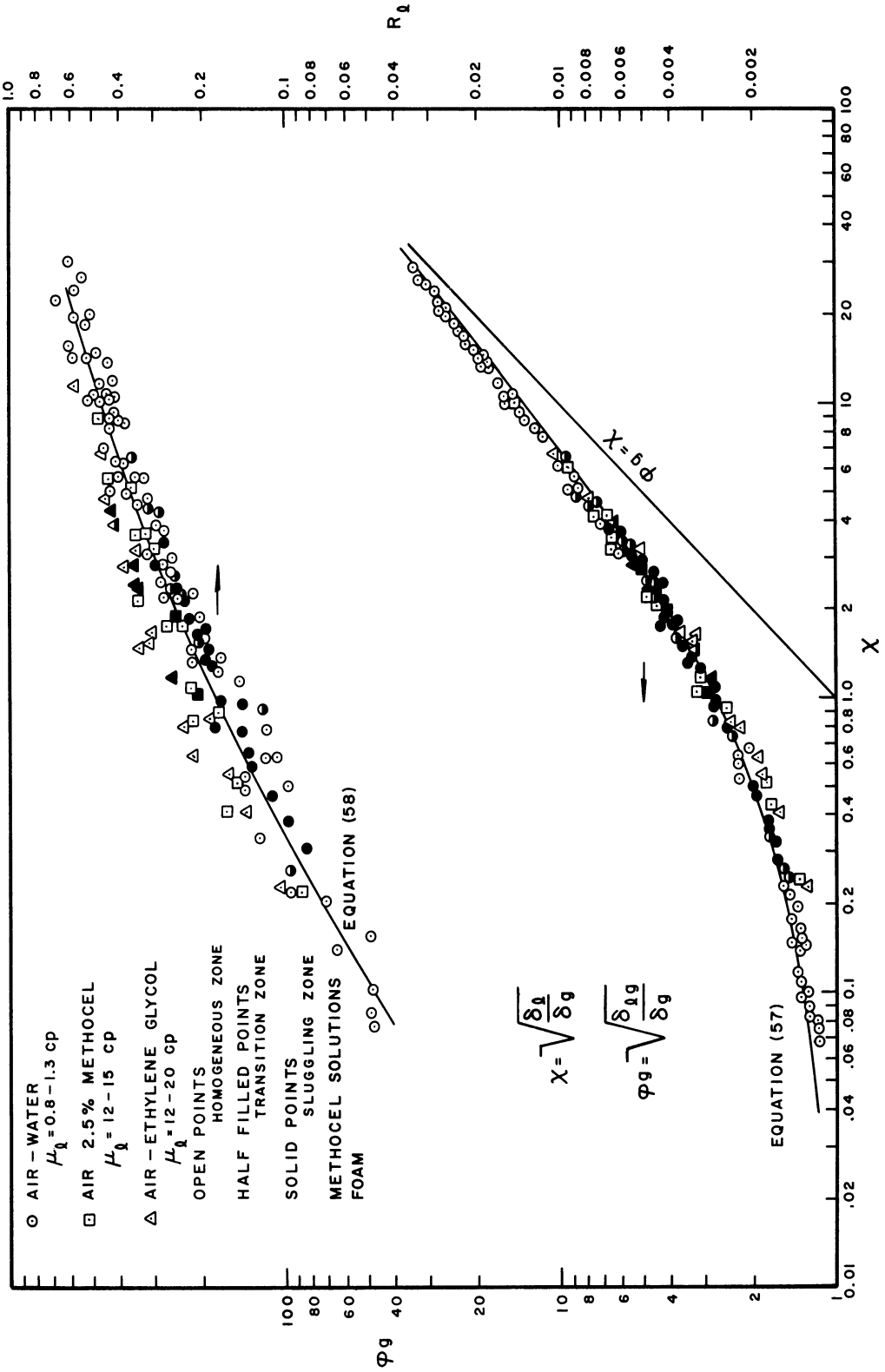

Figure 10. Two-Phase Cocurrent Pressure Drop on 3/8-Inch Raschig Rings

φ_g and X are equal. In order for the data to be consistent with the single-phase relationships, φ_g must approach unity as X approaches zero, and φ_g must approach X, as X approaches infinity. The data on Raschig Rings show that the correlation is valid for this packing, and is not affected by viscosity variations. The points corresponding to the homogeneous mode lie toward the ends of the curve, with points for the slugging mode lying toward the center. The points of transition are well defined, and are a function of the physical properties of liquid phase.

Figure 11 is a plot of the calculated results obtained from data on 3/8-inch spheres. The plot is very similar in form to Figure 10 for Raschig Rings. The liquids used in the runs on spheres were water and ethylene glycol; the runs included lie between 217 and 273. The lines which are drawn in Figure 11 are identical with those of Figure 10, which indicates that there is no change in the correlation obtained on the Raschig Rings as a result of the change in packing or porosity.

Figure 12 is a plot of the calculated results obtained from data on 1/8-inch cylinders. The liquids used were water, foaming Methocel solution, and foaming soap solution. The run numbers lie between 274 and 307. The lines shown in Figure 12 are identical with those in Figures 10 and 11, and the points for water further establish the validity of the correlation over changes in porosity and particle size. The purpose of the points for foaming systems is to establish the effect of foaming on two-phase pressure drop which will be discussed in a later section.

Figure 13 presents the final symmetric correlation of the data on all packing materials, and for all flowing fluids with the

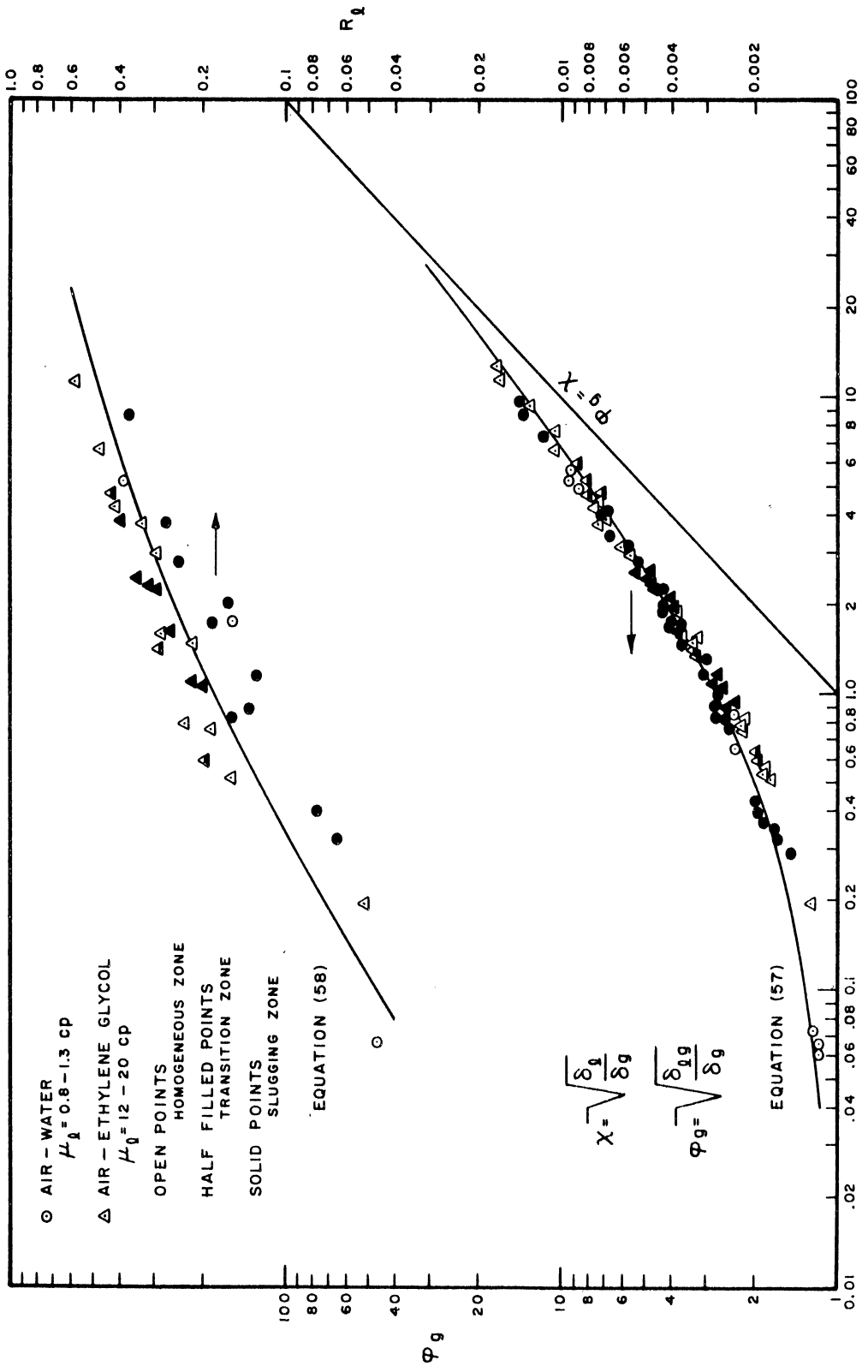

Figure 11. Two-Phase Cocurrent Pressure Drop on 3/8-Inch Spheres.

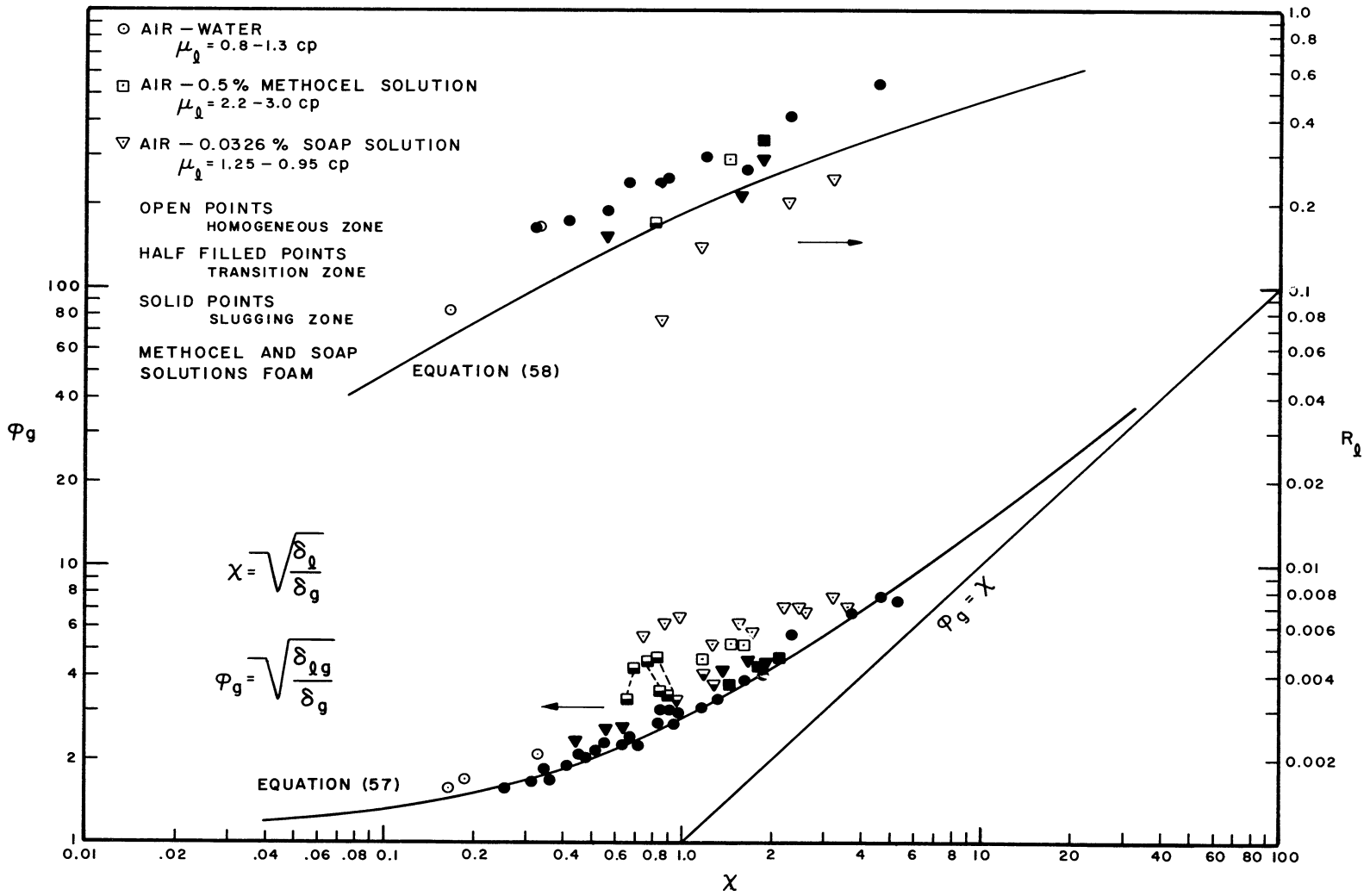

Figure 12. Two-Phase Cocurrent Pressure Drop on 1/8-Inch Cylinders.

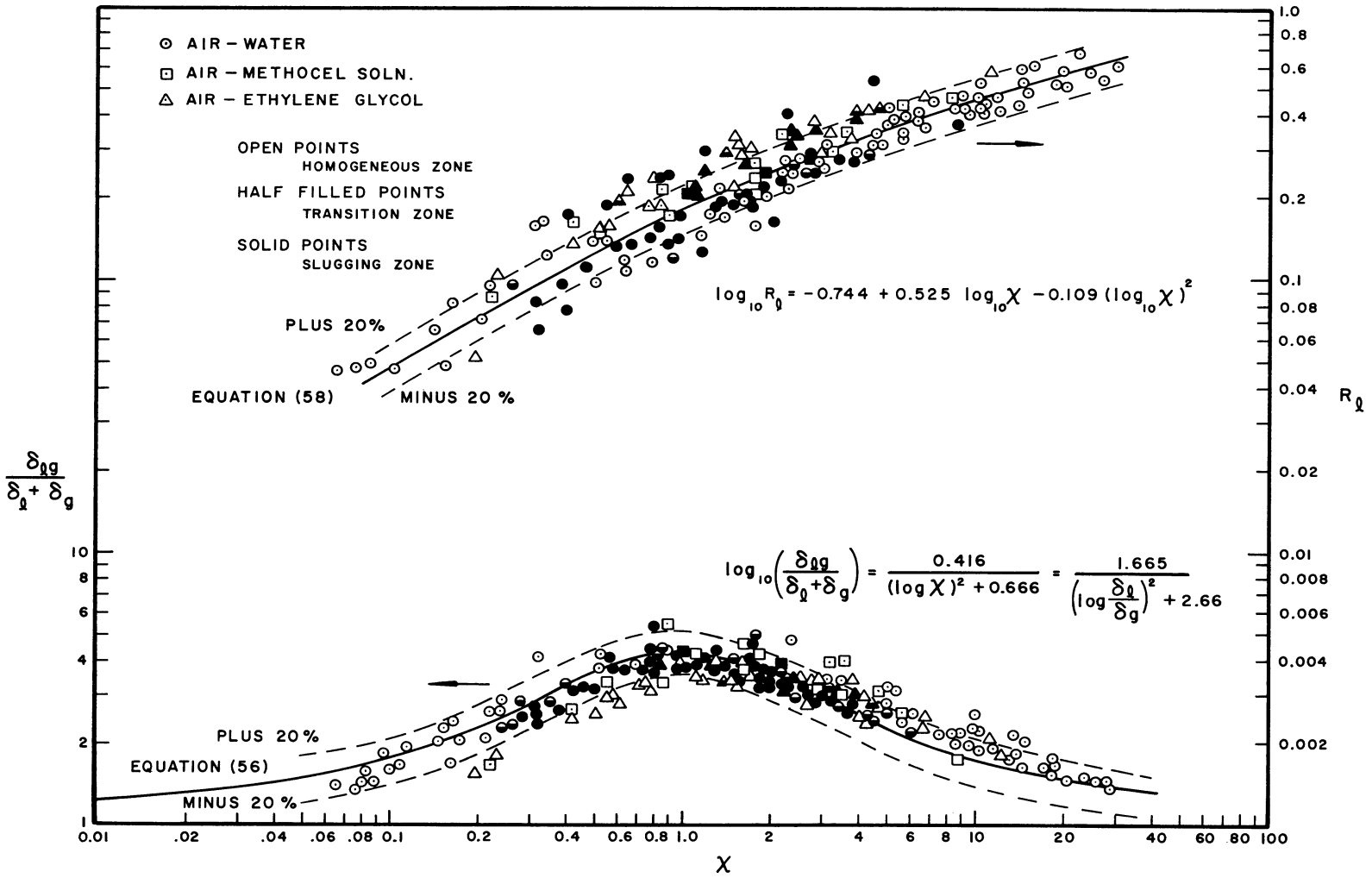

Figure 13. Summary of Two-Phase Pressure Drop on a Symmetrical Basis

exception of the foaming solutions of soap and Methocel. All liquid saturation data is replotted in Figure 13. The data indicate a single relationship for $\frac{\delta_{\ell g}}{\delta_\ell + \delta_g}$ on all packings and for all liquid properties within the range investigated. The correlation reduces to the single-phase case as χ approaches zero or infinity. As a result of the symmetry in Figure 13, the relation between $\frac{\delta_{\ell g}}{\delta_\ell + \delta_g}$ and χ can be fitted by the following equation:

$$\log_{10}\left(\frac{\delta_{\ell g}}{\delta_\ell + \delta_g}\right) = \frac{0.416}{(\log_{10}\chi)^2 + 0.666} . \qquad (56)$$

An expression can be obtained for φ_g from Equation (56) by substitution into and rearrangement of Equation (46) as follows:

$$\log_{10}\varphi_g = 0.5 \log_{10}(1 + \chi^2) + \frac{0.208}{(\log_{10}\chi)^2 + 0.666} . \qquad (57)$$

The reference to Equation (57) in Figures 10, 11, and 12, serves to indicate that all of the curves are the same and are drawn from the above equation. Equation (56) was used to draw the curve shown in Figure 13. The liquid saturation data has also been fitted by an algebraic expression as follows:

$$\log_{10}R_\ell = -0.744 + 0.525(\log_{10}\chi) - 0.109(\log_{10}\chi)^2$$

$$= \log_{10}(1 - R_g) \qquad (58)$$

The above equation is used as a reference in Figures 10 through 13, to indicate that all of the liquid saturation curves are identical and were obtained from Equation (58). No φ_ℓ plots have been presented, since they would be completely dependent upon those which have been presented.

E. Scope and Accuracy of Correlation

1. Comparison of the Three Column Sections

Each experimental run has resulted in three data points, one for the top section of the test column, one for the middle section, and one for the bottom section. Thus, there are some 300 runs and some 900 data points. Not all of the data points have been plotted in the figures described in the previous section because of the confusion of points that would result. Only points obtained from the middle section of the test column have been used in the construction of the figures. All of the variables are constant for a given run, with the exception of the pressure drop and the average pressure, which is used in the calculation of air density. Hence, the three points from a given run should be very close together, but should not be identical. The liquid saturation measurement is an average value for the entire column, and is used in the calculation of all three points from any given run. In certain experimental ranges the liquid saturation may be a large factor in the total energy expression, and the data points from the middle of the column may be expected to have a slightly higher reliability since the average liquid saturation is most valid near the center of the column. Any entrance or exit effects are also eliminated by considering data from the middle section. In every case, the three sections of the column were compared as a check on the validity of the middle section. A typical pattern for three points is shown on an enlarged scale in Figure 14 for run number 46.

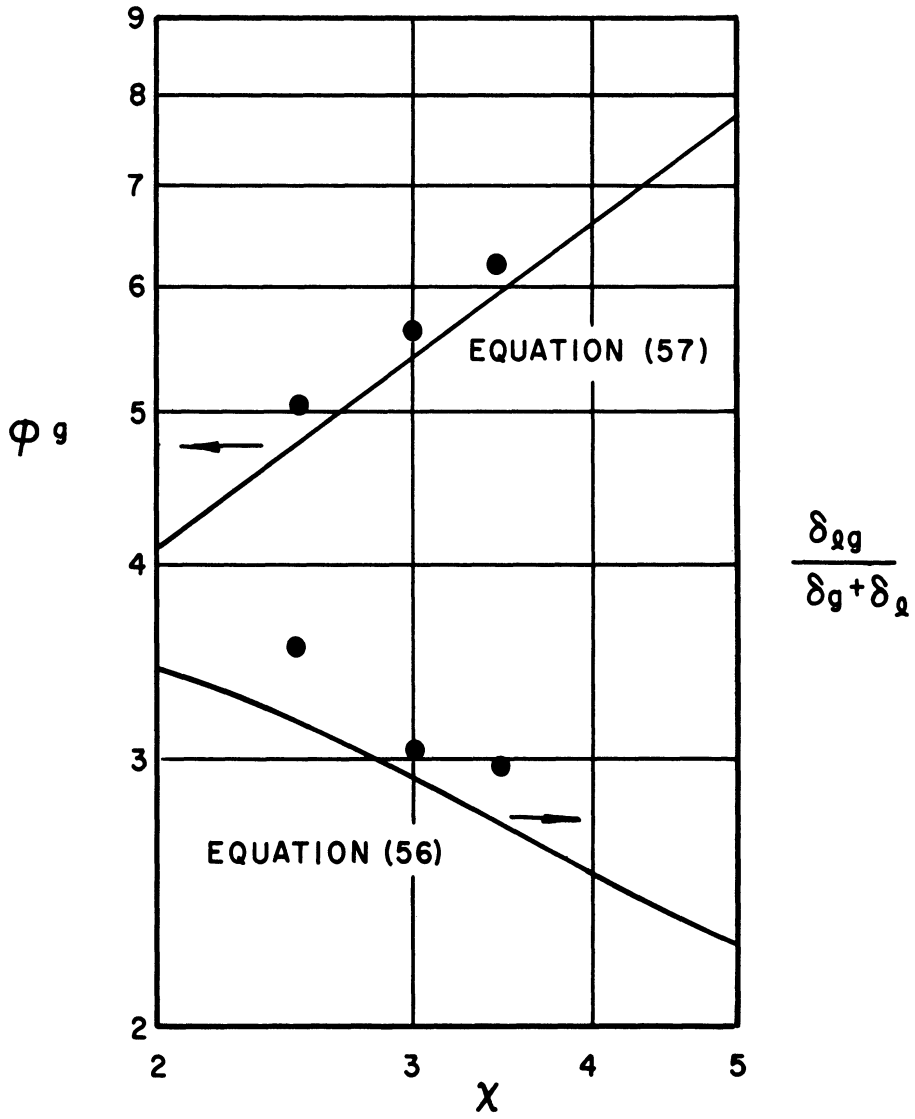

Figure 14. Data from Run 46 Showing Agreement Between the Three Column Sections

2. Range of Experimental Variables

The form of the correlation is such that the range of the pressure drops, Reynolds numbers, etc., cannot be determined by looking at the correlating plots. The curve shown in Figure 13 may be traversed from right to left while holding the rate of either phase constant at any desired value. The parameter X expresses the ratio of energy losses for the liquid and gas phases, but says nothing about their absolute values. The same remark applies to the parameter $\frac{\delta_{lg}}{\delta_l + \delta_g}$. It is necessary, therefore, to determine the level of the Reynolds number, pressure drops, etc., for a given point from the tabulated results. Table VII summarizes the maximum and minimum values of the various parameters which appear in the tabulated data and results.

3. Scatter of the Experimental Data

The number of points plotted in Figure 13 is so large and the curve was traversed from right to left with experimental points so often that a significant portion of the points fall upon one another within one or two per cent of the line defined by Equation (56). The scatter of data in Figure 13 is such that 87 per cent of the data are within plus or minus 20 per cent of the predicted value. The remaining 13 per cent fall well within plus or minus 40 per cent of the values predicted by Equation (56). The standard deviation is 13.2, and is the expected or mean value of the absolute deviation. The errors in $\frac{\delta_{lg}}{\delta_l + \delta_g}$ are those which would result in the design calculation or in the back calculation of the observed pressure drops. When the data is plotted on the basis of φ_g, the scatter is reduced as a result of the square root used in its definition. Since the deviations are small, approximately

TABLE VII

RANGE OF EXPERIMENTAL VARIABLES

Variable	Minimum	Maximum
Column Size, inches	4	4
Packing Diameter, inches	1/8	3/8
Packing Porosity	0.357	0.520
Packing Sphericity	0.53	1.00
Volume Rate of Air, SCFM	1.0	138
Volume Rate of Liquid, gpm	0.715	33.75
Viscosity of Air	0.018	0.019
Viscosity of Liquid, cp	0.75	19.0
Reynolds No. for Air	0.00	6200
Reynolds No. for Liquid	0.00	3405
Pressure Drop, psi/ft	0.004	13.8
Top Column Pressure, psig	2.8	84.0
Fraction Liquid	0.0	1.0

the same 87 per cent of the data falls within plus or minus 10 per cent of the values predicted by Equation (57). The standard deviation is reduced by the same ratio to approximately 6.6 per cent.

The accuracy of the liquid saturation data is not as good as that of the pressure drop data. The curve which has been fitted to the data has been placed so that the scatter is between plus 55 per cent and minus 30 per cent of Equation (58). This arrangement results in maximum errors of 43 per cent from the observed data points. The method used in drawing the curve reflects about an equal confidence in the data points and in the form of the correlation. Examination of the data reveal some upward shift of the liquid saturation points with viscosity, and with a decrease in the packing size. These errors may result from variables of viscosity and packing dimension which have not been included in the correlation, or from the experimental measurements due to the greater difficulty with which air bubbles rise through the packing material in the case of higher viscosities or smaller packings.

F. Analytic Summary of the Final Correlation

Computer applications in chemical engineering design are becoming more common each day. The main obstacle to the use of much of the information in the engineering literature lies in the necessity for fitting equations to the many graphical relationships that are in current use. The symmetric shape of Figure 13 lends itself to the simple algebraic form of Equation (56). The form of the equation is entirely symmetric and reversing the roles of liquid and gases in the definition of X has no effect. This means that the definition of one phase as the gas phase, and another as the liquid phase, is arbitrary.

The liquid saturation data was expressed by a power series in $(\log_{10} X)$ as presented in Equation (58). The expression for liquid saturation is not symmetric; the roles of liquid and gas cannot be interchanged.

A summary of the relationships for two-phase flow in packed beds is given in Table VIII, and a summary of the algebraic equations is given in Table IX. Tabulated values of the algebraic equations are given in Table X at selected values of X. The computation of a pressure drop for a design problem requires the calculation of the total friction energy followed by the use of Equation (49) with the liquid saturation correlation. An assumption of the average pressure will be necessary as in the single-phase calculation for a flowing gas as a result of the dependence of density upon pressure.

G. Saturation Data as a Check on Derivation

Equation (37) of the derivation states that φ_ℓ should be a definite function of the liquid saturation. The only use made of the liquid saturation in the development of the pressure drop correlation was in the calculation of ρ_m for use in Equation (49). In a major portion of the experimental runs, the quantity ρ_m was small compared to the pressure drop observed, and may be considered a correction term. The correlation developed for pressure drop, or for total friction energy, is essentially independent of the measurements of the liquid saturation. Figure 15 is a plot of φ_ℓ versus R_ℓ showing points for water on 3/8-inch Raschig Rings as well as a curve defined by the correlating Equations (57) and (58) which are parametric in X.

TABLE VIII

SUMMARY OF TWO-PHASE RELATIONSHIPS

$$\delta = -\frac{dP}{dL} + \rho$$

$$\chi = \sqrt{\frac{\delta_\ell}{\delta_g}}$$

$$\varphi_g = \sqrt{\frac{\delta_{\ell g}}{\delta_g}} = \varphi_\ell$$

$$\varphi_\ell = \sqrt{\frac{\delta_{\ell g}}{\delta_\ell}} = \frac{\varphi_g}{\chi}$$

$$\frac{\delta_{\ell g}}{\delta_\ell + \delta_g} = \frac{\varphi_g^2}{1 + \chi^2} = \frac{\chi^2 \varphi_\ell^2}{1 + \chi^2}$$

TABLE IX

SUMMARY OF EQUATIONS REPRESENTING CORRELATION

$$\log_{10}\left(\frac{\delta_{\ell g}}{\delta_\ell + \delta_g}\right) = \frac{0.416}{(\log_{10}\chi)^2 + 0.666}$$

$$\log_{10}\varphi_g = \frac{1}{2}\log_{10}(1 + \chi^2) + \frac{0.416}{(\log_{10}\chi)^2 + 0.666}$$

$$\log_{10}\varphi_\ell = \frac{1}{2}\log_{10}\left(\frac{1 + \chi^2}{\chi^2}\right) + \frac{0.416}{(\log_{10}\chi)^2 + 0.666}$$

$$\log_{10}R_\ell = -0.744 + 0.525\log_{10} - 0.109(\log_{10}\chi)^2$$

TABLE X

CORRELATION PARAMETERS AT SELECTED VALUES OF X

X	φ_g	φ_ℓ	$\frac{\delta_{\ell g}}{\delta_\ell+\delta_g}$	R_ℓ	R_g
0.01	1.11	111	1.23		
0.02	1.14	57.2	1.31		
0.04	1.20	30.0	1.44		
0.07	1.27	18.2	1.62		
0.10	1.34	13.4	1.78	0.048	0.952
0.20	1.54	7.70	2.29	0.069	0.931
0.40	1.92	4.81	3.20	0.107	0.893
0.70	2.44	3.48	4.01	0.149	0.851
1.00	2.90	2.90	4.22	0.180	0.820
2.00	4.21	2.10	3.55	0.264	0.736
4.00	6.67	1.64	2.54	0.339	0.661
7.00	10.0	1.43	2.00	0.420	0.580
10.0	13.4	1.34	1.78	0.470	0.530
20.0	24.6	1.23	1.50	0.568	0.432
40.0	46.5	1.16	1.35		
70.0	78.5	1.12	1.27		
100.0	111	1.11	1.23		

Figure 15 indicates a definite correlation between φ_ℓ and R_ℓ as expected from the derivation. The scatter of data is greatest in the region of low liquid saturation where the measurements of saturation are subject to the greatest percentage deviation. A plot of φ_g versus R_g would necessarily show a similar result and confirm Equation (38), since R_g is a function of R_ℓ, and φ_g is a function of φ_ℓ.

H. Effect of Foaming on Pressure Drop

The systems studied in this investigation were non-foaming with the exception of the points indicated in Figure 12. A foam breaker was used to eliminate the foaming of the Methocel solution used with 3/8-inch Raschig Rings. Runs 294 through 307 were taken under conditions of severe foaming in 1/8-inch cylinders. The values observed for the two-phase pressure drop ranged from 1.55 to 5.35 times the values predicted by the non-foaming correlation. The packing served as an excellent agitator which effectively emulsified the air and liquids observed. The resulting emulsion was stable over a period of several minutes, and contained as much as 60 per cent air by volume. The following general statements may be made concerning the data observed:

1. Foaming produces much greater effects in small particle diameter beds. The mild foaming of Methocel solution in 3/8-inch Raschig Rings had a negligible effect.
2. The emulsification of air in the liquid phase is more severe in smaller packings.
3. The effect of foaming on pressure drop becomes smaller as the rate is increased and the pressure

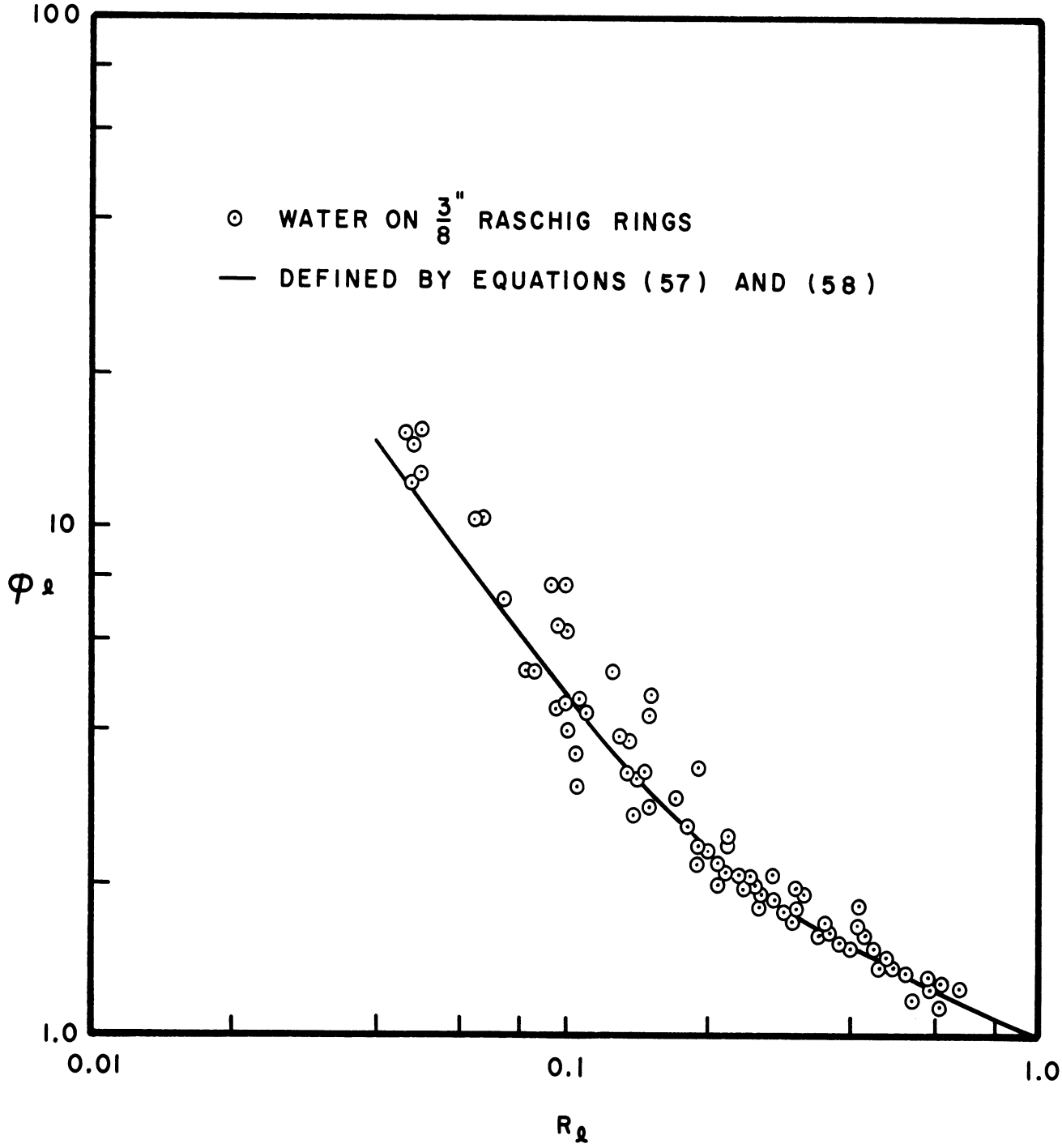

Figure 15. Relation Between φ_ℓ and R_ℓ as Shown by Data for Raschig Rings and by a Curve for the Correlating Equations

drop rises to higher levels. The foaming forces eventually become smaller than the friction forces. The level of pressure drop at which foaming may be neglected varies with the liquid phase and packing diameter.

4. In order to correlate the behavior of foaming mixtures, some correlation must be developed for the amount of foaming as a function of the shearing and mixing of the liquid and gas phases.
5. The addition of a foam breaker reduces the effect of foaming on pressure drop even though some emulsification may still occur.

A correction of the parameters by consideration of the amount of emulsification was attempted with little success. The emulsification of air in the liquid clearly expands the liquid phase and decreases its density. The value of δ_l is inversely proportional to the effective liquid density. For the data observed, the decrease in δ_g caused by the loss of air to the liquid phase is negligible. Further, the increase in mass rate for the liquid phase is negligible. Hence, φ_g is unchanged, and the change in X is inversely proportional to the square root of the change in density or in the volume fraction liquid in the emulsion. Table XI lists the volume fractions of liquid at atmospheric pressure, the corrected values for the column conditions, and the corrected values of X. The change in the values of X is small, and reference to Figure 12, where the original points are plotted, will make it evident that the correction is negligible.

TABLE XI

CORRECTION OF RUNS 301 - 307 FOR EMULSION DENSITY

Run	Volume Fraction Liquid in Emulsion at 14.7 psia	Column Pressure psia	Volume Fraction Liquid in Emulsion at Column Pressure	Calculated Parameters φ_y	Calculated Parameters X	Corrected Parameters φ_y	Corrected Parameters X
301	0.375	26.4	0.518	6.29	0.869	6.29	1.22
302	0.567	37.4	0.768	6.24	1.54	6.24	1.76
303	0.467	51.5	0.753	2.71	0.546	2.71	0.628
304	0.467	56.0	0.768	7.92	3.19	7.92	3.64
305	0.567	64.1	0.850	4.64	1.65	4.64	1.79
306	0.500	52.0	0.780	4.05	1.15	4.05	1.31
307	0.480	45.5	0.740	7.13	2.19	7.13	2.54

I. Comparison with Correlation for Open Channels

Comparison of the correlation for packed beds with the correlation presented by Lockhart and Martinelli[24] reveals a remarkable agreement with the curve obtained for the viscous-viscous mode in open pipes. The agreement between the liquid saturation curves for packed beds and open pipes is also remarkable. These comparisons are made in Figure 16, which shows the four mechanisms in open pipes along with that of packed beds.

The fact that the data of packed beds falls on only one line is probably due to the excellent mixing and distribution obtained in the vertical packed column. This mixing may also account for the significantly smaller scatter in the data for packed beds. The agreement between the liquid saturation for pipes and packed beds may actually be closer than drawn, since Lockhart and Martinelli[24] report that their saturation measurements are probably high.

The close agreement between the correlations for packed beds and open pipes suggest several important conclusions. The data on open pipes were taken for horizontal flow, and the expected applicability of the packed correlation to the horizontal flow problem is somewhat strengthened. Further, a uniform transition appears possible for increasing porosities reaching to 100 per cent, since the packed bed curve falls within the curves for the four mechanisms in open pipes. The assumptions made in the derivations of the correlation parameters were the same for open pipes and packed beds, which further confirms the theoretical derivation. The completely reduced form of the correlations entirely accounts for the properties of the bed or open pipe by the use of the single-phase pressure drops.

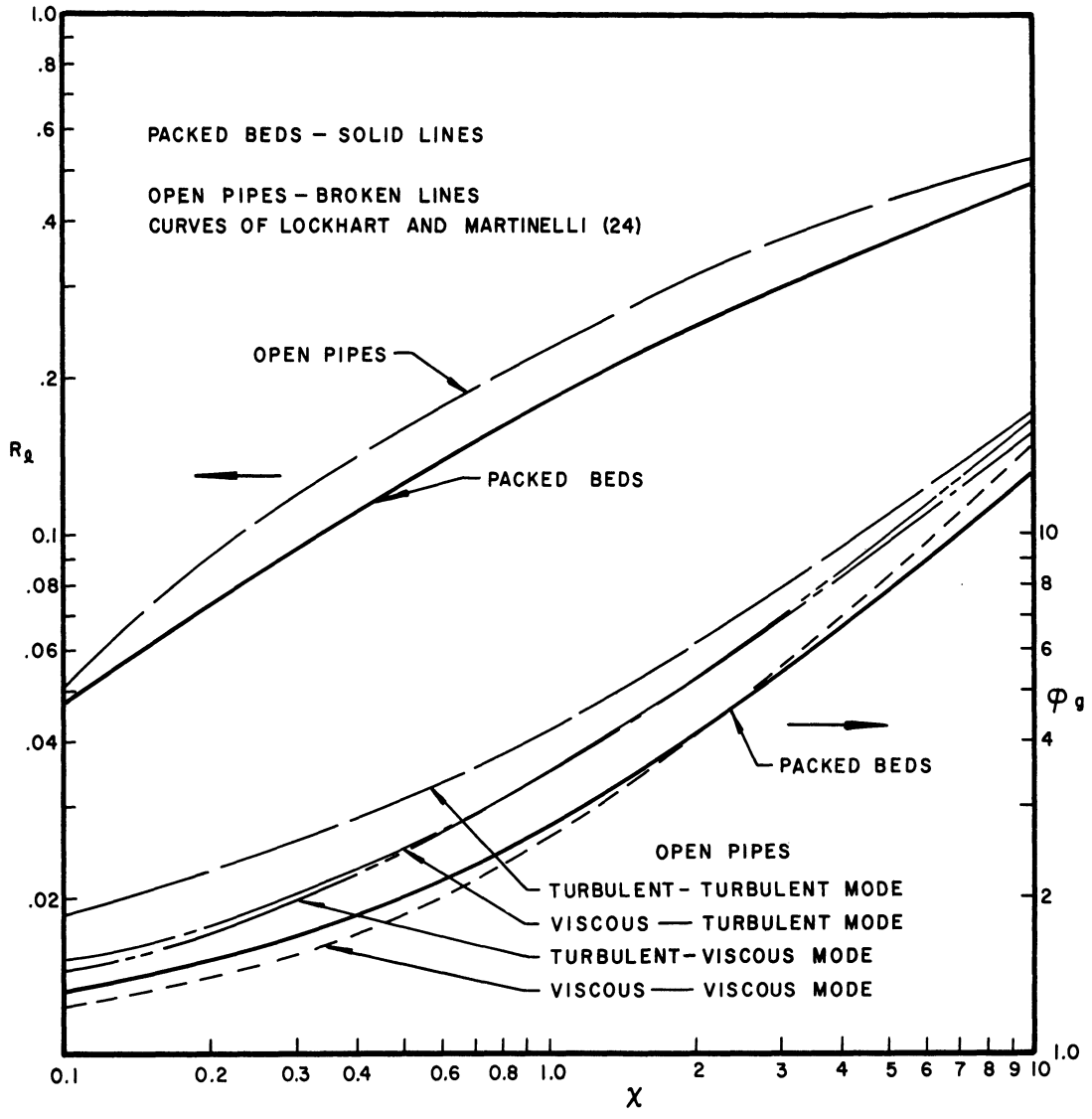

Figure 16. Comparison of Two-Phase Flow Correlations for Pipes and for Packed Beds

J. Application to Other Multiphase Problems

The extension of the pressure drop correlation to the cocurrent flow of liquid and gas in the vertical or horizontal direction is justified in the light of statements by Martinelli, Putnam, and Lockhart[27] and Bergelin[3] who report that the orientation of the tube has a negligible effect on pressure drop at high rates. This result was to be expected since the density correction required to obtain total frictional energy loss becomes small as the pressure drop increases for all orientations. The use of the proper density correction as determined from the energy balance equation would make the correlation valid at low rates for any orientation. The saturation correlation might be expected to be a function of orientation for low rates; but since the correlation is independent of rate for downflow and correct for high rates, only small changes can occur for other orientations with true cocurrent flow.

The correlation is not expected to hold for the flow of two immiscible liquid phases. The compressibility of the gas phase is thought to be the main cause of the larger gas-liquid pressure drops, and the interaction between two immiscible liquids is expected to have a much smaller effect on pressure drop. The flow of two immiscible liquid phases might be approximated by a trial and error calculation based on parallel flow in a partitioned bed. The cross sectional area of the bed may be divided between the liquids with an imaginary partition running the length of the bed. The single-phase pressure drop can be calculated for each liquid after the division of cross sectional area has been been assumed. When the division of area is properly chosen, the pressure drops will be equal to each other, and will be an approximation to the two-phase drop for the immiscible liquids.

The flow of two immiscible liquid phases and a gas phase might be approximated by the use of the correlations for two-phase gas-liquid flow. The speculative method described above may be used to compute the pressure drop for the two liquid phases alone in the bed. Using the combined liquid drop to represent a combined liquid phase, the value of χ can be calculated as the ratio of combined liquid to gas, and the three-phase pressure drop can be estimated from the correlation. The assumption upon which the approximation is based is that the effect of the gas is the same on each of the liquid phases, which is indicated by the dimensionless and symmetrical form of the final correlation, and that the interaction of the liquid phases is negligible.

VI. SUPPORTING DATA ON HYDROCARBON SYSTEMS

A. Agreement of Non-Foaming Systems

Through the courtesy of the Humble Oil and Refining Company, considerable data obtained in their laboratories on two-phase flow in packed beds for hydrocarbon systems have been made available for the further support of this dissertation. Figure 17 presents the data for the non-foaming systems of lube oil with natural gas and lube oil with carbon dioxide on 3 mm glass beads.

The points shown in the figure have been corrected for the density of the flowing mixture on the basis of the liquid saturation Equation (58) since no saturation data were obtained for these runs. The properties of the fluids and packings used are reported in Appendix V along with the tabulated data and the calculated results for the hydrocarbon experiments. The values of the single-phase pressure drops are not reported in the calculated results. The correction of the observed pressure drops, according to Equation (49), requires the calculation of ρ_m from the liquid saturation correlation using χ which is unaffected by the correction. The squaring of the reported value of φ_g permits the computation of δ_g. Having obtained the unknown δ_g, ρ_m can be added to the reported two-phase pressure drop, and the corrected value of φ_g can be computed. Table XII presents both the original and the corrected values for the non-foaming systems with lube oil.

The data points plotted in Figure 17 fall approximately 17 per cent higher than the curve representing Equation (57). The configuration of the data points confirms the shape of the curve, but the points do not seem to converge to the line $\varphi_g = \chi$ at high values of χ.

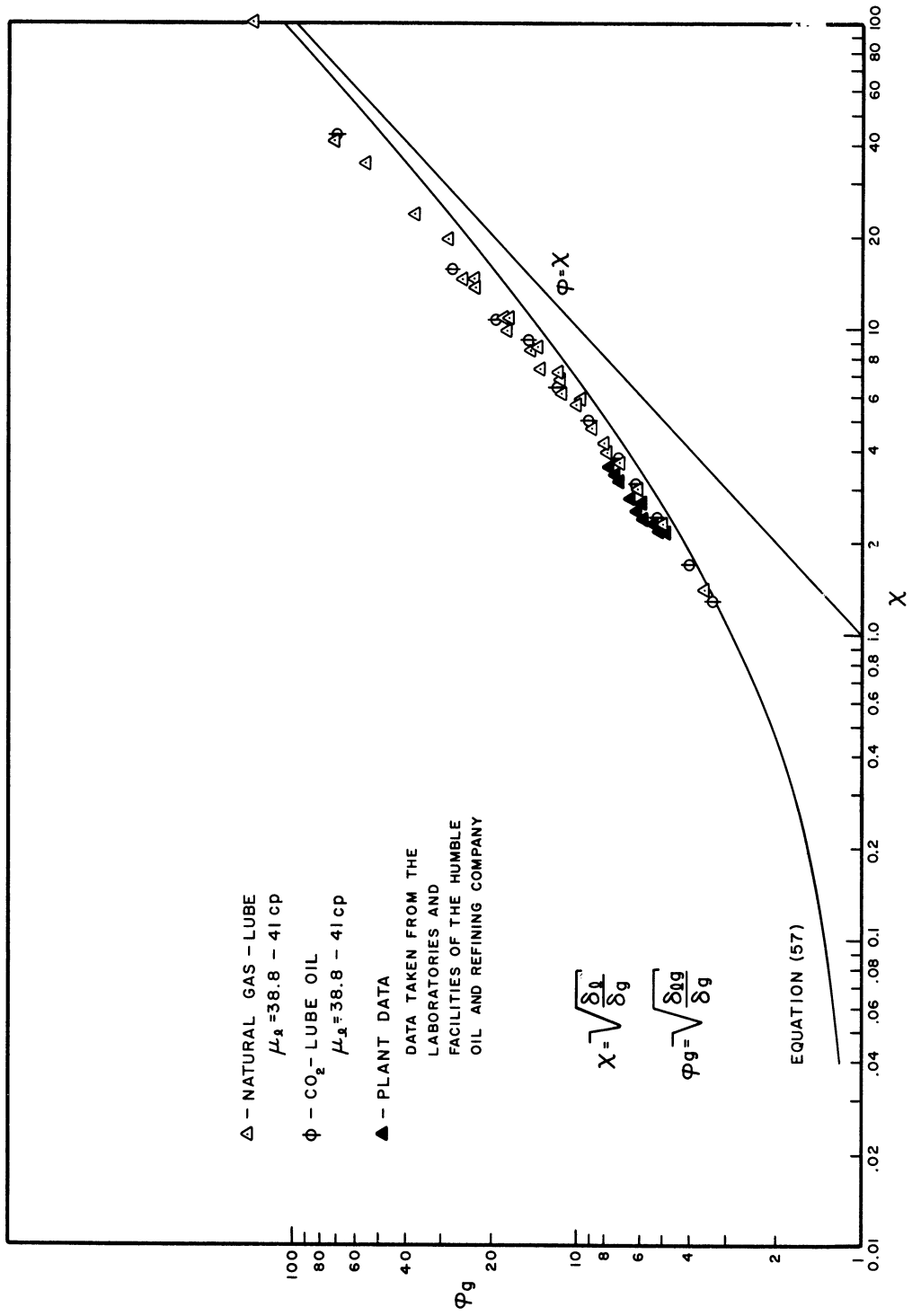

Figure 17. Two-Phase Cocurrent Pressure Drop for Hydrocarbon Systems on 3 mm Glass Beads

TABLE XII

CORRECTION OF HYDROCARBON DATA FOR THE DENSITY OF THE FLOWING MIXTURE AS ESTIMATED BY SATURATION CORRELATION

Two-Phase Pressure Drop psi/ft.	Estimated ρ_m psi/ft.	χ	Reported φ_g	Corrected φ_g
Run No. 15				
0.311	0.260	41.23	53.12	72.00
0.383	0.194	14.44	20.64	25.30
0.431	0.171	9.88	14.98	17.70
0.467	0.157	7.40	11.68	13.50
0.491	0.145	6.07	9.82	11.20
0.539	0.134	4.72	8.00	8.93
0.599	0.123	3.63	6.49	7.12
0.670	0.115	3.00	5.68	6.15
0.790	0.107	2.29	4.69	5.00
1.155	0.080	1.39	3.45	3.57
Run No. 16				
1.532	0.298	99.76	127.37	139.00
2.119	0.242	34.88	52.37	55.41
2.119	0.227	23.72	35.63	37.59
2.179	0.216	19.58	26.77	28.13
2.131	0.197	14.56	21.92	23.03
2.226	0.197	14.60	22.46	23.41
2.167	0.179	10.79	16.39	17.05
2.310	0.178	10.82	16.96	17.65
2.274	0.164	8.65	13.46	13.93
2.412	0.164	8.68	13.90	14.40
2.346	0.156	7.14	11.28	11.65
2.454	0.156	7.15	11.55	11.90
2.490	0.145	5.82	9.47	9.73
2.597	0.145	5.83	9.70	9.95
2.777	0.126	3.91	6.73	6.90
2.861	0.126	3.92	6.84	6.98
Run No. 17				
0.302	0.261	40.41	51.26	70.02
0.383	0.205	15.65	22.39	27.79
0.431	0.178	10.69	16.24	19.32
0.455	0.160	7.71	12.02	13.95
0.491	0.149	6.43	10.42	11.94
0.551	0.134	4.68	8.03	8.95
0.613	0.122	3.69	6.69	7.32
0.682	0.114	3.02	5.77	6.23
0.766	0.104	2.43	4.91	5.22
0.982	0.090	1.70	3.89	4.06
1.209	0.820	1.29	3.27	3.38

The region of high χ is the region of approach to 100 per cent liquid, and the failure of ϕ_g to approach χ in magnitude casts some doubt upon the calculation of the single-phase pressure drops for the liquid phase, and perhaps for the gas phase. An error of 37 per cent in the single-phase correlation would account for the separation between the data points and the correlation. The single-phase pressure drops were calculated from Equation (11) with no adjustments to the constants. Some check runs were obtained for the 1/8-inch catalyst cylinders at low gas rates, but the single-phase correlation was not checked for the liquid phase alone as a result of the design of the equipment. The deviation at high χ values implies a necessary correction to the constants of Equation (11) for 3 mm glass spheres of approximately 35 per cent.

Since some adjustment is necessary to make the hydrocarbon data self-consistent for high χ, and since the spread between the data points and the correlation is essentially constant, the data on hydrocarbon systems is considered to support the correlation. The range of viscosities investigated now reaches to a maximum of 41 centipoise.

B. Agreement of Plant Data

A few data points from operating plant equipment are included in Figure 17. Table XIII presents the original and corrected values of the correlation parameters for the plant data. Corrections to the reported values were made by the method of the previous section.

The plant data agree with the other points reported for nonfoaming hydrocarbon systems, and are subject to the same errors through the calculation of the single-phase pressure drops. An error of 35 per cent in the single-phase prediction is within the error for the

TABLE XIII

CORRECTION OF PLANT DATA FOR THE DENSITY OF THE FLOWING MIXTURE AS ESTIMATED BY SATURATION CORRELATION

Two-Phase Pressure Drop psi/ft.	Estimated ρ_m psi/ft.	X	Reported φ_g	Corrected φ_g
0.215	0.091	2.66	5.01	6.00
0.240	0.086	2.36	4.66	5.43
0.218	0.085	2.33	4.28	5.05
0.324	0.088	2.52	5.46	6.15
0.507	0.091	2.69	5.87	6.37
0.575	0.101	3.34	6.82	7.40
0.216	0.084	2.32	4.46	5.26
0.335	0.090	2.62	5.69	6.40
0.515	0.102	3.47	7.11	7.79
0.238	0.085	2.29	4.63	5.40
0.300	0.099	3.28	6.46	7.48
0.462	0.098	3.21	6.58	7.25
0.238	0.090	2.61	5.43	6.40
0.275	0.088	2.45	5.24	6.02
0.216	0.085	2.25	4.45	5.25

uncorrected correlation, and the plant data are considered to check the two-phase correlation.

C. Observations of Foaming and Surging

In addition to the data presented in Figure 17 for non-foaming hydrocarbon systems, a large number of points have been reported for the foaming system of kerosene and natural gas. This data forms the major portion of the tabulation in Appendix V, and is plotted in Figure 18.

The points shown in Figure 18 have not been corrected for the density of the flowing mixture, and hence, φ_g is based on the observed pressure drop per unit length. The correction of the points would cause all of the points to lie above the viscous-viscous line shown in Figure 18 from the open pipe correlation. These data further illustrate the deviations and scatter which occur in the foaming systems. The non-foaming data is also included in Figure 18 in the uncorrected form, and shows excellent agreement with the viscous-viscous curve for pipes.

A new form of instability was observed in the test section when foaming occurred at low values of the two-phase pressure drop. Pressure surges as high as plus and minus 40 per cent of the average value of the pressure drop are reported in the case of kerosene and natural gas. These surges were found to have a reproducible magnitude and frequency. The time between peaks was of the order of magnitude of five or ten seconds, and varied with the flow rates. The observation of pressure surges were accompanied by a filling and emptying of the column with foam. The column appeared to fill with foam as the pressure drop was observed to increase. The foam then seemed to collapse and be swept from the column in a wave-like motion with a corresponding decrease

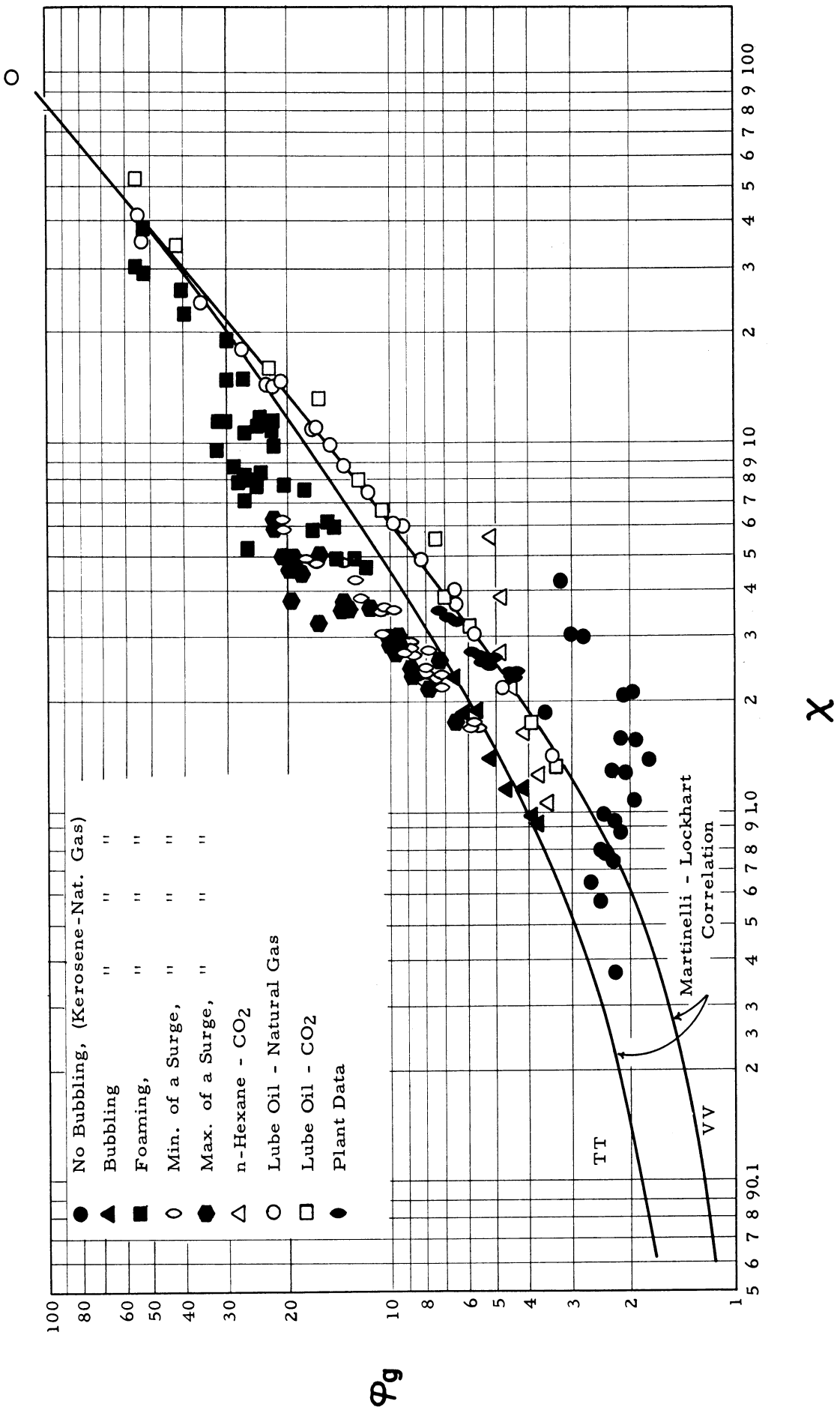

Figure 18. Data on Foaming Hydrocarbon Systems

in pressure drop. The surging phenomena were observed in fairly narrow ranges of the experimental variables and disappeared at low liquid rates as well as at high liquid rates.

The points in Figure 18 have been coded for the surging runs to indicate the maximum and minimum values observed. Figure 19 shows one of the surging regions observed with kerosene and natural gas, and it illustrates the range of rates and the magnitude of the pressure drop over which the surging region is defined.

The form of instability observed in the foaming kerosene systems was also observed in Run 294 of Appendix III and Appendix IV. The instability appeared in tests with 0.50 per cent solution of foaming Methocel on 1/8-inch cylinders. The phenomena was found to occur near the lower limit of rates which could be measured in the experimental equipment. The surges were apparent with fresh Methocel solutions, but disappeared as the solutions aged. The surges which have been described are felt to be a definite function of the foaming system employed, and probably represents a balance between the rate of emulsification and the pressure difference acting upon the foam. As the foam begins to build up, the rates are at their highest values and effect the maximum shear. The foam filling the pores causes the pressure drop to increase across the bed when constant feed rates to the column are maintained. At some point, the restriction of flow and the forces on the foam combine to reduce the foaming tendency and force the foam to break. The cycle is then able to repeat itself as the pressure drop decreases and the flow is unrestricted.

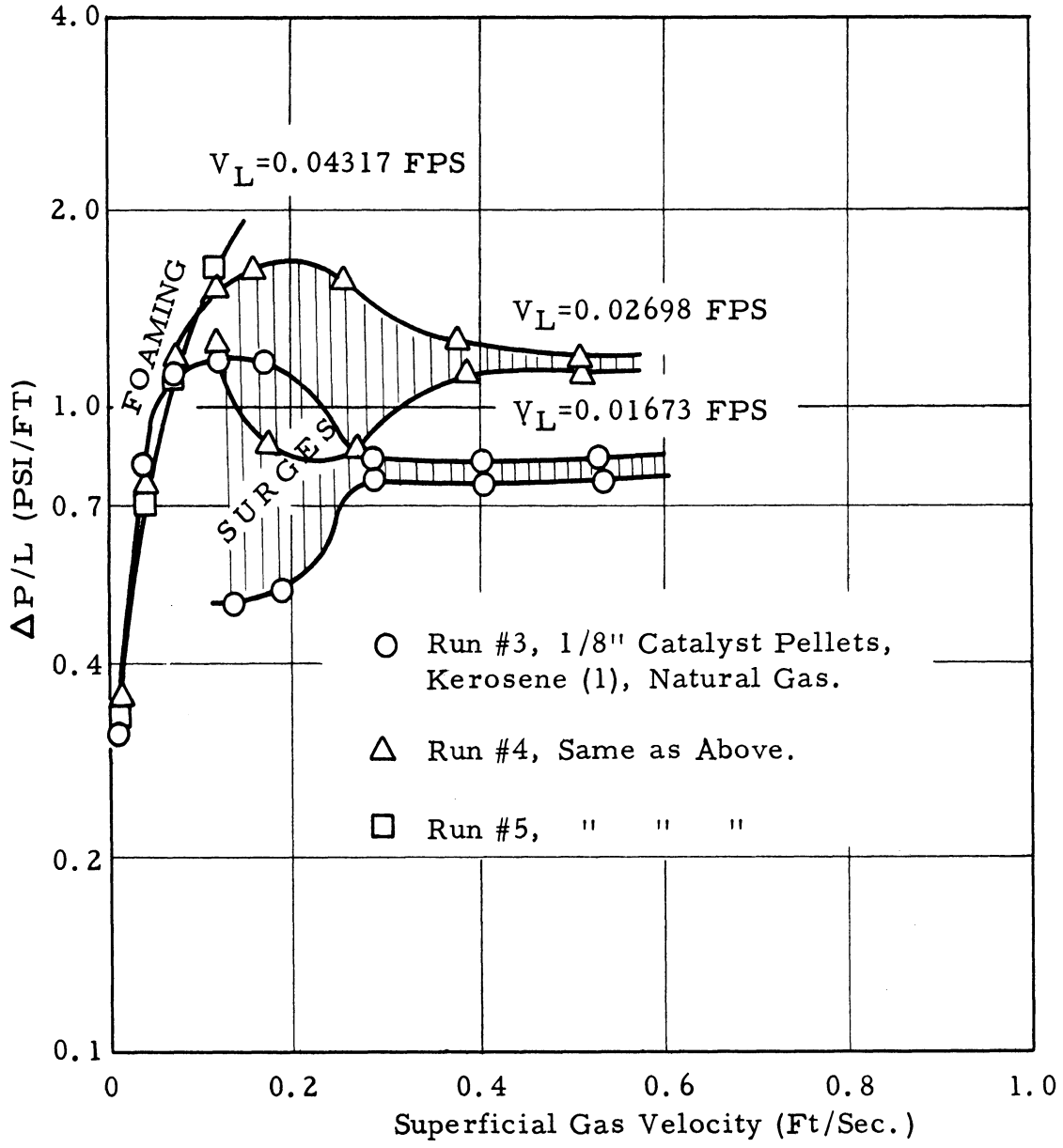

Figure 19. A Foaming Hydrocarbon System in the Unstable Region

VII. SOLUTION OF SAMPLE PROBLEM

The application of the correlations which have been presented for two-phase downward flow in packed beds is illustrated in this section by the solution of an example problem.

Predict the pressure drop and liquid saturation for the flow of air and water through a vertical packed section filled with 1/8-inch cylinders under the following conditions:

Water rate.....	4300	lb/(hr)(sq ft)
Air rate.....	328.0	lb/(hr)(sq ft)
Temperature.....	60.0	°F
Inlet pressure...	30.0	psig
Length of bed....	10.0	ft.

The properties of the packing and fluids are as follows:

Viscosity of water at 60°F.....	2.72	lb mass/(ft)(hr)
Viscosity of air at 60°F.....	0.0455	lb mass/(ft)(hr)
Density of water at 60°F.....	62.4	lb/cu ft
Density of air at 60°F, 30 psig...	0.233	lb/cu ft
Porosity of packed bed.....	0.357	
Length and diameter of particles...	0.0104	ft.

The single-phase pressure drop for horizontal flow over 1/8 x 1/8-inch cylinders is correlated by

$$-\left(\frac{\Delta P}{\Delta L}\right) = \delta = \frac{Re(150 + 1.75Re)}{\frac{g_c \rho D_p^3}{2}\left(\frac{\epsilon}{1-\epsilon}\right)^3}$$

where

$$Re = \frac{GD_p}{\mu(1-\epsilon)} .$$

The Reynolds number for air alone in the bed is

$$Re_g = \frac{G_g D_p}{\mu_g (1 - \epsilon)} = \frac{(328.0)(0.0104)}{(0.0455)(1 - 0.357)} = 116.5 .$$

The Reynolds number for liquid alone in the bed is

$$Re_\ell = \frac{G_\ell D_p}{\mu_\ell (1 - \epsilon)} = \frac{(4300)(0.0104)}{(2.72)(1 - 0.357)} = 25.55 .$$

The calculation of the single-phase friction loss for the gas requires a knowledge of the average pressure in the packed section. Therefore, the pressure drop across the bed is assumed as follows:

Assumed pressure drop = 3.0 psi

Inlet pressure = 30.0 psig

Outlet pressure = 27.0 psig

Average pressure = 28.5 psig.

The density of air at the average pressure in the bed is

$$\rho_g = \frac{0.233(28.5 + 14.7)}{(30.0 + 14.7)} = 0.225 \text{ lb/cu ft.}$$

The frictional loss for the air flowing alone is

$$\delta_g = \frac{Re_g(150 + 1.75Re_g)}{\frac{g_c \rho_g D_p^3}{\mu_g^2} \left(\frac{\epsilon}{1 - \epsilon}\right)^3}$$

$$= \frac{116.5(150 + 1.75 \times 116.5)}{\frac{(32.17)(3600)^2(0.2065)(0.0104)^3}{(0.0455)^2} \left(\frac{0.357}{1 - 0.357}\right)^3}$$

$$= 4.05 \text{ lb/sq ft/ft} = 0.0281 \text{ psi/ft.}$$

The frictional loss for the liquid flowing alone is

$$\delta_\ell = \frac{Re_\ell(150 + 1.75Re_\ell)}{\frac{g_c \rho_\ell D_p^3}{\mu_\ell^2}\left(\frac{\epsilon}{1-\epsilon}\right)^3}$$

$$= \frac{25.55(150 + 1.75 \times 25.55)}{\frac{(32.17)(3600)^2(62.4)(0.0104)^3}{(2.72)^2}\left(\frac{0.357}{1-0.357}\right)^3}$$

$$= 7.33 \text{ lb/sq ft/ft} = 0.0509 \text{ psi/ft.}$$

Calculate the correlation parameter defined by Equation (39).

$$\chi = \sqrt{\frac{\delta_\ell}{\delta_g}} = \sqrt{\frac{0.0509}{0.0281}} = 1.35$$

The correlation parameter $\frac{\delta_\ell}{\delta_\ell + \delta_g}$ is obtained from Equation (56).

$$\log_{10}\left(\frac{\delta_{\ell g}}{\delta_\ell + \delta_g}\right) = \frac{0.416}{(\log_{10}\chi)^2 + 0.666} = \frac{0.416}{(\log_{10}1.35)^2 + 0.666}$$

$$= 0.610$$

and

$$\frac{\delta_{\ell g}}{\delta_\ell + \delta_g} = \frac{\delta_{\ell g}}{0.0509 + 0.0281} = 4.07$$

The two-phase frictional loss is calculated as

$$\delta_{\ell g} = (0.0509 + 0.0281)(4.07) = 0.322 \text{ psi/ft.}$$

The liquid saturation is calculated from Equation (58).

$$\log_{10}R_\ell = -0.744 + 0.525(\log_{10}\chi) - 0.109(\log_{10}\chi)^2.$$

$$= -0.744 + 0.525(\log_{10}1.35) - 0.109(\log_{10}1.35)^2.$$

$$= -0.678.$$

$$R_\ell = 0.210 \text{ (fraction of voids occupied by liquid).}$$

The density of the flowing mixture is

$$\rho_m = R_\ell \rho_\ell + R_g \rho_g = (0.210)(62.4) + (1 - 0.210)(0.225)$$

$$= 13.3 \text{ lb/cu ft}$$

$$= 0.092 \text{ lb/sq in/ft or psi/ft.}$$

The pressure drop per unit length is obtained from Equation (49).

$$-\left(\frac{\Delta P}{\Delta L}\right)_{\ell g} = \delta_{\ell g} - \rho_m = 0.322 - 0.092 = 0.230 \text{ psi/ft.}$$

The pressure drop over the length of the bed is

$$\Delta P = (10.0)(-0.230) = -2.30 \text{ psi.}$$

The assumed pressure drop used in the calculation of the average pressure and δ_g was 3.0 psi. A new assumption might be made of 2.30 psi, and the calculation could be carried out again to obtain a more accurate computation. However, the change in δ_g from the last calculation is less than 2 per cent, and is well within the accuracy of the correlation.

The result of the computation is as follows:

Pressure drop = 2.30 psi

Inlet pressure = 30.0 psig

Outlet pressure = 27.7 psig

Average saturation = 0.210.

VIII. CONCLUSIONS

This dissertation presents a correlation of two-phase pressure drop data for downward flow in vertical packed beds, and a correlation of the liquid saturation data accompanying the two-phase flow. The conclusions which may be drawn from the investigation are listed below in the order of their development. The most important conclusions are marked with an asterisk.

*1. The correlation of pressure drop and liquid saturation for non-foaming mixtures has been established over a wide range of porosities, effective packing diameters, liquid viscosities, and flow rates.

2. The correlations for two-phase pressure drop and liquid saturation are based on the single independent variable, X, which is the square root of the ratio of the friction loss of the liquid to the friction loss of the gas, assuming each phase flowing separately. This ratio can be obtained from single-phase data or correlations.

*3. The correction of the single-phase pressure drop equations on the basis of observed data eliminates error in the two-phase correlation from the single-phase predictions. Therefore, any single-phase data or correlation may be used with the two-phase correlation.

4. Both curves and algebraic equations have been presented for the correlation of pressure drop and liquid saturation in order to facilitate their use with digital computers.

5. The incorporation of all fluid and packing properties in the single-phase pressure drops and their elimination from the final form of the correlations facilitates extrapolation of the relationships.

*6. The agreement between correlations for open pipes and packed beds supports the wide extrapolation of porosities.

*7. The correlation is expected to hold at higher rates in both horizontal and upward flow, as well as for downward flow. No significant change in the liquid saturation correlation is expected for horizontal and upward flow when true cocurrent flow is maintained. The use of the proper energy balance with the proposed liquid saturation correlation is expected to give good results for any orientation.

*8. The effect of foaming on pressure drop is large for small packing diameters and low rates. The effect is decreased as the packing diameter or flow rates are increased. Further work is required to characterize the foaming tendencies of mixtures in order to correlate foaming pressure drop.

*9. The symmetry of the pressure drop correlation shows that the effect of the liquid on the gas is identical to that of the gas on the liquid, and the roles of liquid and gas can be interchanged in the definition of χ. The correlation is not thought to hold for immiscible liquid phases since the compressibility of the gas is thought to be the

main cause of the larger gas-liquid pressure effects. Further work is required to determine the behavior of immiscible liquid phases in flow.

10. The prediction of three-phase pressure drops for the flow of two immiscible liquid phases and a gas phase might be subject to the correlation, if pressure drop data on the simultaneous flow of the two immiscible phases is obtained and used with the single-phase drop for the gas to calculate χ. Considering the liquids as a single-phase assumes negligible interaction between the immiscible liquid phases.

IX. APPENDIX I - SAMPLE CALCULATIONS

A. Calculation of Correlation Parameters

1. Data on Run 46

Data for the middle section of the test column are obtained from Table III for water and air on Raschig Rings as follows:

Liquid Rate	- 23.2 gpm
Air Rate	- 52.8 SCFM
Average Pressure in Section	- 32.9 psig
Pressure Drop in Section	- 7.01 psi/ft
Column Temperature	- 64.0°F
Liquid Viscosity	- 1.064 cp
Liquid Saturation	- 25.8%

Table II gives the porosity of the Raschig Rings as 52.0 per cent, and the inside diameter of 4-inch pipe is 4.03 inches.

2. Mass Rates

$$G_\ell = \frac{(\text{gpm})(\rho_\ell)}{A} = \frac{(23.2)(8.337)}{\pi(4.03/24)^2} = 2184.5 \text{ lb/(sq ft)(min)}$$

$$G_g = \frac{(\text{SCFM})(\rho_g)}{A} = \frac{(52.8)(0.0765)}{\pi(4.03/24)^2} = 45.44 \text{ lb/(sq ft)(min)}$$

3. Calculation of $\delta_{\ell g}$

The correction of the observed pressure drop for the unequal liquid legs of the manometer requires the subtraction of the liquid density in psi/ft.

$$-\left(\frac{\Delta P}{\Delta L}\right)_{\ell g} = 7.01 - 0.4356 = 6.5744 \text{ psi/ft.}$$

Equation (49) is applied with the assumption that ρ_m is equal to the fraction liquid times the liquid density in psi/ft since the density of air is small and ρ_m is a correction.

$$\delta_{lg} = 6.5744 + (0.258)(0.4356) = 6.6898 \text{ psi/ft.}$$

4. Reynolds Numbers

The effective diameter of the packing particles is calculated from Equation (8) using the specific surface given in Table II.

$$D_p = \frac{6(1 - \epsilon)}{S} = \frac{6(1 - 0.520)}{148} = 0.0195 \text{ ft.}$$

The Reynolds number is calculated from the definition given in Equation (12).

$$Re_l = \frac{D_p G_l}{\mu_l (1 - \epsilon)} = \frac{(0.0195)(2184.5)(60)}{(1.064)(1 - 0.52)(2.42)} = 2061.8$$

$$Re_g = \frac{D_p G_g}{\mu (1 - \epsilon)} = \frac{(0.0195)(45.44)(60)}{\mu_g (1 - 0.52)(2.42)} = \frac{45.6}{\mu_g}$$

The viscosity of air is obtained from Equation (51)

$$\mu_g = 0.01709(524.0/460)^{.768} = 0.0189 \text{ cp}$$

$$Re_g = 45.6/0.0189 = 2416$$

5. Single-Phase Pressure Drops

Figure 9 is consulted for the proper constants for Equation (47).

$$-\left(\frac{dP}{dL}\right) = \frac{Re(266 + 2.33Re)}{\frac{g_c \rho D_p^3}{\mu^2} \left(\frac{\epsilon}{1 - \epsilon}\right)^3}$$

The density of air is calculated from Equation (51).

$$\rho_g = 2.708 \left(\frac{32.9 + 14.7}{64.0 + 460}\right) = 0.245 \text{ lb/cu ft.}$$

The density of the liquid phase is obtained from Table I.

$$-\left(\frac{dP}{dL}\right)_g = \frac{(2416)(266 + 2.33 \times 2416)}{\frac{(32.17)(.245)(.01945)^3}{(.0189 \times .000672)^2}\left(\frac{.52}{1 - .52}\right)^3} = 31.0 \text{ lb/sq ft/ft} = 0.215 \text{ psi/ft.}$$

$$-\left(\frac{dP}{dL}\right)_\ell = \frac{(2061.8)(266 + 2.33 \times 2061.8)}{\frac{(32.17)(62.4)(.01945)^3}{(1.064 \times .000672^2}\left(\frac{.52}{1 - .52}\right)^3} = 284 \text{ lb/sq ft/ft} = 1.975 \text{ psi/ft.}$$

6. Correlation Parameters

Since the pressure drop correlations are for horizontal flow, no correction for density is required.

$$\chi = \sqrt{\frac{\delta_\ell}{\delta_g}} = \sqrt{\frac{1.975}{0.215}} = 3.03$$

$$\varphi_\ell = \sqrt{\frac{\delta_{\ell g}}{\delta_\ell}} = \sqrt{\frac{6.6898}{1.975}} = 1.84$$

$$\varphi_g = \sqrt{\frac{\delta_{\ell g}}{\delta_g}} = \sqrt{\frac{6.6898}{0.215}} = 5.58$$

$$\frac{\delta_{\ell g}}{\delta_\ell + \delta_g} = \frac{6.6898}{1.975 + 0.215} = 3.05$$

7. Comparison with Correlations

$$\log_{10}\left(\frac{\delta_{\ell g}}{\delta_\ell + \delta_g}\right) = \frac{0.416}{(\log_{10} 3.03)^2 + 0.666} = .464$$

$$\frac{\delta_{\ell g}}{\delta_\ell + \delta_g} = 2.91$$

A calculated value of 2.91 is obtained which deviates 4.6 per cent from the observed value of 3.05.

$$\log_{10} R_\ell = -0.744 + 0.525(\log_{10} 3.03) - 0.109(\log_{10} 3.03)^3 = -0.5163$$

$R_\ell = 0.304$ which deviates 15 per cent from the observed value of 0.258.

B. Correction of Results for Emulsion Density

1. Assumptions

a. The expanded liquid phase flows with the viscosity of the liquid.

b. The mass flow rate for the expanded phase is the same as that of the liquid.

c. The amount of air lost in the emulsion does not affect the air drop.

2. Data

Consider the data for Run 301 which are as follows:

$\varphi_g = 6.29$

$\chi = 0.869$

Average pressure in middle section - 26.4 psia

Fraction Liquid in emulsion at 14.7 psia - 0.375

If the drop for the gas phase is not affected by the loss of volume to the liquid phase, φ_g is not altered. The liquid pressure drop is inversely proportional to the density of the liquid phase, and if the mass of the air is neglected, the pressure drop for the expanded phase is inversely proportional to the fraction liquid in the emulsion.

3. Correction of Fraction Liquid to Column Conditions

Take a basis of one cubic foot of emulsion.

Air volume at 14.7 psia - 0.625 cu ft

Liquid volume at 14.7 psia - 0.375 cu ft

Air volume at 26.4 psia -

$$0.625(14.7/26.4) = 0.348 \text{ cu ft}$$

Fraction Liquid in emulsion at 26.4 psia

$$\frac{0.375}{0.375 + 0.348} = 0.518$$

4. Correction of χ

Since δ_ℓ is inversely proportional to the fraction liquid in the emulsion, χ is inversely proportional to the square root of the fraction liquid.

$$\chi_2 = \chi_1\sqrt{\frac{1.0}{0.518}} = 0.869\sqrt{\frac{1.0}{0.518}} = 1.22$$

C. Outline of the Design Calculation

Given the porosity of a packed bed, the flow rates of the liquid and gas streams, the viscosity of the liquid and gas, and the density of the liquid and gas; compute the rate of change of pressure with distance, assuming that the single-phase correlation is given. The pressure must be known at some point in the packed bed to carry out the following steps:

1. Calculate δ_ℓ and δ_g from the single-phase relationships at the known pressure.
2. Calculate $\delta_{\ell g}$ from Equation (56), and R_ℓ from Equation (58), using the definition of χ given in Equation (39).
3. Use the liquid saturation to calculate ρ_m by Equation (50).

4. Obtain the rate of change of observed pressure with distance down the column from Equation (24).

If the pressure drop over a short section is desired, and the pressure at the beginning of the section is given, estimate the average pressure in the section and use it to carry out the four steps above. Change the differentials to deltas and multiply by the length. Check the assumed value of the average pressure, and repeat the calculation if necessary.

If the pressure drop over a long section is desired and the pressure at the beginning of the section is given, a step-wise computation may be made. Assume an increment in pressure, and compute the average pressure in the increment. Calculate the average rate of pressure drop as above, and use it to compute the length required for the assumed drop in pressure.

X. APPENDIX II - COMPUTER PROCESSING OF DATA

A. Description of Data Processing Equipment

The use of a high-speed electronic computer made it possible to consider a large number of experimental runs, to test proposed correlations with ease, and to eliminate the human error from the calculations. The original data for each run was transferred to a single IBM punched card. The processing was subject to no further manual treatment.

The processing of the data was executed within an IBM-650 computer which accepts a deck of cards containing a series of instructions to be executed, accepts data for the calculations on punched cards, and performs the given instructions in order to obtain the desired results. The computer is capable of performing 78,000 additions or subtractions per minute; 5,000 ten by ten multiplications per minute; 3,700 divisions per minute; or 138,000 logical decisions per minute. The IBM-650 operates with ten digit numbers, and any number with less than ten digits must be filled in with leading or trailing zeros before arithmetic operations can be performed. The output of the IBM-650 is on punched cards, and may be printed on the IBM-407 tabulator. The printer reads 150 cards per minute, and prints the same number of lines. The final form of the output of the IBM-650 was put through an IBM-513 reproducing punch in order to convert the form of the numbers to fixed point and to insert the decimal points, which are not carried inside the 650.

The most convenient form of numbers within the computer is known as the floating point form. The advantage of this form is that

the proper location of the decimal point can always be determined by looking at the number. A typical number in floating point has the following form:

8945012353+ ,

and may be separated into two portions, 89450123+ and 53. The eight digits toward the left are called the mantissa, and the decimal point is considered to follow the first digit, i.e., +8.9450123. Each location in the machine carries a sign which is associated with the mantissa. The two digits at the right of the number are a code for the exponent to which 10 must be raised in order to properly shift the decimal point of the number. The exponent is obtained by subtracting 50 from the last two digits of a floating point number. The number 8954012353+ in floating point is to be interpreted as the number

$$+8.9450123 \times 10^{3} = 8945.0123.$$

The code is expressed as 50 plus the exponent since only one sign is available for each location, and both plus and minus exponents are required. This coding allows the exponent to range from -49 to +49 without changing the sign of the number.

Both numbers and instructions are composed of ten digits in the IBM-650, and 2,000 locations are available for the storage of instructions or numbers. The locations are numbered from 0000 to 1999. A typical instruction in the machine has the following form:

+3209000100 ,

which may be separated into three important parts, +32, 0900, and 0100. The above instruction tells the machine to perform an addition of two floating point numbers by designating the operation code 32. One of

the numbers to be added is in the lower accumulator of the machine, and the other number to be added is in location 0900. When the addition has been performed, the machine is to look at location 0100 for its next instruction. By performing a series of such instructions, complex calculations can be carried out.

The calculations required to output all of the processed data and calculated results for this dissertation takes a little less than 45 minutes of IBM-650 time. The instructions for the calculations are contained on approximately 250 IBM cards. Some 150 of these cards are not specific to the particular program and are termed subroutines. Subroutines are short programs which are used many times in a calculation, and are included as a package to reduce the number of instructions which must be written for a specific program. Typical subroutines are available for the calculation of sine, cosine, logarithms, anti-logarithms, and other specific functions. The number of instruction cards required for this problem is approximately 100, and the number of instructions on the cards is approximately 500. The method followed in the calculation is that presented in Appendix I.

B. Steps in the Development of Processed Data

Table XIV shows the series of cards used in the development of the processed data. The first card shown in the table is an original data card for Run 46. The card is divided into eight ten-digit words, and each word contains two five-digit pieces of data packed together. Comparison of the headings with the sample data sheet in Figure 6 will indicate the pieces of data recorded.

TABLE XIV

STEPS IN THE DEVELOPMENT OF THE PROCESSED DATA

EXPERIMENTAL DATA

Run Code	Liq. Rate Gpm	Air Rate % of Max.	Air Meter Const	Air Meter Temp. °F	Air Meter Pres. psig	Top Col. Pres. psig	Top Sec. ΔP psig	Mid Sec. ΔP psig	Btm. Sec. ΔP psig	Col. Temp. °F	Liq. Vis. cp.	Liq. Hold-Up ft^3
0046113040	23200	04920	00302	00925	05485	05320	13310	27300	44200	00640	01064	00086

PROCESSED DATA (Two Cards per Run) - Floating Point Numbers

Run Code	Liquid Rate gpm	Air Rate SCFM	Mass Rate for Liquid #/(ft^2-min)	Mass Rate for Gas #/(ft^2-min)	Liquid Saturation %	Avg. Pres. Top Sec. psig	Pres. Drop Top Sec. psi/ft
0046113040	2320000051	5271746751	2184535253	4544245751	2574850351	4654500051	6689786950

Run Code	Avg. Pres. Mid. Sec. psig	Pres. Drop Mid. Sec. psi/ft	Avg. Pres. Btm.Sec. psig	Pres. Drop Btm.Sec. psi/ft	Column Temperature °F	Liquid Saturation %	Liquid Viscosity centipoise
0046113040	3289500051	7013234450	1745000051	8363024550	6400000051	2574850351	1064000050

PROCESSED DATA (Two Cards per Run) - Fixed Point Numbers

Run Code	Liquid Rate		Air Rate		Avg. Pres. Top Sec. psig	Pres. Drop Top Sec. psig
	Volume Rate gpm	Mass Rate #/(ft^2-min)	Volume Rate SCFM	Mass Rate #/(ft^2-min)		
46113040	23.200	2184.535	52.7174	45.4424	46.54500	6.68978

Run Code	Avg. Pres. Mid. Sec. psig	Pres. Drop Mid. Sec. psi/ft	Avg. Pres. Btm.Sec. psig	Pres. Drop Btm.Sec. psi/ft	Column Temperature °F	Liquid Viscosity centipoise	Liquid Saturation %
46113040	32.89500	7.01323	17.45000	8.36302	64.0	1.064	25.748

The original data cards were read into the IBM-650 with instructions required to execute the desired computation. The first step in the computer program was to split the packed five-digit words apart and place them in two separate locations in the form of floating point numbers. The output of the program consisted of two cards of answers for every card of original data. The output was in the form of ten-digit floating point numbers. The output of the IBM-650 was converted with the IBM-513 into fixed point numbers as presented in the final tabulation of the processed data. In the final process, the numbers were shifted as indicated by the exponent of the number, the decimal point was inserted, and the exponent code was stripped from the numbers. Some rearrangement of order was also performed. The number of digits reported could have been reduced by manual handling of the cards, but possibility of human errors in the process outweighs any confusion the extra digits may cause. The reporting of calculated numbers to a greater accuracy than justified by the data, does not introduce any additional error in the numbers.

C. Steps in the Development of Calculated Results

Table XV shows the series of cards used in the development of the calculated results. The calculation of the results was performed in two steps. The first step consisted of the calculation of the Reynolds numbers, single-phase pressure drops, and corrected two-phase pressure drop. Three cards were produced from each data card, since a calculation is desired for each section of the column. The second calculation step produced the correlation parameters and the saturations for the liquid and gas. Three cards were again produced for each data card.

The two cards corresponding to each column section were combined to form the final contents of the tabulated results. Some values were deleted in the conversion to fixed point numbers, and some values were copied from the processed data. The cards were rearranged and converted into the fixed point form by the IBM-513 reproducing punch, and the final printing was made on an IBM-407 printer.

Both the tabulation of the processed data and calculated results were printed in two parts by the IBM-407, and pasted together for photographing. The numbers in the final tabulations were actually calculated, modified, and printed by IBM equipment.

TABLE XV

STEPS IN THE DEVELOPMENT OF THE CALCULATED RESULTS

CALCULATED RESULTS (Six Cards per Run) - Floating Point Numbers

Run Code	Section Number	Liquid Saturation %	Reynolds No. for Air	One-Phase Pres. Drop for Air psi/ft	Reynolds No. for Liquid	One-Phase Pres. Drop for Liquid psi/ft	Two-Phase Pres. Drop Corrected psi/ft
0046113040	3333333333	2574850351	2415835253	1671553349	2061843753	1974728550	6366347450
0046113040	2222222222	2574850351	2415835253	2150946149	2061843753	1974728550	6689794950
0046113040	1111111111	2574850351	2415835253	3184270049	2061843753	1974728550	8039585050

Run Code	Section Number	$\frac{\delta_{lg}}{\delta_l + \delta_g}$	χ	φ_l	φ_g	Liquid Saturation %	Gas Saturation %
0046113040	3333333333	2972312250	3437110550	1795525150	6171418450	2574850351	7425149751
0046113040	2222222222	3054947650	3029974650	1840570650	5576882550	2574850351	7425149751
0046113040	1111111111	3505904950	2490284650	2017729750	5024721550	2574850351	7425149751

CALCULATED RESULTS (Six Cards per Run) - Fixed Point Numbers

Run Code	Column Section	Mass Rates		Reynolds Numbers		Two-Phase Pres. Drop Corrected psi/ft	One-Phase Pres.Drop for Liquid psi/ft
		Liquid #/(ft^2-min)	Gas #/(ft^2-min)	Liquid	Gas		
46113040	TOP	2184.535	45.4424	2061.843	2415.835	6.36634	1.97472
46113040	MID	2184.535	45.4424	2061.843	2415.835	6.68979	1.97472
46113040	BTM	2184.535	45.4424	2061.843	2415.835	8.03958	1.97472

Run Code	Column Section	One-Phase Pres. Drop for Air psi/ft	Liquid Saturation %	χ	φ_l	φ_g	$\frac{\delta_{lg}}{\delta_l + \delta_g}$
46113040	TOP	.16715	25.7485	3.4371	1.7955	6.1714	2.9723
46113040	MID	.21509	25.7485	3.0299	1.8405	5.5768	3.0549
46113040	BTM	.31842	25.7485	2.4902	2.0177	5.0247	3.5059

XI. APPENDIX III - TABULATION OF PROCESSED DATA

The following pages are a tabulation of the processed data which is described in Subsection D of Section III. The following pages are referred to as Table XVI in the List of Tables.

The run codes and run numbers associated with various systems of fluids and packings are indexed in Table IV.

The detailed meaning of the run code is explained in Table V.

Single-phase data are indicated by a zero rate for one of the phases.

TABLE XVI

TABULATION OF PROCESSED DATA

	Liquid Rate		Air Rate		Top Section		Middle Section		Bottom Section				
Run Code	gpm	#/(ft^2 - min)	SCFM	#/(ft^2 - min)	Avg. Pres. psig	Pres. Drop psi/ft	Avg. Pres. psig	Pres. Drop psi/ft	Avg. Pres. psig	Pres. Drop psi/ft	Column Temperature °F	Liquid Viscosity cp	Liquid Saturation %
1111000	33.750	3177.933	.0000	.0000	31.91500	4.60896	23.26500	4.07559	14.75000	4.40419	73.0	.937	100.000
2111000	32.700	3079.064	.0000	.0000	29.52500	4.29734	21.47500	3.78484	13.65000	4.00831	73.5	.930	100.000
3111000	31.400	2956.655	.0000	.0000	27.07500	3.94551	19.70000	3.45899	12.52500	3.68665	74.0	.925	100.000
4111000	29.000	2730.669	.0000	.0000	27.40000	3.31724	21.20000	2.90755	15.05000	3.21654	75.0	.913	100.000
5111000	26.100	2457.602	.0000	.0000	22.30000	2.71411	17.28500	2.32103	12.47500	2.46931	76.0	.901	100.000
6111000	23.200	2184.535	.0000	.0000	21.84500	2.16626	17.74000	1.95508	13.72000	2.04869	76.5	.895	100.000
7111000	20.300	1911.468	.0000	.0000	20.59500	1.71391	17.39500	1.49889	14.28500	1.59837	77.0	.890	100.000
8111000	17.400	1638.401	.0000	.0000	18.32500	1.28166	15.93000	1.12291	13.60500	1.19259	77.0	.890	100.000
9111000	14.500	1365.334	.0000	.0000	20.27000	.93486	18.52000	.82213	16.81500	.87589	78.0	.880	100.000
10111000	11.600	1092.267	.0000	.0000	15.58500	.61821	14.44000	.53138	13.32000	.58392	78.5	.875	100.000
11111000	10.400	979.274	.0000	.0000	14.52750	.47496	13.64750	.40856	12.79000	.44536	78.5	.875	100.000
12111000	9.360	881.346	.0000	.0000	21.11000	.39203	20.38000	.34088	19.68000	.35629	79.0	.870	100.000
13111000	8.320	783.419	.0000	.0000	16.68250	.31915	16.08250	.28323	15.49000	.30680	79.5	.865	100.000
14111000	7.280	685.492	.0000	.0000	12.04350	.25784	11.56700	.22057	11.10250	.24198	79.5	.865	100.000
15111000	11.600	1092.267	9.9753	8.5987	10.72500	1.58323	7.17500	1.98014	3.33500	1.84580	72.5	.943	42.215
16111000	11.600	1092.267	17.2670	14.8841	13.28500	2.22657	8.83500	2.24082	4.21500	2.36045	78.0	.880	31.137
17112120	11.600	1092.267	26.1090	22.5059	15.99000	2.62364	10.81500	2.57168	5.12500	3.09283	78.5	.875	27.544
18113120	11.600	1092.267	35.8926	30.9394	20.37500	2.94028	13.90000	3.55925	6.82500	3.48871	62.0	1.095	22.155
19113080	11.600	1092.267	51.0245	43.9831	24.21000	3.60876	16.81000	3.81993	8.20000	4.75059	63.0	1.080	18.263
20113060	11.600	1092.267	72.4231	62.4287	30.16000	4.46320	21.46000	4.27110	11.45000	5.69081	65.0	1.050	14.970
21113040	11.600	1092.267	94.8608	81.7700	36.05000	4.97587	25.85000	5.26368	13.80000	6.73000	67.0	1.020	11.377
22111000	14.500	1365.334	10.6930	9.2174	14.41500	2.39746	9.71000	2.32604	4.79500	2.56828	70.0	.975	41.616
23112000	14.500	1365.334	23.3601	20.1364	19.80000	3.31724	13.42500	3.08301	6.72500	3.58768	72.0	.950	32.335
24112080	14.500	1365.334	35.2733	30.4056	23.61000	3.70928	16.30000	3.62943	8.34000	4.29532	73.0	.937	23.353
25113100	14.500	1365.334	47.8620	41.2570	28.02000	4.20184	19.62000	4.23100	10.15000	5.19596	74.0	.925	19.161
26113060	14.500	1365.334	64.2168	55.3549	33.37500	4.85022	23.67500	4.88770	12.45000	6.28463	75.0	.913	17.065
27113030	14.500	1365.334	81.3087	70.0881	38.80000	5.32770	27.80000	5.71485	14.75000	7.27434	75.0	.913	14.970
28114000	14.500	1365.334	93.9453	80.9808	41.72500	5.60414	30.22500	5.94044	16.35000	7.86817	76.0	.900	14.970
29111000	17.400	1638.401	7.5890	6.5417	17.07500	2.94028	11.37500	2.78223	5.50000	3.06809	60.5	1.118	44.011
30111000	17.400	1638.401	18.2182	15.7041	22.22500	3.69420	14.97500	3.58431	7.45000	3.90934	63.0	1.080	35.628
31112180	17.400	1638.401	40.9671	35.3136	27.71000	4.51347	19.01000	4.22097	9.65000	5.09699	64.0	1.065	26.047

TABLE XVI (CONT'D)

Run Code	Liquid Rate		Air Rate		Top Section		Middle Section		Bottom Section		Column Temperature	Liquid Viscosity	Liquid Saturation
	gpm	#/(ft^2 - min)	SCFM	#/(ft^2 - min)	Avg. Pres. psig	Pres. Drop psi/ft	Avg. Pres. psig	Pres. Drop psi/ft	Avg. Pres. psig	Pres. Drop psi/ft	°F	cp	%
32113120	17.400	1638.401	46.1492	39.7806	32.96000	5.06634	23.01000	4.92279	11.92500	6.11144	66.0	1.035	21.257
33113060	17.400	1638.401	61.6022	53.1011	38.20000	5.42822	27.00000	5.81511	14.10000	7.02692	67.5	1.012	20.359
34113040	17.400	1638.401	79.2741	68.3342	43.55000	5.98110	31.35000	6.26629	16.80000	8.21456	68.5	.998	19.760
35114000	17.400	1638.401	93.0390	80.1996	47.55000	6.38319	34.50000	6.71746	18.75000	8.95684	70.0	.975	19.161
36111000	20.300	1911.468	11.6393	10.0331	20.72000	3.29714	14.22000	3.22839	7.05000	3.90934	74.0	.925	48.203
37112240	20.300	1911.468	25.3785	21.8763	27.56000	4.26216	19.13500	4.19590	9.77500	5.12173	75.0	.913	33.532
38112120	20.300	1911.468	35.2894	30.4194	32.20000	4.82509	22.55000	4.86264	11.75000	5.88875	75.5	.908	29.341
39113050	20.300	1911.468	47.3618	40.8259	37.00000	5.42822	26.10000	5.51433	13.80000	6.73000	76.0	.901	27.544
40113030	20.300	1911.468	61.8995	53.3573	42.83500	5.99618	30.58500	6.30138	16.45000	7.76920	77.0	.890	24.850
41113020	20.300	1911.468	77.4539	66.7653	48.20000	6.53397	34.75000	6.96811	18.90000	8.80839	78.0	.880	21.856
42114000	20.300	1911.468	94.2125	81.2111	53.49000	7.04664	38.84000	7.65991	21.55000	9.55067	78.0	.880	20.658
43111000	23.200	2184.535	16.0696	13.8520	29.42000	4.40289	20.41000	4.64206	10.24000	5.48297	60.0	1.126	43.712
44112000	23.200	2184.535	28.5327	24.5952	35.57000	5.55890	24.52000	5.53438	12.50000	6.43309	61.5	1.103	36.227
45113060	23.200	2184.535	40.0881	34.5559	40.91000	6.12183	28.71000	6.12592	15.15000	7.37331	63.0	1.080	29.041
46113040	23.200	2184.535	52.7174	45.4424	46.54500	6.68978	32.89500	7.01323	17.45000	8.36302	64.0	1.064	25.748
47113030	23.200	2184.535	71.8506	61.9352	53.75000	7.38841	38.50000	7.92059	20.80000	9.69912	66.0	1.035	24.550
48114000	23.200	2184.535	86.3775	74.4574	57.95000	7.99155	42.00000	8.02085	23.20000	10.68883	67.0	1.020	23.952
49114000	23.200	2184.535	96.6754	83.3342	61.30000	8.34338	44.75000	8.27150	25.10000	11.28266	68.0	1.005	24.251
50111000	26.100	2457.602	13.8410	11.9309	30.35500	4.87032	20.60500	4.91778	10.05000	5.59184	73.5	.930	49.401
51112000	26.100	2457.602	26.4911	22.8354	38.07000	5.86047	26.42000	5.83517	13.40000	7.12589	74.0	.925	38.323
52112001	26.100	2457.602	36.7283	31.6598	43.04000	6.49376	30.29000	6.30639	15.70000	8.21456	75.0	.913	31.437
53113081	26.100	2457.602	48.4819	41.7914	48.57500	7.16224	34.37500	7.09344	18.10000	9.10530	76.0	.900	27.844
54113040	26.100	2457.602	66.9815	57.7381	56.45500	7.98653	40.50500	8.02586	21.85000	10.54038	76.0	.900	27.544
55113023	26.100	2457.602	83.2792	71.7867	63.10000	8.74547	45.70000	8.72267	25.05000	11.82699	76.5	.896	26.347
56114003	26.100	2457.602	94.4460	81.4124	66.65000	9.19782	47.85000	9.67515	26.35000	11.72802	77.0	.891	23.952
57111001	29.000	2730.669	15.1737	13.0797	39.02500	6.40832	26.57500	6.09083	13.20000	7.22486	59.0	1.142	47.005
58111001	29.000	2730.669	25.0602	21.6019	45.46000	7.27784	31.16000	7.07840	15.80000	8.21456	61.0	1.110	39.820
59111002	29.000	2730.669	36.1593	31.1693	51.24000	8.00160	35.44000	7.86043	18.05000	9.45170	63.0	1.080	34.730
60112003	29.000	2730.669	49.3522	42.5416	57.50500	8.74045	40.25500	8.57730	20.95000	10.63935	65.0	1.050	28.742

TABLE XVI (CONT'D)

Run Code	Liquid Rate		Air Rate		Top Section		Middle Section		Bottom Section		Column Temperature	Liquid Viscosity	Liquid Saturation
	gpm	#/(ft^2 - min)	SCFM	#/(ft^2 - min)	Avg. Pres. psig	Pres. Drop psi/ft	Avg. Pres. psig	Pres. Drop psi/ft	Avg. Pres. psig	Pres. Drop psi/ft	°F	cp	%
61112005	29.000	2730.669	65.6747	56.6116	64.40000	9.44913	45.60000	9.42450	24.15000	11.92597	67.0	1.020	29.341
62112006	29.000	2730.669	81.5887	70.3295	70.35000	10.10253	50.40000	9.92580	27.40000	12.96516	68.0	1.005	30.239
63113066	29.000	2730.669	91.4694	78.8467	74.00000	10.05227	53.65000	10.37698	29.50000	13.65795	70.0	.975	26.646
64111000	7.800	734.455	9.1662	7.9012	7.42000	1.28669	4.96000	1.18307	2.40000	1.36579	74.0	.925	33.532
65112000	7.800	734.455	24.2760	20.9259	10.74000	1.86972	7.09000	1.79466	3.45000	1.83095	75.0	.913	22.455
66113060	7.800	734.455	40.5219	34.9299	15.06500	2.44772	10.21000	2.42630	5.13000	2.63262	76.0	.901	17.664
67113050	7.800	734.455	54.3370	46.8385	18.49000	2.82468	12.74000	2.94766	6.32500	3.43923	76.5	.896	14.371
68113040	7.800	734.455	68.9411	59.4272	22.17500	3.24185	15.50000	3.45899	8.02500	3.98357	77.0	.891	10.479
69114001	7.800	734.455	93.8250	80.8771	27.64000	3.88017	19.69000	4.10066	10.30000	5.24544	77.5	.886	9.880
72112000	5.200	489.637	28.9846	24.9847	9.12500	1.48271	6.05000	1.60417	2.87500	1.55878	80.5	.855	19.161
73113080	5.200	489.637	43.7631	37.7238	11.90000	1.90993	7.98500	2.02025	3.88500	2.06353	80.5	.855	13.173
74113080	5.200	489.637	59.4884	51.2790	15.59000	2.42259	10.75500	2.43132	5.42000	2.88004	80.5	.855	11.077
75113080	5.200	489.637	74.9192	64.5803	18.23000	2.78447	12.78000	2.68698	6.55000	3.51346	80.5	.855	9.880
76113080	5.200	489.637	94.1927	81.1941	22.26000	3.25693	15.78500	3.24343	8.27500	4.23099	80.5	.855	8.383
79111000	2.600	244.818	23.3459	20.1242	5.53500	.97004	3.61500	.95748	1.75500	.89568	81.0	.850	15.568
80112000	2.600	244.818	36.4657	31.4334	7.38000	1.32689	4.82500	1.23821	2.62500	.95506	81.0	.850	12.574
81112000	2.600	244.818	51.6625	44.5330	9.65500	1.65359	6.43000	1.58411	3.17000	1.66270	80.5	.855	9.880
82111000	2.600	244.818	66.5122	57.3335	12.03000	1.98029	8.07000	1.99518	3.96500	2.09323	80.5	.855	7.185
83111000	2.600	244.818	94.8190	81.7340	17.06000	2.65379	11.81000	2.61680	6.10500	3.06314	80.5	.855	4.790
86111000	1.040	97.927	24.9041	21.4673	4.41000	.79412	2.82000	.80208	1.18500	.82640	79.0	.870	9.880
87111000	1.040	97.927	41.4752	35.7516	6.56000	1.14595	4.29000	1.13294	2.05000	1.09857	77.0	.891	6.586
88111000	1.040	97.927	59.6361	51.4063	9.21000	1.49778	6.21500	1.50892	3.06500	1.62806	76.5	.896	4.790
89111000	1.040	97.927	76.8061	66.2068	11.41500	1.89485	7.68000	1.85482	3.73000	2.07838	76.0	.901	4.790
90111000	1.040	97.927	93.5268	80.6201	13.86500	2.17631	9.53000	2.17565	4.74500	2.58808	76.0	.901	4.790
99111000	11.600	1092.267	.0000	.0000	12.09000	.61318	10.97750	.50380	9.90250	.56660	80.0	.860	100.000
102111000	11.600	1092.267	6.2752	5.4092	71.91000	1.09569	69.84500	.97754	67.82500	1.03424	80.0	.860	63.772
103111000	11.600	1092.267	5.6079	4.8340	52.45000	1.25653	50.06500	1.13795	47.70500	1.21239	79.0	.870	60.778
104111000	11.600	1092.267	4.7421	4.0877	32.99000	1.41737	30.27500	1.30840	27.53500	1.42022	78.5	.875	53.293
105111000	11.600	1092.267	6.4538	5.5632	29.85500	1.55307	26.79000	1.52396	23.63500	1.61817	77.0	.891	48.203

TABLE XVI (CONT'D)

Run Code	Liquid Rate		Air Rate		Top Section		Middle Section		Bottom Section		Column Temperature °F	Liquid Viscosity cp	Liquid Saturation %
	gpm	#/(ft^2 - min)	SCFM	#/(ft^2 - min)	Avg. Pres. psig	Pres. Drop psi/ft	Avg. Pres. psig	Pres. Drop psi/ft	Avg. Pres. psig	Pres. Drop psi/ft			
108111000	17.400	1638.401	.0000	.0000	32.94000	1.26658	30.58000	1.10286	28.29000	1.17775	76.0	.901	100.000
109111000	17.400	1638.401	5.8268	5.0227	57.32500	1.98532	53.55000	1.80469	49.85000	1.88044	75.0	.913	67.664
110111000	17.400	1638.401	5.7958	4.9960	42.52500	2.23663	38.24500	2.06035	33.96500	2.20209	74.0	.925	58.982
111111000	17.400	1638.401	4.9673	4.2818	15.16500	2.64877	9.98500	2.55163	4.74500	2.66726	72.5	.943	49.401
112111000	17.400	1638.401	7.4274	6.4024	17.04500	2.97044	11.25000	2.84740	5.28000	3.09778	71.0	.963	44.910
113111000	23.200	2184.535	.0000	.0000	48.67500	2.13610	44.71000	1.84479	40.90000	1.94972	82.0	.840	100.000
116111000	23.200	2184.535	4.0757	3.5132	19.01000	3.30719	12.63500	3.09304	6.07500	3.43923	80.0	.860	59.880
117111000	23.200	2184.535	5.7356	4.9441	22.13500	3.78468	14.73000	3.64948	7.04500	4.00336	79.0	.870	52.994
118111000	23.200	2184.535	10.1808	8.7758	25.92500	4.39786	17.37000	4.19089	8.34500	4.79513	78.5	.875	42.514
119111000	23.200	2184.535	14.1599	12.2058	28.63500	4.78990	19.18500	4.69721	9.35000	5.09699	76.5	.896	38.622
120111000	29.000	2730.669	.0000	.0000	16.66500	3.35243	10.44000	2.89753	4.52000	2.99881	81.7	.842	100.000
122111000	29.000	2730.669	4.5211	3.8972	26.15000	4.47326	17.50000	4.21094	8.50000	4.75059	85.0	.835	61.976
123111000	29.000	2730.669	5.4775	4.7216	28.80000	4.82509	19.30000	4.71225	9.30000	5.24544	84.9	.835	55.089
124111000	29.000	2730.669	8.4168	7.2553	32.32000	5.30759	21.89500	5.15841	10.75000	5.93824	84.0	.820	50.598
125111000	29.000	2730.669	12.4416	10.7246	35.54000	5.89063	24.04000	5.65470	11.75000	6.58155	84.0	.820	43.712
126111000	29.000	2730.669	16.7909	14.4738	39.07000	6.36308	26.52000	6.23621	13.05000	7.17537	83.0	.830	40.419
127111000	7.800	734.455	.0000	.0000	31.02100	.28045	30.50050	.24212	30.00950	.24693	87.5	.786	100.000
130111000	7.800	734.455	6.1915	5.3371	69.06000	.84439	67.45000	.77200	65.84000	.83135	73.0	.937	54.491
134111000	5.200	489.637	.0000	.0000	44.03500	.16586	43.74500	.12532	43.49950	.11925	89.0	.772	100.000
135111000	5.200	489.637	.0000	.0000	52.59650	.10404	52.37750	.11580	52.13450	.12618	95.0	.730	100.000
140111000	5.200	489.637	10.3597	8.9300	13.31000	1.09569	11.13000	1.09284	8.93000	1.09857	75.0	.913	28.443
143111000	2.600	244.818	.0000	.0000	4.85650	.04372	4.77350	.03960	4.68900	.04453	94.0	.740	100.000
144112000	2.600	244.818	2.6905	2.3192	3.37850	.52422	2.43750	.42059	1.54400	.46912	89.0	.772	28.742
150111000	1.040	97.927	.0000	.0000	3.39600	.00402	3.38800	.00401	3.37600	.00791	94.0	.740	100.000
154111000	1.040	97.927	9.9991	8.6192	3.52600	.52673	2.48450	.51884	1.47600	.48594	87.0	.792	14.071
155111000	.000	.000	20.0613	17.2929	3.49500	.60816	2.29500	.59655	1.12500	.56908	69.0	1.000	.000
156111000	.000	.000	40.2171	34.6671	6.11500	.88962	4.28000	.95247	2.31500	1.00455	56.0	1.000	.000
157111000	.000	.000	61.2811	52.8243	7.72500	1.28166	5.07500	1.37858	2.45000	1.23713	52.0	1.000	.000
158111000	.000	.000	80.9977	69.8200	10.36500	1.64354	7.01500	1.71947	3.50000	1.78147	49.0	1.000	.000

TABLE XVI (CONT'D)

Run Code	Liquid Rate		Air Rate		Top Section		Middle Section		Bottom Section		Column Temperature °F	Liquid Viscosity cp	Liquid Saturation %
	gpm	#/(ft^2 - min)	SCFM	#/(ft^2 - min)	Avg. Pres. psig	Pres. Drop psi/ft	Avg. Pres. psig	Pres. Drop psi/ft	Avg. Pres. psig	Pres. Drop psi/ft			
159111000	.000	.000	99.7343	85.9709	13.42500	1.98532	9.36500	2.09043	4.62500	2.62767	49.0	1.000	.000
160111000	.000	.000	119.7921	103.2608	16.50500	2.50804	11.62500	2.39121	6.27000	2.93942	59.0	1.000	.000
161111000	.000	.000	132.5883	114.2911	18.50000	2.61359	13.25000	2.65690	7.05000	3.51346	47.5	1.000	.000
162111000	.760	71.562	.0000	.0000	11.55500	.04523	11.46500	.04511	11.37500	.04453	72.5	13.700	100.000
163111000	3.040	286.249	.0000	.0000	11.44150	.25985	11.02000	.16342	10.66100	.19398	75.0	13.000	100.000
164111000	4.940	465.155	.0000	.0000	4.45250	.34931	3.80200	.30378	3.16200	.33353	78.5	12.250	100.000
165111000	7.420	698.674	.0000	.0000	9.51000	.59308	8.40000	.52135	7.38000	.49485	80.5	11.500	100.000
166111000	11.670	1098.858	.0000	.0000	14.11000	1.09569	11.92000	1.10286	9.80000	1.00950	87.0	10.250	100.000
167111000	16.540	1557.422	.0000	.0000	17.60500	1.90490	13.97500	1.73952	10.36000	1.86064	89.0	10.000	100.000
168111000	1.140	107.343	.0000	.0000	5.26150	.23974	4.85250	.17094	4.43100	.24841	83.0	11.200	100.000
170111000	1.140	107.343	26.3008	22.6713	25.46500	1.04041	23.35500	1.07780	21.21500	1.05403	84.0	11.100	17.365
171111000	1.140	107.343	38.9680	33.5904	8.84500	1.46260	6.07000	1.32344	3.32500	1.41033	70.0	14.600	14.970
172111000	1.140	107.343	117.7046	101.4614	23.65000	2.66385	17.97000	3.03789	11.59500	3.31057	70.0	14.600	8.682
173111000	7.420	698.674	10.4823	9.0357	13.65000	2.16123	9.25000	2.25586	4.55000	2.42478	82.0	11.500	35.928
174111000	7.420	698.674	38.5402	33.2217	24.50000	3.51829	17.15000	3.86003	8.90000	4.35471	83.0	11.250	23.053
176111000	16.540	1557.422	13.8070	11.9016	31.10000	5.42822	20.45000	5.26368	9.80000	5.34441	76.0	12.700	43.712
177111000	16.540	1557.422	46.2273	39.8480	55.00000	7.53920	41.25000	6.26629	26.75000	8.16508	78.0	12.200	34.431
178114000	16.300	1534.824	96.8526	83.4870	64.25000	8.79573	46.00000	9.52476	24.00000	12.37133	71.0	14.400	24.251
179111000	7.420	698.674	104.1617	89.7874	37.75000	5.27744	26.85000	5.66472	14.35000	6.77949	70.5	14.650	21.556
180111000	21.200	1996.213	33.1800	28.6011	48.25000	7.28789	33.25000	7.77020	17.00000	8.41250	74.0	13.300	43.712
181111000	3.040	286.249	8.9609	7.7243	7.22500	1.23140	4.83500	1.16803	2.56000	1.09857	75.5	12.800	29.940
182111000	3.040	286.249	30.4599	26.2564	11.39400	2.00643	7.51900	1.88389	3.81750	1.80374	76.0	12.700	21.856
183111000	3.040	286.249	105.7328	91.1417	26.92500	3.94551	19.09000	3.92019	10.44000	4.69121	73.0	13.600	16.167
184114000	21.200	1996.213	79.5776	68.5959	67.00000	10.05227	47.00000	10.02606	25.15000	11.72802	73.5	13.450	27.544
185111000	4.940	465.155	20.5468	17.7113	12.01750	2.12354	7.90750	2.00270	3.95500	1.93487	75.0	13.000	34.431
186114000	4.940	465.155	47.6033	41.0341	18.82000	3.14636	12.67000	3.02787	6.37500	3.24129	77.5	12.300	21.257
187111000	11.670	1098.858	26.9189	23.2041	29.67500	4.44813	20.22500	5.03809	10.10000	5.04750	79.0	12.000	32.335
188111000	11.670	1098.858	63.8712	55.0569	45.25000	6.48371	32.05000	6.76759	16.75000	8.46199	79.7	11.800	26.646
190111000	2.860	298.923	.0000	.0000	10.90750	.29402	10.33400	.28173	9.75150	.29839	94.0	12.100	100.000

TABLE XVI (CONT'D)

Run Code	Liquid Rate gpm	Liquid Rate #/(ft^2 - min)	Air Rate SCFM	Air Rate #/(ft^2 - min)	Top Section Avg. Pres. psig	Top Section Pres. Drop psi/ft	Middle Section Avg. Pres. psig	Middle Section Pres. Drop psi/ft	Bottom Section Avg. Pres. psig	Bottom Section Pres. Drop psi/ft	Column Temperature °F	Liquid Viscosity cp	Liquid Saturation %
191111000	4.650	486.012	.0000	.0000	13.05900	.39304	12.31650	.35241	11.58250	.37856	94.0	12.100	100.000
192111000	6.975	729.018	.0000	.0000	39.18400	.68958	37.85900	.64066	36.57500	.63836	92.0	12.400	100.000
193111000	10.950	1144.479	.0000	.0000	17.79500	1.41234	15.17500	1.21816	12.72500	1.22228	90.0	12.800	100.000
194111000	15.550	1625.265	.0000	.0000	23.96000	2.35223	19.58500	2.04030	15.50000	2.02889	86.3	13.750	100.000
195111000	19.920	2082.012	.0000	.0000	18.05000	3.66907	11.27500	3.13314	5.57500	2.54849	84.0	14.300	100.000
196111000	10.960	1145.525	11.0996	9.5679	15.91500	2.90008	10.36500	2.67194	5.14000	2.53365	93.0	12.200	47.305
197113080	10.960	1145.525	40.3213	34.7569	28.00000	4.52352	19.30000	4.21094	9.90000	5.14647	94.0	12.100	34.131
198114000	10.960	1145.525	96.4013	83.0979	46.22500	6.55910	33.35000	6.36655	18.60000	8.31353	94.0	12.100	25.449
199111000	2.860	298.923	11.3505	9.7841	20.94500	.94993	19.05000	.95247	17.18250	.90805	95.5	11.900	34.431
200111000	2.860	298.923	28.6771	24.7197	41.10500	1.11077	38.84000	1.16302	36.51500	1.15300	95.5	11.900	30.538
201111000	2.860	298.923	47.0233	40.5340	20.36000	1.86972	16.78000	1.72448	13.16500	1.87549	95.2	11.900	23.053
202111000	.715	74.730	9.9743	8.5979	13.09600	.39605	12.15100	.55243	11.05250	.54186	85.2	14.000	20.359
203111000	.715	74.730	24.1567	20.8231	24.96500	.66847	23.54500	.75696	22.01500	.76702	88.0	13.300	18.562
204111000	.715	74.730	33.6270	28.9865	18.40000	.90470	16.61000	.89232	14.73500	.97486	87.5	13.400	15.868
205111000	.715	74.730	44.3847	38.2596	17.29000	1.09569	15.10000	1.10286	12.92750	1.06146	87.0	13.600	13.473
206111000	.715	74.730	100.5127	86.6419	34.35000	1.96019	30.58500	1.81973	26.88500	1.86559	85.0	14.100	10.179
207111000	19.920	2082.012	15.1292	13.0414	37.57500	6.60936	25.10000	5.91538	12.55000	6.58155	73.0	17.600	58.083
208112000	19.920	2082.012	54.1929	46.7142	58.90000	9.14756	41.55000	8.27150	22.15000	11.03523	77.0	16.300	41.616
209114000	19.920	2082.012	76.9974	66.3717	68.30000	10.25331	48.15000	9.97593	25.65000	12.42082	78.5	15.800	35.029
210111000	15.550	1625.265	29.6474	25.5560	36.18500	6.01628	24.55000	5.66472	12.70000	6.13618	80.5	15.300	44.311
211113050	15.550	1625.265	68.5130	59.0582	52.00000	7.53920	36.75000	7.77020	20.00000	8.90736	83.0	14.600	34.431
212111000	6.975	729.018	24.3347	20.9765	20.68500	2.39746	16.16000	2.14557	11.49500	2.49901	84.7	14.100	38.622
213112000	6.975	729.018	60.3315	52.0057	41.14500	3.66405	34.17000	3.33868	27.12000	3.68171	82.0	14.800	33.532
214111000	4.650	486.012	9.7839	8.4337	11.00500	1.41234	8.44000	1.16302	6.01000	1.25692	84.0	14.300	42.514
215111000	4.650	486.012	37.0945	31.9754	24.36000	2.17129	20.19750	2.00772	16.10750	2.06601	86.0	13.800	31.137
216111000	4.650	486.012	103.3672	89.1025	37.13000	4.15158	29.18000	3.82995	20.48000	4.82977	87.0	13.600	21.257
217121000	19.920	2082.012	.0000	.0000	18.77000	2.98552	12.84500	2.96270	6.79000	3.06809	82.5	14.800	100.000
218121000	15.550	1625.265	.0000	.0000	16.80000	1.90993	12.95000	1.95508	8.88500	2.09323	84.0	14.300	100.000
219121000	10.960	1145.525	.0000	.0000	13.09000	1.09569	10.86000	1.14297	8.77500	.93527	86.2	13.800	100.000

TABLE XVI (CONT'D)

Run Code	Liquid Rate		Air Rate		Top Section		Middle Section		Bottom Section		Column Temperature °F	Liquid Viscosity cp	Liquid Saturation %
	gpm	#/(ft^2 - min)	SCFM	#/(ft^2 - min)	Avg. Pres. psig	Pres. Drop psi/ft	Avg. Pres. psig	Pres. Drop psi/ft	Avg. Pres. psig	Pres. Drop psi/ft			
220121000	6.975	729.018	.0000	.0000	18.54300	.54985	17.43800	.55945	16.35250	.52207	88.0	13.300	100.000
221121000	4.650	486.012	.0000	.0000	24.64400	.32770	23.99150	.32735	23.33150	.33006	90.0	12.800	100.000
224121000	10.960	1145.525	11.1499	9.6112	16.68000	2.69400	11.17000	2.83737	5.72500	2.58808	95.0	11.900	46.781
225123040	10.960	1145.525	40.3213	34.7569	29.08500	4.10635	20.42500	4.58692	10.72500	5.07224	95.0	11.900	30.042
226124000	10.960	1145.525	107.5875	92.7404	50.00000	6.03136	36.50000	7.51955	20.25000	8.65993	94.0	12.100	20.600
227123080	6.975	729.018	22.9069	19.7457	15.14500	2.21652	10.47000	2.47643	5.75000	2.22684	93.0	12.200	33.905
228123100	6.975	729.018	62.3473	53.7434	26.77500	3.59368	18.97500	4.23601	10.12500	4.57739	93.5	12.100	21.459
229121000	19.920	2082.012	15.4518	13.3195	40.40000	5.93084	27.55000	6.96811	13.60000	6.92794	69.8	19.000	58.369
230124000	19.920	2082.012	55.3708	47.7297	63.45000	8.39364	45.30000	9.82554	24.12500	11.25791	74.8	17.000	39.055
231122000	15.550	1625.265	29.8959	25.7702	37.47500	5.40309	25.95000	6.16603	13.30000	6.43309	77.2	16.200	42.489
232123030	15.550	1625.265	69.6483	60.0368	54.80000	7.03659	39.40000	8.42189	21.20000	9.69912	79.8	15.500	32.188
233124000	15.550	1625.265	107.8632	92.9781	68.45000	8.19260	49.95000	10.37698	27.67500	11.80225	82.0	14.800	26.180
234121000	4.650	486.012	10.3630	8.9329	13.77000	1.33695	11.04500	1.39863	8.32500	1.31136	83.6	14.400	41.630
235122000	4.650	486.012	40.5940	34.9920	28.88500	2.09589	24.58500	2.22077	20.22000	2.12787	85.4	14.000	29.613
236122000	4.650	486.012	108.6054	93.6178	43.06000	3.57860	35.52500	3.98536	27.65000	3.85985	87.0	13.600	19.742
237121000	2.860	298.923	21.4471	18.4874	16.05000	1.25653	13.55000	1.25325	11.15500	1.13321	89.5	13.000	28.326
238121000	2.860	298.923	53.0373	45.7182	29.78000	1.78930	26.15500	1.84980	22.53500	1.75673	90.5	12.750	23.175
239121000	.715	74.730	9.4625	8.1567	10.43000	.58303	9.27000	.58151	8.09500	.58887	87.0	13.600	21.888
240121000	.715	74.730	19.4954	16.8051	11.26500	.73884	9.80000	.73190	8.34500	.71753	88.0	13.300	18.884
241121000	.715	74.730	35.2674	30.4005	21.38000	.88459	19.63500	.86725	17.88500	.87589	87.5	13.400	15.450
242121000	.715	74.730	108.5542	93.5737	32.48000	1.99034	28.37500	2.13053	24.07000	2.15756	84.5	14.200	5.150
243121000	1.430	149.461	6.1191	5.2746	9.14750	.65591	7.85250	.64417	6.60500	.59877	92.5	12.300	29.613
244121000	2.145	224.192	7.1582	6.1704	17.76500	.76899	16.22500	.77702	14.67500	.76702	94.8	12.000	33.476
245121000	3.040	286.249	.0000	.0000	3.40600	.09449	3.21750	.09474	3.02850	.09352	57.0	1.175	100.000
246121000	6.080	572.498	.0000	.0000	29.90700	.19400	29.52100	.19350	29.13500	.19101	58.5	1.150	100.000
248121000	7.420	698.674	.0000	.0000	19.62500	.26638	19.09500	.26569	18.56500	.26227	60.0	1.125	100.000
249121000	11.660	1097.917	.0000	.0000	22.61000	.57297	21.47000	.57148	20.32500	.56908	61.0	1.110	100.000
250121000	16.540	1557.422	.0000	.0000	21.40000	1.06554	19.28000	1.06276	17.16000	1.04908	62.0	1.095	100.000
251121000	21.200	1996.213	.0000	.0000	22.43500	1.65359	19.14500	1.64928	15.85000	1.63301	62.5	1.087	100.000

TABLE XVI (CONT'D)

Run Code	Liquid Rate		Air Rate		Top Section		Middle Section		Bottom Section		Column Temperature	Liquid Viscosity	Liquid Saturation
	gpm	#/(ft^2 - min)	SCFM	#/(ft^2 - min)	Avg. Pres. psig	Pres. Drop psi/ft	Avg. Pres. psig	Pres. Drop psi/ft	Avg. Pres. psig	Pres. Drop psi/ft	°F	cp	%
252121000	.000	.000	109.3936	94.2972	13.25000	1.75914	9.25000	2.25586	4.55000	2.42478	48.2	1.000	.000
256121000	.760	71.562	107.4868	92.6536	25.17000	1.94008	21.15000	2.09544	16.95500	2.08333	61.0	1.110	4.721
257124000	21.200	1996.213	13.2228	11.3980	26.86000	3.88017	18.30000	4.71225	9.05000	4.50316	67.0	1.020	36.909
258124000	21.200	1996.213	51.5245	44.4141	43.96500	5.79513	31.60000	6.61720	17.00000	7.91765	68.0	1.005	24.034
259124000	21.200	1996.213	77.8279	67.0877	53.75000	6.28266	39.35000	8.17124	22.05000	9.05581	68.5	.998	15.879
261123000	3.040	286.249	45.5388	39.2545	16.52000	1.42742	13.58250	1.52145	10.55250	1.49693	70.0	.977	7.725
262124000	16.540	1557.422	30.5706	26.3518	42.83850	3.47959	35.33850	4.04902	27.25000	4.00831	73.5	.930	27.038
263124000	16.540	1557.422	61.5447	53.0515	39.70000	5.02613	28.85000	5.86524	16.25000	6.68052	73.5	.930	11.158
264124000	16.540	1557.422	107.4025	92.5809	54.00000	6.03136	40.15000	7.87046	23.65000	8.56096	67.0	1.020	12.446
265121000	4.940	465.155	9.4004	8.1031	8.99500	1.05046	6.85000	1.10286	4.62000	1.11836	68.5	.998	23.175
266123080	4.940	465.155	33.1624	28.5860	16.25000	1.50784	13.16250	1.59163	10.03250	1.52662	70.0	.977	15.450
267123040	4.940	465.155	107.8641	92.9788	33.25000	2.86489	27.16500	3.24343	20.66500	3.23139	70.0	.977	4.721
268121000	11.670	1098.858	10.7014	9.2246	14.81500	1.82448	10.90000	2.10547	6.76500	2.01405	71.5	.955	39.055
269123060	11.670	1098.858	38.7202	33.3768	24.93000	2.94531	18.60500	3.40385	11.73000	3.44418	72.0	.950	18.025
270124000	11.670	1098.858	108.0774	93.1627	43.83500	4.86027	33.15000	5.86524	19.60000	7.62074	71.0	.961	8.583
271122000	7.420	698.674	20.4509	17.6287	13.32500	1.73401	9.76000	1.84479	6.13000	1.77157	72.2	.946	23.175
272123060	7.420	698.674	49.6501	42.7984	23.34250	2.34971	18.36750	2.64437	12.90500	2.79592	73.0	.936	13.304
273131000	.000	.000	107.9447	93.0483	45.00000	5.02613	33.35000	6.66733	17.45000	9.15479	46.5	1.000	.000
274131000	21.200	1996.213	.0000	.0000	48.62500	8.16747	31.75000	8.77280	13.85000	9.05581	64.8	1.052	100.000
275131000	16.540	1557.422	.0000	.0000	32.10000	5.42822	20.85000	5.86524	9.00000	5.93824	65.0	1.050	100.000
276131000	11.660	1097.917	.0000	.0000	19.80000	3.11620	13.35000	3.35873	6.75000	3.21654	95.0	1.050	100.000
277131000	7.420	698.674	.0000	.0000	13.90500	1.41234	11.00500	1.49889	7.96000	1.53404	66.0	1.035	100.000
278131000	3.040	286.249	.0000	.0000	21.54750	.44481	20.73150	.37447	19.97900	.37509	67.0	1.020	100.000
281133000	3.040	286.249	27.7828	23.9488	30.91500	4.40792	21.36500	5.17846	10.20000	5.93824	60.5	1.118	24.782
282134000	3.040	286.249	46.7906	40.3335	40.40000	5.42822	28.65000	6.36655	14.50000	7.71971	61.0	1.110	19.565
283134000	3.040	286.249	69.2457	59.6898	52.22500	6.55910	38.10000	7.61981	20.27500	10.11975	61.5	1.105	17.826
284134000	3.040	286.249	102.3186	88.1987	67.75000	7.79051	50.00000	10.02606	26.50000	13.36104	61.5	1.103	16.956
285131000	.760	71.562	23.2787	20.0662	18.61500	2.32710	13.71000	2.59675	8.20500	2.88499	63.0	1.080	16.956
286131000	.760	71.562	58.3776	50.3215	35.75000	4.77482	25.85000	5.16342	13.90000	6.73000	60.5	1.118	8.260

TABLE XVI (CONT'D)

Run Code	Liquid Rate		Air Rate		Top Section		Middle Section		Bottom Section		Column Temperature °F	Liquid Viscosity cp	Liquid Saturation %
	gpm	#/(ft^2 - min)	SCFM	#/(ft^2 - min)	Avg. Pres. psig	Pres. Drop psi/ft	Avg. Pres. psig	Pres. Drop psi/ft	Avg. Pres. psig	Pres. Drop psi/ft			
288133000	11.660	1097.917	17.8726	15.4061	57.45000	6.48371	41.50000	9.52476	20.15000	11.72802	66.0	1.035	54.782
289133000	7.420	698.674	34.5473	29.7798	53.00000	7.03659	37.50000	8.52215	18.75000	10.14449	68.5	.998	26.521
290133000	7.420	698.674	58.2140	50.1804	70.50000	8.54443	51.00000	11.02867	26.00000	13.85589	49.6	1.325	30.000
291133000	4.940	465.155	13.4888	11.6273	29.19000	4.31242	19.99000	4.92279	9.54000	5.48297	53.5	1.238	42.608
292133000	4.940	465.155	51.7230	44.5852	53.40000	7.13711	37.65000	8.67254	18.75000	10.14449	56.5	1.185	24.347
293133000	4.940	465.155	75.5763	65.1467	66.00000	8.04181	48.00000	10.02606	24.75000	13.11361	58.5	1.150	24.347
294132000	.760	71.562	13.7065	11.8150	21.50000	2.01045	15.50000	4.01042	6.85000	4.60213	56.0	2.850	16.956
295132000	.760	71.562	13.7065	11.8150	19.25000	2.26176	12.60000	4.41146	5.10000	3.06809	56.0	2.850	16.956
296131000	3.040	286.249	20.5817	17.7414	41.60000	5.62927	28.90000	7.11850	13.35000	8.36302	65.0	2.400	30.000
297133000	7.420	698.674	38.1051	32.8466	66.95000	9.29835	47.00000	10.72789	23.65000	12.51979	71.0	2.150	35.652
301131000	.760	715.623	7.7192	6.6539	17.92500	2.94028	11.71500	3.29356	5.31500	3.08293	54.0	1.230	7.826
302131000	3.040	286.249	14.3767	12.3928	33.27500	4.49839	22.65000	6.16603	10.30000	6.13618	58.0	1.160	22.173
303131000	3.040	286.249	51.0442	44.0001	52.15000	6.68476	36.75000	8.77280	17.85000	10.04552	63.5	1.070	15.217
304133000	7.420	698.674	17.6266	15.1941	56.85000	6.18214	41.25000	9.47463	19.90000	11.77751	66.0	1.035	24.782
305133000	7.420	698.674	38.4785	33.1685	69.40000	8.14234	49.40000	11.93102	24.00000	13.36104	67.5	1.010	29.565
306131000	4.940	465.155	34.5044	29.7428	54.00000	7.53920	37.25000	9.27411	18.00000	9.89707	68.0	1.005	13.913
307132000	4.940	465.155	15.8960	13.7023	44.90000	6.13188	30.80000	8.20854	13.90000	8.80839	70.5	.970	20.869

XII. APPENDIX IV - TABULATION OF CALCULATED RESULTS

The following pages are a tabulation of the calculated results which are described in Subsection C of Section V. The following pages are referred to as Table XVII in the List of Tables.

The run codes and run numbers associated with the various systems of fluids and packings are indexed in Table IV.

The detailed meaning of the run code is explained in Table V.

Single-phase results are indicated by a zero rate for one of the phases.

Values which are infinite are reported as the number 999.9999.

TABLE XVII

TABULATION OF CALCULATED RESULTS

Run Code	Column Section	Mass Rates: Liquid #/(ft² - min)	Mass Rates: Air #/(ft² - min)	Reynolds Number: Liquid	Reynolds Number: Air	$\delta_{\ell g}$	δ_{ℓ}	δ_g	Liquid Saturation %	X	Φ_{ℓ}	Φ_g	$\frac{\delta_{\ell g}}{\delta_{\ell}+\delta_g}$
1111000	TOP	3177.933	.0000	3405.991	.000	4.60896	4.09253	.00000	100.0000	999.9999	1.0612	999.9999	1.1261
1111000	MID	3177.933	.0000	3405.991	.000	4.07559	4.09253	.00000	100.0000	999.9999	.9979	999.9999	.9958
1111000	BTM	3177.933	.0000	3405.991	.000	4.40419	4.09253	.00000	100.0000	999.9999	1.0373	999.9999	1.0761
2111000	TOP	3079.064	.0000	3324.866	.000	4.29734	3.84489	.00000	100.0000	999.9999	1.0572	999.9999	1.1176
2111000	MID	3079.064	.0000	3324.866	.000	3.78484	3.84489	.00000	100.0000	999.9999	.9921	999.9999	.9843
2111000	BTM	3079.064	.0000	3324.866	.000	4.00831	3.84489	.00000	100.0000	999.9999	1.0210	999.9999	1.0425
3111000	TOP	2956.655	.0000	3209.942	.000	3.94551	3.54947	.00000	100.0000	999.9999	1.0543	999.9999	1.1115
3111000	MID	2956.655	.0000	3209.942	.000	3.45899	3.54947	.00000	100.0000	999.9999	.9871	999.9999	.9745
3111000	BTM	2956.655	.0000	3209.942	.000	3.68665	3.54947	.00000	100.0000	999.9999	1.0191	999.9999	1.0386
4111000	TOP	2730.669	.0000	3003.562	.000	3.31724	3.03475	.00000	100.0000	999.9999	1.0455	999.9999	1.0930
4111000	MID	2730.669	.0000	3003.562	.000	2.90755	3.03475	.00000	100.0000	999.9999	.9788	999.9999	.9580
4111000	BTM	2730.669	.0000	3003.562	.000	3.21654	3.03475	.00000	100.0000	999.9999	1.0295	999.9999	1.0599
5111000	TOP	2457.602	.0000	2739.208	.000	2.71411	2.46684	.00000	100.0000	999.9999	1.0489	999.9999	1.1002
5111000	MID	2457.602	.0000	2739.208	.000	2.32103	2.46684	.00000	100.0000	999.9999	.9699	999.9999	.9408
5111000	BTM	2457.602	.0000	2739.208	.000	2.46931	2.46684	.00000	100.0000	999.9999	1.0005	999.9999	1.0010
6111000	TOP	2184.535	.0000	2451.175	.000	2.16626	1.95827	.00000	100.0000	999.9999	1.0517	999.9999	1.1062
6111000	MID	2184.535	.0000	2451.175	.000	1.95508	1.95827	.00000	100.0000	999.9999	.9991	999.9999	.9983
6111000	BTM	2184.535	.0000	2451.175	.000	2.04869	1.95827	.00000	100.0000	999.9999	1.0228	999.9999	1.0461
7111000	TOP	1911.468	.0000	2156.827	.000	1.71391	1.50840	.00000	100.0000	999.9999	1.0659	999.9999	1.1362
7111000	MID	1911.468	.0000	2156.827	.000	1.49889	1.50840	.00000	100.0000	999.9999	.9968	999.9999	.9936
7111000	BTM	1911.468	.0000	2156.827	.000	1.59837	1.50840	.00000	100.0000	999.9999	1.0293	999.9999	1.0596
8111000	TOP	1638.401	.0000	1848.709	.000	1.28166	1.11750	.00000	100.0000	999.9999	1.0709	999.9999	1.1469
8111000	MID	1638.401	.0000	1848.709	.000	1.12291	1.11750	.00000	100.0000	999.9999	1.0024	999.9999	1.0048
8111000	BTM	1638.401	.0000	1848.709	.000	1.19259	1.11750	.00000	100.0000	999.9999	1.0330	999.9999	1.0671
9111000	TOP	1365.334	.0000	1558.097	.000	.93486	.78446	.00000	100.0000	999.9999	1.0916	999.9999	1.1917
9111000	MID	1365.334	.0000	1558.097	.000	.82213	.78446	.00000	100.0000	999.9999	1.0237	999.9999	1.0480
9111000	BTM	1365.334	.0000	1558.097	.000	.87589	.78446	.00000	100.0000	999.9999	1.0566	999.9999	1.1165
10111000	TOP	1092.267	.0000	1253.600	.000	.61821	.51038	.00000	100.0000	999.9999	1.1005	999.9999	1.2112
10111000	MID	1092.267	.0000	1253.600	.000	.53138	.51038	.00000	100.0000	999.9999	1.0203	999.9999	1.0411
10111000	BTM	1092.267	.0000	1253.600	.000	.58392	.51038	.00000	100.0000	999.9999	1.0696	999.9999	1.1440
11111000	TOP	979.274	.0000	1123.918	.000	.47496	.41419	.00000	100.0000	999.9999	1.0708	999.9999	1.1467

TABLE XVII (CONT'D)

Run Code	Column Section	Mass Rates: Liquid #/(ft² - min)	Mass Rates: Liquid #/(ft² - min)	Reynolds Number: Liquid	Reynolds Number: Air	$\delta_{\ell g}$	δ_ℓ	δ_g	Liquid Saturation %	χ	Φ_ℓ	Φ_g	$\frac{\delta_{\ell g}}{\delta_\ell+\delta_g}$
11111000	MID	979.274	.0000	1123.918	.000	.40856	.41419	.00000	100.0000	999.9999	.9931	999.9999	.9863
11111000	BTM	979.274	.0000	1123.918	.000	.44536	.41419	.00000	100.0000	999.9999	1.0369	999.9999	1.0752
12111000	TOP	881.346	.0000	1017.339	.000	.39203	.33874	.00000	100.0000	999.9999	1.0757	999.9999	1.1573
12111000	MID	881.346	.0000	1017.339	.000	.34088	.33874	.00000	100.0000	999.9999	1.0031	999.9999	1.0063
12111000	BTM	881.346	.0000	1017.339	.000	.35629	.33874	.00000	100.0000	999.9999	1.0255	999.9999	1.0518
13111000	TOP	783.419	.0000	909.529	.000	.31915	.27084	.00000	100.0000	999.9999	1.0855	999.9999	1.1783
13111000	MID	783.419	.0000	909.529	.000	.28323	.27084	.00000	100.0000	999.9999	1.0226	999.9999	1.0457
13111000	BTM	783.419	.0000	909.529	.000	.30680	.27084	.00000	100.0000	999.9999	1.0643	999.9999	1.1327
14111000	TOP	685.492	.0000	795.837	.000	.25784	.21067	.00000	100.0000	999.9999	1.1062	999.9999	1.2238
14111000	MID	685.492	.0000	795.837	.000	.22057	.21067	.00000	100.0000	999.9999	1.0232	999.9999	1.0469
14111000	BTM	685.492	.0000	795.837	.000	.24198	.21067	.00000	100.0000	999.9999	1.0717	999.9999	1.1486
15111000	TOP	1092.267	8.5987	1163.203	451.515	1.33152	.51369	.01752	42.2155	5.4137	1.6099	8.7160	2.5065
15111000	MID	1092.267	8.5987	1163.203	451.515	1.72843	.51369	.02037	42.2155	5.0215	1.8343	9.2112	3.2363
15111000	BTM	1092.267	8.5987	1163.203	451.515	1.59409	.51369	.02470	42.2155	4.5595	1.7615	8.0321	2.9607
16111000	TOP	1092.267	14.8841	1246.478	775.417	1.92661	.51062	.04414	31.1377	3.4011	1.9424	6.6065	3.4728
16111000	MID	1092.267	14.8841	1246.478	775.417	1.94086	.51062	.05248	31.1377	3.1190	1.9496	6.0809	3.4466
16111000	BTM	1092.267	14.8841	1246.478	775.417	2.06048	.51062	.06530	31.1377	2.7962	2.0087	5.6170	3.5776
17112120	TOP	1092.267	22.5059	1253.600	1171.655	2.30802	.51038	.28811	27.5449	2.4067	2.1265	5.1179	3.8563
17112120	MID	1092.267	22.5059	1253.600	1171.655	2.25607	.51038	.10598	27.5449	2.1944	2.1024	4.6137	3.6602
17112120	BTM	1092.267	22.5059	1253.600	1171.655	2.77722	.51038	.13640	27.5449	1.9343	2.3326	4.5122	4.2938
18113120	TOP	1092.267	30.9394	1001.735	1649.655	2.60119	.52109	.13760	22.1556	1.9459	2.2342	4.3477	3.9489
18113120	MID	1092.267	30.9394	1001.735	1649.655	3.22016	.52109	.16876	22.1556	1.7571	2.4858	4.3682	4.6678
18113120	BTM	1092.267	30.9394	1001.735	1649.655	3.14962	.52109	.22423	22.1556	1.5244	2.4585	3.7478	4.2258
19113080	TOP	1092.267	43.9831	1015.648	2341.689	3.25272	.52036	.24635	18.2634	1.4533	2.5001	3.6336	4.2423
19113080	MID	1092.267	43.9831	1015.648	2341.689	3.46388	.52036	.30421	18.2634	1.3078	2.5800	3.3743	4.2008
19113080	BTM	1092.267	43.9831	1015.648	2341.689	4.39454	.52036	.41859	18.2634	1.1149	2.9060	3.2401	4.6802
20113060	TOP	1092.267	62.4287	1044.667	3314.012	4.09281	.51890	.42624	14.9700	1.1033	2.8084	3.0987	4.3303
20113060	MID	1092.267	62.4287	1044.667	3314.012	3.90071	.51890	.52880	14.9700	.9905	2.7417	2.7159	3.7231
20113060	BTM	1092.267	62.4287	1044.667	3314.012	5.32042	.51890	.73122	14.9700	.8423	3.2020	2.6974	4.2559

TABLE XVII (CONT'D)

Run Code	Column Section	Mass Rates: Liquid #/(ft² - min)	Mass Rates: Air #/(ft² - min)	Reynolds Number: Liquid	Reynolds Number: Air	$\delta_{\ell g}$	δ_ℓ	δ_g	Liquid Saturation %	X	Φ_ℓ	Φ_g	$\frac{\delta_{\ell g}}{\delta_\ell+\delta_g}$
21113040	TOP	1092.267	81.7700	1075.392	4328.084	4.58983	.51744	.64380	11.3772	.8965	2.9782	2.6700	3.9525
21113040	MID	1092.267	81.7700	1075.392	4328.084	4.87764	.51744	.80574	11.3772	.8013	3.0702	2.4604	3.6862
21113040	BTM	1092.267	81.7700	1075.392	4328.084	6.34396	.51744	1.14642	11.3772	.6718	3.5014	2.3523	3.8127
22111000	TOP	1365.334	9.2174	1406.283	485.755	2.14314	.79024	.01725	41.6167	6.7672	1.6468	11.1444	2.6540
22111000	MID	1365.334	9.2174	1406.283	485.755	2.07173	.79024	.02058	41.6167	6.1963	1.6191	10.0328	2.5550
22111000	BTM	1365.334	9.2174	1406.283	485.755	2.31397	.79024	.02577	41.6167	5.5375	1.7111	9.4757	2.8356
23112000	TOP	1365.334	20.1364	1443.290	1058.119	3.02250	.78872	.06258	32.3353	3.5501	1.9575	6.9496	3.5504
23112000	MID	1365.334	20.1364	1443.290	1058.119	2.78826	.78872	.07676	32.3353	3.2053	1.8802	6.0267	3.2216
23112000	BTM	1365.334	20.1364	1443.290	1058.119	3.29294	.78872	.10077	32.3353	2.7976	2.0432	5.7164	3.7020
24112080	TOP	1365.334	30.4056	1463.314	1595.435	3.37541	.78793	.12451	23.3532	2.5155	2.0697	5.2065	3.6993
24112080	MID	1365.334	30.4056	1463.314	1595.435	3.29556	.78793	.15387	23.3532	2.2628	2.0451	4.6278	3.4991
24112080	BTM	1365.334	30.4056	1463.314	1595.435	3.96145	.78793	.20703	23.3532	1.9508	2.2422	4.3742	3.9814
25113100	MID	1365.334	41.2570	1482.298	2161.715	3.87886	.78720	.20236	19.1616	1.9723	2.2114	4.3615	3.8903
25113100	BTM	1365.334	41.2570	1482.298	2161.715	4.84383	.78720	.25189	19.1616	1.7677	2.2197	3.9241	3.7329
25113100	TOP	1365.334	41.2570	1482.298	2161.715	3.84971	.78720	.34789	19.1616	1.5042	2.4805	3.7314	4.2673
26113060	TOP	1365.334	55.3549	1501.780	2896.230	4.48896	.78647	.32019	17.0658	1.5672	2.3890	3.7442	4.0562
26113060	MID	1365.334	55.3549	1501.780	2896.230	4.52644	.78647	.40113	17.0658	1.4002	2.3990	3.3591	3.8114
26113060	BTM	1365.334	55.3549	1501.780	2896.230	5.92337	.78647	.56698	17.0658	1.1777	2.7443	3.2322	4.3764
27113030	TOP	1365.334	70.0881	1501.780	3667.087	4.95731	.78647	.45760	14.9700	1.3109	2.5106	3.2913	3.9847
27113030	MID	1365.334	70.0881	1501.780	3667.087	5.34446	.78647	.57603	14.9700	1.1684	2.6068	3.0459	3.9225
27113030	BTM	1365.334	70.0881	1501.780	3667.087	6.90395	.78647	.83129	14.9700	.9726	2.9628	2.8818	4.2675
28114000	TOP	1365.334	80.9808	1523.473	4230.934	5.23375	.78567	.57796	14.9700	1.1659	2.5809	3.0092	3.8380
28114000	MID	1365.334	80.9808	1523.473	4230.934	5.57005	.78567	.72591	14.9700	1.0403	2.6626	2.7700	3.6848
28114000	BTM	1365.334	80.9808	1523.473	4230.934	7.49778	.78567	1.05030	14.9700	.8648	3.0891	2.6718	4.0837
29111000	TOP	1638.401	6.5417	1471.691	349.570	2.69640	1.13415	.00840	44.0119	11.6189	1.5419	17.9152	2.3599
29111000	MID	1638.401	6.5417	1471.691	349.570	2.53835	1.13415	.01023	44.0119	10.5253	1.4960	15.7461	2.2180
29111000	BTM	1638.401	6.5417	1471.691	349.570	2.82420	1.13415	.01321	44.0119	9.2640	1.5780	14.6187	2.4614
30111000	TOP	1638.401	15.7041	1523.473	836.099	3.41380	1.13137	.03586	35.6287	5.6164	1.7370	9.7561	2.9246
30111000	MID	1638.401	15.7041	1523.473	836.099	3.30391	1.13137	.04462	35.6287	5.0349	1.7088	8.6041	2.8094

TABLE XVII (CONT'D)

Run Code	Column Section	Mass Rates: Liquid #/(ft² - min)	Mass Rates: Air #/(ft² - min)	Reynolds Number: Liquid	Reynolds Number: Air	$\delta_{\ell g}$	δ_ℓ	δ_g	Liquid Saturation %	X	φ_ℓ	φ_g	$\frac{\delta_{\ell g}}{\delta_\ell+\delta_g}$
30111000	BTM	1638.401	15.7041	1523.473	836.099	3.62894	1.13137	.05978	35.6287	4.3500	1.7909	7.7907	3.0465
31112180	TOP	1638.401	35.3136	1544.930	1877.364	4.19133	1.13028	.14766	26.0479	2.7666	1.9256	5.3277	3.2797
31112180	MID	1638.401	35.3136	1544.930	1877.364	3.89883	1.13028	.18577	26.0479	2.4666	1.8572	4.5811	2.9625
31112180	BTM	1638.401	35.3136	1544.930	1877.364	4.77485	1.13028	.25718	26.0479	2.0963	2.0553	4.3088	3.4414
32113120	TOP	1638.401	39.7806	1589.711	2108.664	4.72334	1.12809	.16632	21.2574	2.6043	2.0462	5.3290	3.6490
32113120	MID	1638.401	39.7806	1589.711	2108.664	4.57979	1.12809	.21021	21.2574	2.3165	2.0148	4.6676	3.4220
32113120	BTM	1638.401	39.7806	1589.711	2108.664	5.76843	1.12809	.29772	21.2574	1.9465	2.2612	4.4016	4.0456
33113060	TOP	1638.401	53.1011	1625.841	2808.596	5.08131	1.12641	.26433	20.3592	2.0642	2.1239	4.3843	3.6536
33113060	MID	1638.401	53.1011	1625.841	2808.596	5.46820	1.12641	.33533	20.3592	1.8327	2.2032	4.0381	3.7408
33113060	BTM	1638.401	53.1011	1625.841	2808.596	6.68000	1.12641	.48553	20.3592	1.5231	2.4352	3.7091	4.1440
34113040	TOP	1638.401	68.3342	1648.648	3609.046	5.63157	1.12539	.39485	19.7604	1.6882	2.2369	3.7765	3.7043
34113040	MID	1638.401	68.3342	1648.648	3609.046	5.91676	1.12539	.49945	19.7604	1.5010	2.2929	3.4418	3.6414
34113040	BTM	1638.401	68.3342	1648.648	3609.046	7.86504	1.12539	.73016	19.7604	1.2414	2.6436	3.2820	4.2386
35114000	TOP	1638.401	80.1996	1687.539	4226.500	6.03106	1.12371	.50808	19.1616	1.4871	2.3166	3.4452	3.6959
35114000	MID	1638.401	80.1996	1687.539	4226.500	6.36533	1.12371	.64285	19.1616	1.3221	2.3800	3.1466	3.6032
35114000	BTM	1638.401	80.1996	1687.539	4226.500	8.60471	1.12371	.94554	19.1616	1.0901	2.7672	3.0166	4.1583
36111000	TOP	1911.468	10.0331	2075.217	525.697	3.07152	1.51139	.01668	48.2035	9.5167	1.4255	13.5668	2.0100
36111000	MID	1911.468	10.0331	2075.217	525.697	3.00276	1.51139	.02043	48.2035	8.5993	1.4095	12.1209	1.9602
36111000	BTM	1911.468	10.0331	2075.217	525.697	3.68371	1.51139	.02717	48.2035	7.4575	1.5611	11.6426	2.3942
37112240	TOP	1911.468	21.8763	2102.493	1144.593	3.97263	1.51036	.46019	33.5329	5.0091	1.6218	8.1239	2.5294
37112240	MID	1911.468	21.8763	2102.493	1144.593	3.90637	1.51036	.47518	33.5329	4.4821	1.6082	7.2082	2.4637
37112240	BTM	1911.468	21.8763	2102.493	1144.593	4.83220	1.51036	.10393	33.5329	3.8121	1.7886	6.8186	2.9933
38112120	TOP	1911.468	30.4194	2114.071	1590.437	4.51730	1.50994	.10230	29.3413	3.8418	1.7296	6.6450	2.8018
38112120	MID	1911.468	30.4194	2114.071	1590.437	4.55485	1.50994	.12880	29.3413	3.4238	1.7368	5.9466	2.7794
38112120	BTM	1911.468	30.4194	2114.071	1590.437	5.58096	1.50994	.18139	29.3413	2.8851	1.9225	5.5467	3.2997
39113050	TOP	1911.468	40.8259	2130.495	2132.996	5.11261	1.50934	.16446	27.5449	3.0294	1.8404	5.5755	3.0544
39113050	MID	1911.468	40.8259	2130.495	2132.996	5.19872	1.50934	.20840	27.5449	2.6911	1.8558	4.9945	3.0264
39113050	BTM	1911.468	40.8259	2130.495	2132.996	6.41439	1.50934	.29834	27.5449	2.2492	2.0615	4.6367	3.5483
40113030	TOP	1911.468	53.3573	2156.827	2783.723	5.66882	1.50840	.24990	24.8502	2.4568	1.9385	4.7627	3.2240

TABLE XVII (CONT'D)

Run Code	Column Section	Mass Rates: Liquid #/(ft^2 - min)	Mass Rates: Liquid #/(ft^2 - min)	Reynolds Number: Liquid	Reynolds Number: Air	$\delta_{\ell g}$	δ_ℓ	δ_g	Liquid Saturation %	X	Φ_ℓ	Φ_g	$\frac{\delta_{\ell g}}{\delta_\ell+\delta_g}$
40113030	MID	1911.468	53.3573	2156.827	2783.723	5.97403	1.50840	.31750	24.8502	2.1796	1.9900	4.3377	3.2718
40113030	BTM	1911.468	53.3573	2156.827	2783.723	7.44184	1.50840	.46157	24.8502	1.8077	2.2211	4.0153	3.7776
41113020	TOP	1911.468	66.7653	2181.336	3478.260	6.19358	1.50755	.35574	21.8562	2.0585	2.0269	4.1725	3.3239
41113020	MID	1911.468	66.7653	2181.336	3478.260	6.62772	1.50755	.45250	21.8562	1.8252	2.0967	3.8270	3.3813
41113020	BTM	1911.468	66.7653	2181.336	3478.260	8.46799	1.50755	.66596	21.8562	1.5045	2.3700	3.5658	3.8959
42114000	TOP	1911.468	81.2111	2181.336	4230.844	6.70103	1.50755	.48276	20.6586	1.7671	2.1083	3.7256	3.3668
42114000	MID	1911.468	81.2111	2181.336	4230.844	7.31430	1.50755	.61486	20.6586	1.5658	2.2026	3.4490	3.4462
42114000	BTM	1911.468	81.2111	2181.336	4230.844	9.20506	1.50755	.90813	20.6586	1.2884	2.4710	3.1837	3.8105
43111000	TOP	2184.535	13.8520	1948.314	740.756	4.15770	1.98076	.02357	43.7125	9.1654	1.4488	13.2789	2.0743
43111000	MID	2184.535	13.8520	1948.314	740.756	4.39688	1.98076	.02963	43.7125	8.1761	1.4898	12.1816	2.1870
43111000	BTM	2184.535	13.8520	1948.314	740.756	5.23778	1.98076	.04171	43.7125	6.8910	1.6261	11.2057	2.5897
44112000	TOP	2184.535	24.5952	1988.940	1312.354	5.28111	1.97852	.06162	36.2275	5.6662	1.6337	9.2573	2.5885
44112000	MID	2184.535	24.5952	1988.940	1312.354	5.25659	1.97852	.07898	36.2275	5.0048	1.6299	8.1578	2.5548
44112000	BTM	2184.535	24.5952	1988.940	1312.354	6.15530	1.97852	.11389	36.2275	4.1679	1.7638	7.3515	2.9417
45113060	TOP	2184.535	34.5559	2031.297	1839.781	5.81274	1.97628	.10775	29.0419	4.2826	1.7150	7.3447	2.7891
45113060	MID	2184.535	34.5559	2031.297	1839.781	5.81683	1.97628	.13803	29.0419	3.7838	1.7156	6.4915	2.7511
45113060	BTM	2184.535	34.5559	2031.297	1839.781	7.06422	1.97628	.20073	29.0419	3.1376	1.8906	5.9322	3.2448
46113040	TOP	2184.535	45.4424	2061.843	2415.835	6.36634	1.97472	.16715	25.7485	3.4371	1.7955	6.1714	2.9723
46113040	MID	2184.535	45.4424	2061.843	2415.835	6.68979	1.97472	.21509	25.7485	3.0299	1.8405	5.5768	3.0549
46113040	BTM	2184.535	45.4424	2061.843	2415.835	8.03958	1.97472	.31842	25.7485	2.4902	2.0177	5.0247	3.5059
47113030	TOP	2184.535	61.9352	2119.615	3283.015	7.05976	1.97190	.27555	24.5508	2.6750	1.8921	5.0615	3.1412
47113030	MID	2184.535	61.9352	2119.615	3283.015	7.59193	1.97190	.35455	24.5508	2.3583	1.9621	4.6274	3.2633
47113030	BTM	2184.535	61.9352	2119.615	3283.015	9.37047	1.97190	.53132	24.5508	1.9264	2.1799	4.1995	3.7433
48114000	TOP	2184.535	74.4574	2150.786	3941.029	7.66029	1.97044	.37383	23.9520	2.2958	1.9716	4.5267	3.2676
48114000	MID	2184.535	74.4574	2150.786	3941.029	7.68958	1.97044	.47899	23.9520	2.0282	1.9754	4.0067	3.1393
48114000	BTM	2184.535	74.4574	2150.786	3941.029	10.35757	1.97044	.71659	23.9520	1.6582	2.2926	3.8018	3.8546
49114000	TOP	2184.535	83.3342	2182.887	4404.465	8.01342	1.96898	.44716	24.2514	2.0984	2.0173	4.2332	3.3166
49114000	MID	2184.535	83.3342	2182.887	4404.465	7.94154	1.96898	.57164	24.2514	1.8559	2.0083	3.7272	3.1258
49114000	BTM	2184.535	83.3342	2182.887	4404.465	10.95270	1.96898	.85387	24.2514	1.5185	2.3585	3.5814	3.8800

TABLE XVII (CONT'D)

Run Code	Column Section	Mass Rates: Liquid #/(ft^2 - min)	Mass Rates: Liquid #/(ft^2 - min)	Reynolds Number: Liquid	Reynolds Number: Air	$\delta_{\ell g}$	δ_ℓ	δ_g	Liquid Saturation %	X	Φ_ℓ	Φ_g	$\frac{\delta_{\ell g}}{\delta_\ell+\delta_g}$
50111000	TOP	2457.602	11.9309	2653.792	625.589	4.64991	2.47001	.01800	49.4011	11.7121	1.3720	16.0698	1.8689
50111000	MID	2457.602	11.9309	2653.792	625.589	4.69737	2.47001	.02297	49.4011	10.3677	1.3790	14.2975	1.8842
50111000	BTM	2457.602	11.9309	2653.792	625.589	5.37143	2.47001	.03277	49.4011	8.6806	1.4746	12.8011	2.1461
51112000	TOP	2457.602	22.8354	2668.137	1196.489	5.59181	2.46947	.05221	38.3233	6.8767	1.5047	10.3480	2.2174
51112000	MID	2457.602	22.8354	2668.137	1196.489	5.56650	2.46947	.06701	38.3233	6.0704	1.5013	9.1139	2.1945
51112000	BTM	2457.602	22.8354	2668.137	1196.489	6.85722	2.46947	.09806	38.3233	5.0181	1.6663	8.3621	2.6707
52112001	TOP	2457.602	31.6598	2703.205	1656.478	6.19510	2.46815	.08968	31.4371	5.2459	1.5843	8.3111	2.4220
52112001	MID	2457.602	31.6598	2703.205	1656.478	6.00773	2.46815	.11510	31.4371	4.6306	1.5601	7.2245	2.3256
52112001	BTM	2457.602	31.6598	2703.205	1656.478	7.91590	2.46815	.17034	31.4371	3.8064	1.7908	6.8169	3.0001
53113081	TOP	2457.602	41.7914	2742.252	2183.439	6.84793	2.46673	.14064	27.8443	4.1879	1.6661	6.9777	2.6263
53113081	MID	2457.602	41.7914	2742.252	2183.439	6.77913	2.46673	.18134	27.8443	3.6881	1.6577	6.1141	2.5600
53113081	BTM	2457.602	41.7914	2742.252	2183.439	8.79099	2.46673	.27132	27.8443	3.0152	1.8878	5.6921	3.2106
54113040	TOP	2457.602	57.7381	2742.252	3016.591	7.67091	2.46673	.23545	27.5449	3.2367	1.7634	5.7078	2.8387
54113040	MID	2457.602	57.7381	2742.252	3016.591	7.71025	2.46673	.30347	27.5449	2.8509	1.7679	5.0404	2.7832
54113040	BTM	2457.602	57.7381	2742.252	3016.591	10.22476	2.46673	.45837	27.5449	2.3198	2.0359	4.7229	3.4955
55113023	TOP	2457.602	71.7867	2754.494	3747.891	8.42464	2.46629	.33082	26.3473	2.7303	1.8482	5.0463	3.0119
55113023	MID	2457.602	71.7867	2754.494	3747.891	8.40184	2.46629	.42612	26.3473	2.4057	1.8457	4.4403	2.9047
55113023	BTM	2457.602	71.7867	2754.494	3747.891	11.50616	2.46629	.64749	26.3473	1.9516	2.1599	4.2154	3.6952
56114003	TOP	2457.602	81.4124	2769.951	4247.394	8.86656	2.46574	.40588	23.9520	2.4647	1.8962	4.6738	3.0876
56114003	MID	2457.602	81.4124	2769.951	4247.394	9.34389	2.46574	.52787	23.9520	2.1612	1.9466	4.2072	3.1212
56114003	BTM	2457.602	81.4124	2769.951	4247.394	11.39676	2.46574	.80434	23.9520	1.7508	2.1498	3.7641	3.4851
57111001	TOP	2730.669	13.0797	2401.271	700.493	6.17748	3.06263	.01736	47.0059	13.2807	1.4202	18.8617	2.0056
57111001	MID	2730.669	13.0797	2401.271	700.493	5.85999	3.06263	.02260	47.0059	11.6407	1.3832	16.1020	1.8993
57111001	BTM	2730.669	13.0797	2401.271	700.493	6.99401	3.06263	.03343	47.0059	9.5705	1.5111	14.4628	2.2590
58111001	TOP	2730.669	21.6019	2470.497	1153.490	7.01570	3.05873	.04012	39.8203	8.7312	1.5144	13.2233	2.2639
58111001	MID	2730.669	21.6019	2470.497	1153.490	6.81626	3.05873	.05263	39.8203	7.6232	1.4928	11.3800	2.1907
58111001	BTM	2730.669	21.6019	2470.497	1153.490	7.95242	3.05873	.07913	39.8203	6.2169	1.6124	10.0242	2.5343
59111002	TOP	2730.669	31.1693	2539.122	1659.476	7.71729	3.05508	.07440	34.7305	6.4079	1.5893	10.1844	2.4659
59111002	MID	2730.669	31.1693	2539.122	1659.476	7.57612	3.05508	.09784	34.7305	5.5877	1.5747	8.7992	2.4028

TABLE XVII (CONT'D)

Run Code	Column Section	Mass Rates: Liquid #/(ft^2 - min)	Mass Rates: Air #/(ft^2 - min)	Reynolds Number: Liquid	Reynolds Number: Air	$\delta_{\ell g}$	δ_ℓ	δ_g	Liquid Saturation %	X	Φ_ℓ	Φ_g	$\frac{\delta_{\ell g}}{\delta_\ell+\delta_g}$
59111002	BTM	2730.669	31.1693	2539.122	1659.476	9.16738	3.05508	.14980	34.7305	4.5159	1.7322	7.8227	2.8604
60112003	TOP	2730.669	42.5416	2611.668	2258.311	8.43005	3.05143	.12488	28.7425	4.9430	1.6621	8.2158	2.6540
60112003	MID	2730.669	42.5416	2611.668	2258.311	8.26690	3.05143	.16408	28.7425	4.3123	1.6459	7.0979	2.5709
60112003	BTM	2730.669	42.5416	2611.668	2258.311	10.32895	3.05143	.25294	28.7425	3.4732	1.8398	6.3901	3.1258
61112005	TOP	2730.669	56.6116	2688.482	2996.454	9.14134	3.04778	.20024	29.3413	3.9012	1.7318	6.7564	2.8144
61112005	MID	2730.669	56.6116	2688.482	2996.454	9.11671	3.04778	.26268	29.3413	3.4062	1.7295	5.8912	2.7539
61112005	BTM	2730.669	56.6116	2688.482	2996.454	11.61818	3.04778	.40771	29.3413	2.7341	1.9524	5.3381	3.3622
62112006	TOP	2730.669	70.3295	2728.609	3717.126	9.79865	3.04595	.28592	30.2395	3.2638	1.7935	5.8540	2.9408
62112006	MID	2730.669	70.3295	2728.609	3717.126	9.62193	3.04595	.37355	30.2395	2.8555	1.7773	5.0752	2.8138
62112006	BTM	2730.669	70.3295	2728.609	3717.126	12.66128	3.04595	.57762	30.2395	2.2963	2.0388	4.6818	3.4941
63113066	TOP	2730.669	78.8467	2812.566	4155.201	9.73274	3.04230	.34480	26.6467	2.9703	1.7886	5.3128	2.8734
63113066	MID	2730.669	78.8467	2812.566	4155.201	10.05745	3.04230	.44746	26.6467	2.6074	1.8182	4.7409	2.8819
63113066	BTM	2730.669	78.8467	2812.566	4155.201	13.33843	3.04230	.69195	26.6467	2.0968	2.0938	4.3905	3.5719
64111000	TOP	734.455	7.9012	797.374	413.997	.99716	.24178	.01737	33.5329	3.7308	2.0308	7.5767	3.8477
64111000	MID	734.455	7.9012	797.374	413.997	.89354	.24178	.01954	33.5329	3.5173	1.9224	6.7617	3.4192
64111000	BTM	734.455	7.9012	797.374	413.997	1.07626	.24178	.02246	33.5329	3.2803	2.1098	6.9209	4.0728
65112000	TOP	734.455	20.9259	807.854	1094.869	1.53193	.24139	.09186	22.4550	1.6209	2.5191	4.0835	4.5968
65112000	MID	734.455	20.9259	807.854	1094.869	1.45688	.24139	.10725	22.4550	1.5001	2.4566	3.6855	4.1786
65112000	BTM	734.455	20.9259	807.854	1094.869	1.49317	.24139	.12876	22.4550	1.3691	2.4871	3.4052	4.0338
66113060	TOP	734.455	34.9299	818.614	1824.952	2.08907	.24099	.21090	17.6646	1.0689	2.9442	3.1472	4.6228
66113060	MID	734.455	34.9299	818.614	1824.952	2.06765	.24099	.25201	17.6646	.9779	2.9290	2.8643	4.1939
66113060	BTM	734.455	34.9299	818.614	1824.952	2.27396	.24099	.31657	17.6646	.8725	3.0717	2.6801	4.0783
67113050	TOP	734.455	46.8385	823.182	2445.377	2.45168	.24083	.33532	14.3712	.8474	3.1906	2.7039	4.2552
67113050	MID	734.455	46.8385	823.182	2445.377	2.57466	.24083	.40559	14.3712	.7705	3.2696	2.5195	3.9829
67113050	BTM	734.455	46.8385	823.182	2445.377	3.06623	.24083	.52934	14.3712	.6745	3.5681	2.4067	3.9811
68113040	TOP	734.455	59.4272	827.801	3100.395	2.85190	.24067	.48172	10.4790	.7068	3.4423	2.4331	3.9478
68113040	MID	734.455	59.4272	827.801	3100.395	3.06904	.24067	.58820	10.4790	.6396	3.5709	2.2842	3.7026
68113040	BTM	734.455	59.4272	827.801	3100.395	3.59361	.24067	.78167	10.4790	.5548	3.8641	2.1441	3.5150
69114001	TOP	734.455	80.8771	832.473	4216.453	3.48761	.24050	.77048	9.8802	.5587	3.8080	2.1275	3.4496

TABLE XVII (CONT'D)

Run Code	Column Section	Mass Rates: Liquid #/(ft² - min)	Mass Rates: Air #/(ft² - min)	Reynolds Number: Liquid	Reynolds Number: Air	$\delta_{\ell g}$	δ_{ℓ}	δ_{g}	Liquid Saturation %	X	Φ_{ℓ}	Φ_{g}	$\frac{\delta_{\ell g}}{\delta_{\ell}+\delta_{g}}$
69114001	MID	734.455	80.8771	832.473	4216.453	3.70810	.24050	.94860	9.8802	.5035	3.9265	1.9771	3.1183
69114001	BTM	734.455	80.8771	832.473	4216.453	4.85288	.24050	1.30489	9.8802	.4293	4.4919	1.9284	3.1402
72112000	TOP	489.637	24.9847	575.104	1297.001	1.13057	.11266	.13919	19.1616	.8996	3.1678	2.8499	4.4889
72112000	MID	489.637	24.9847	575.104	1297.001	1.25203	.11266	.15982	19.1616	.8395	3.3336	2.7988	4.5948
72112000	BTM	489.637	24.9847	575.104	1297.001	1.20665	.11266	.18869	19.1616	.7726	3.2726	2.5287	4.0040
73113080	TOP	489.637	37.7238	575.104	1958.309	1.53171	.11266	.27646	13.1736	.6383	3.6872	2.3538	3.9363
73113080	MID	489.637	37.7238	575.104	1958.309	1.64203	.11266	.32417	13.1736	.5895	3.8177	2.2506	3.7589
73113080	BTM	489.637	37.7238	575.104	1958.309	1.68532	.11266	.39569	13.1736	.5335	3.8677	2.0637	3.3152
74113080	TOP	489.637	51.2790	575.104	2661.983	2.03525	.11266	.44207	11.0778	.5048	4.2503	2.1456	3.6688
74113080	MID	489.637	51.2790	575.104	2661.983	2.04397	.11266	.52604	11.0778	.4627	4.2594	1.9711	3.2001
74113080	BTM	489.637	51.2790	575.104	2661.983	2.49270	.11266	.66553	11.0778	.4114	4.7037	1.9353	3.2031
75113080	TOP	489.637	64.5803	575.104	3352.476	2.39191	.11266	.63948	9.8802	.4197	4.6077	1.9340	3.1801
75113080	MID	489.637	64.5803	575.104	3352.476	2.29442	.11266	.76631	9.8802	.3834	4.5128	1.7303	2.6103
75113080	BTM	489.637	64.5803	575.104	3352.476	3.12089	.11266	.99097	9.8802	.3371	5.2632	1.7746	2.8278
76113080	TOP	489.637	81.1941	575.104	4214.927	2.85785	.11266	.89454	8.3832	.3548	5.0365	1.7873	2.8374
76113080	MID	489.637	81.1941	575.104	4214.927	2.84435	.11266	1.08454	8.3832	.3223	5.0246	1.6194	2.3758
76113080	BTM	489.637	81.1941	575.104	4214.927	3.83191	.11266	1.43906	8.3832	.2797	5.8320	1.6318	2.4694
79111000	TOP	244.818	20.1242	289.243	1043.938	.60226	.03277	.10851	15.5688	.5495	4.2866	2.3558	4.2626
79111000	MID	244.818	20.1242	289.243	1043.938	.58970	.03277	.11988	15.5688	.5228	4.2417	2.2178	3.8627
79111000	BTM	244.818	20.1242	289.243	1043.938	.52790	.03277	.13344	15.5688	.4955	4.0132	1.9889	3.1759
80112000	TOP	244.818	31.4334	289.243	1630.604	.94607	.03277	.23402	12.5748	.3742	5.3726	2.0106	3.5460
80112000	MID	244.818	31.4334	289.243	1630.604	.85739	.03277	.26464	12.5748	.3519	5.1146	1.7999	2.8827
80112000	BTM	244.818	31.4334	289.243	1630.604	.57424	.03277	.29825	12.5748	.3315	4.1857	1.3875	1.7347
81112000	TOP	244.818	44.5330	287.552	2311.788	1.26103	.03283	.41724	9.8802	.2805	6.1976	1.7384	2.8018
81112000	MID	244.818	44.5330	287.552	2311.788	1.19155	.03283	.48092	9.8802	.2612	6.0244	1.5740	2.3193
81112000	BTM	244.818	44.5330	287.552	2311.788	1.27014	.03283	.56866	9.8802	.2402	6.2199	1.4945	2.1116
82111000	TOP	244.818	57.3335	287.552	2976.282	1.57599	.03283	.62351	7.1856	.2294	6.9285	1.5898	2.4011
82111000	MID	244.818	57.3335	287.552	2976.282	1.59088	.03283	.73194	7.1856	.2117	6.9611	1.4742	2.0801
82111000	BTM	244.818	57.3335	287.552	2976.282	1.68893	.03283	.89292	7.1856	.1917	7.1724	1.3753	1.8243

TABLE XVII (CONT'D)

Run Code	Column Section	Mass Rates: Liquid #/(ft^2 - min)	Mass Rates: Air #/(ft^2 - min)	Reynolds Number: Liquid	Reynolds Number: Air	$\delta_{\ell g}$	δ_ℓ	δ_g	Liquid Saturation %	X	Φ_ℓ	Φ_g	$\frac{\delta_{\ell g}}{\delta_\ell+\delta_g}$
83111000	TOP	244.818	81.7340	287.552	4242.951	2.23906	.03283	1.05471	4.7904	.1764	8.2584	1.4570	2.0588
83111000	MID	244.818	81.7340	287.552	4242.951	2.20207	.03283	1.26358	4.7904	.1611	8.1898	1.3201	1.6985
83111000	BTM	244.818	81.7340	287.552	4242.951	2.64841	.03283	1.61008	4.7904	.1427	8.9816	1.2825	1.6120
86111000	TOP	97.927	21.4673	113.037	1116.788	.40156	.00755	.12943	9.8802	.2416	7.2893	1.7614	2.9313
86111000	MID	97.927	21.4673	113.037	1116.788	.40952	.00755	.14117	9.8802	.2313	7.3612	1.7031	2.7533
86111000	BTM	97.927	21.4673	113.037	1116.788	.43384	.00755	.15570	9.8802	.2203	7.5766	1.6692	2.6572
87111000	TOP	97.927	35.7516	110.373	1865.211	.73905	.00764	.30951	6.5868	.1572	9.8294	1.5452	2.3301
87111000	MID	97.927	35.7516	110.373	1865.211	.72603	.00764	.34651	6.5868	.1485	9.7425	1.4474	2.0499
87111000	BTM	97.927	35.7516	110.373	1865.211	.69166	.00764	.39285	6.5868	.1395	9.5091	1.3268	1.7269
88111000	TOP	97.927	51.4063	109.757	2683.859	1.08305	.00767	.55846	4.7904	.1171	11.8822	1.3925	1.9130
88111000	MID	97.927	51.4063	109.757	2683.859	1.09419	.00767	.63844	4.7904	.1096	11.9431	1.3091	1.6935
88111000	BTM	97.927	51.4063	109.757	2683.859	1.21333	.00767	.75164	4.7904	.1010	12.5766	1.2705	1.5979
89111000	TOP	97.927	66.2068	109.148	3459.051	1.48012	.00769	.83958	4.7904	.0957	13.8709	1.3277	1.7469
89111000	MID	97.927	66.2068	109.148	3459.051	1.44008	.00769	.97970	4.7904	.0886	13.6820	1.2124	1.4584
89111000	BTM	97.927	66.2068	109.148	3459.051	1.66365	.00769	1.18968	4.7904	.0804	14.7057	1.1825	1.3894
90111000	TOP	97.927	80.6201	109.148	4212.085	1.76158	.00769	1.13165	4.7904	.0824	15.1324	1.2476	1.5461
90111000	MID	97.927	80.6201	109.148	4212.085	1.76092	.00769	1.33412	4.7904	.0759	15.1295	1.1488	1.3123
90111000	BTM	97.927	80.6201	109.148	4212.085	2.17335	.00769	1.66242	4.7904	.0680	16.8082	1.1433	1.3013
99111000	TOP	1092.267	.0000	1275.466	.000	.61318	.50965	.00000	100.0000	999.9999	1.0968	999.9999	1.2031
99111000	MID	1092.267	.0000	1275.466	.000	.50380	.50965	.00000	100.0000	999.9999	.9942	999.9999	.9885
99111000	BTM	1092.267	.0000	1275.466	.000	.56660	.50965	.00000	100.0000	999.9999	1.0543	999.9999	1.1117
102111000	TOP	1092.267	5.4092	1275.466	281.004	.93789	.50965	.00231	63.7724	14.8289	1.3565	20.1163	1.8319
102111000	MID	1092.267	5.4092	1275.466	281.004	.81973	.50965	.00237	63.7724	14.6510	1.2682	18.5809	1.6009
102111000	BTM	1092.267	5.4092	1275.466	281.004	.87643	.50965	.00243	63.7724	14.4749	1.3113	18.9819	1.7115
103111000	TOP	1092.267	4.8340	1260.805	251.481	1.08568	.51013	.00246	60.7784	14.3893	1.4588	20.9917	2.1179
103111000	MID	1092.267	4.8340	1260.805	251.481	.96710	.51013	.00255	60.7784	14.1314	1.3768	19.4572	1.8863
103111000	BTM	1092.267	4.8340	1260.805	251.481	1.04154	.51013	.00265	60.7784	13.8716	1.4288	19.8208	2.0311
104111000	TOP	1092.267	4.0877	1253.600	212.804	1.21391	.51038	.00261	53.2934	13.9600	1.5422	21.5294	2.3663
104111000	MID	1092.267	4.0877	1253.600	212.804	1.10494	.51038	.00277	53.2934	13.5568	1.4713	19.9471	2.1532

TABLE XVII (CONT'D)

Run Code	Column Section	Mass Rates: Liquid #/(ft² - min)	Mass Rates: Air #/(ft² - min)	Reynolds Number: Liquid	Reynolds Number: Air	$\delta_{\ell g}$	δ_ℓ	δ_g	Liquid Saturation %	X	Φ_ℓ	Φ_g	$\frac{\delta_{\ell g}}{\delta_\ell+\delta_g}$
104111000	BTM	1092.267	4.0877	1253.600	212.804	1.21677	.51038	.00295	53.2934	13.1373	1.5440	20.2845	2.3703
105111000	TOP	1092.267	5.5632	1231.089	290.240	1.32745	.51116	.00469	48.2035	10.4338	1.6115	16.8141	2.5732
105111000	MID	1092.267	5.5632	1231.089	290.240	1.29833	.51116	.00504	48.2035	10.0685	1.5937	16.0465	2.5151
105111000	BTM	1092.267	5.5632	1231.089	290.240	1.39254	.51116	.00545	48.2035	9.6781	1.6505	15.9742	2.6955
108111000	TOP	1638.401	.0000	1826.139	.000	1.26658	1.11830	.00000	100.0000	999.9999	1.0642	999.9999	1.1325
108111000	MID	1638.401	.0000	1826.139	.000	1.10286	1.11830	.00000	100.0000	999.9999	.9930	999.9999	.9861
108111000	BTM	1638.401	.0000	1826.139	.000	1.17775	1.11830	.00000	100.0000	999.9999	1.0262	999.9999	1.0531
109111000	TOP	1638.401	5.0227	1802.137	262.795	1.84447	1.11918	.00242	67.6646	21.4681	1.2837	27.5600	1.6444
109111000	MID	1638.401	5.0227	1802.137	262.795	1.66383	1.11918	.00256	67.6646	20.8979	1.2192	25.4805	1.4832
109111000	BTM	1638.401	5.0227	1802.137	262.795	1.73959	1.11918	.00270	67.6646	20.3235	1.2467	25.3380	1.5505
110111000	TOP	1638.401	4.9960	1778.758	261.774	2.05795	1.12005	.00302	58.9820	19.2522	1.3554	26.0962	1.8324
110111000	MID	1638.401	4.9960	1778.758	261.774	1.88168	1.12005	.00326	58.9820	18.5182	1.2961	24.0023	1.6750
110111000	BTM	1638.401	4.9960	1778.758	261.774	2.02342	1.12005	.00355	58.9820	17.7539	1.3440	23.8626	1.8008
111111000	TOP	1638.401	4.2818	1744.805	224.839	2.42836	1.12137	.00445	49.4011	15.8692	1.4715	23.3527	2.1569
111111000	MID	1638.401	4.2818	1744.805	224.839	2.33122	1.12137	.00538	49.4011	14.4275	1.4418	20.8021	2.0689
111111000	BTM	1638.401	4.2818	1744.805	224.839	2.44685	1.12137	.00683	49.4011	12.8049	1.4771	18.9150	2.1687
112111000	TOP	1638.401	6.4024	1708.568	336.920	2.73047	1.12283	.00829	44.9101	11.6357	1.5594	18.1449	2.4139
112111000	MID	1638.401	6.4024	1708.568	336.920	2.60743	1.12283	.01014	44.9101	10.5202	1.5238	16.0314	2.3013
112111000	BTM	1638.401	6.4024	1708.568	336.920	2.85781	1.12283	.01317	44.9101	9.2311	1.5953	14.7269	2.5156
113111000	TOP	2184.535	.0000	2611.668	.000	2.13610	1.95291	.00000	100.0000	999.9999	1.0458	999.9999	1.0938
113111000	MID	2184.535	.0000	2611.668	.000	1.84479	1.95291	.00000	100.0000	999.9999	.9719	999.9999	.9446
113111000	BTM	2184.535	.0000	2611.668	.000	1.94972	1.95291	.00000	100.0000	999.9999	.9991	999.9999	.9983
116111000	TOP	2184.535	3.5132	2550.932	182.511	3.13243	1.95486	.00290	59.8802	25.9471	1.2658	32.8451	1.6000
116111000	MID	2184.535	3.5132	2550.932	182.511	2.91828	1.95486	.00358	59.8802	23.3651	1.2218	28.5478	1.4901
116111000	BTM	2184.535	3.5132	2550.932	182.511	3.26447	1.95486	.00471	59.8802	20.3694	1.2922	26.3225	1.6659
117111000	TOP	2184.535	4.9441	2521.611	257.208	3.57992	1.95583	.00466	52.9940	20.4741	1.3529	27.6997	1.8260
117111000	MID	2184.535	4.9441	2521.611	257.208	3.44473	1.95583	.00583	52.9940	18.3008	1.3271	24.2874	1.7560
117111000	BTM	2184.535	4.9441	2521.611	257.208	3.79860	1.95583	.00790	52.9940	15.7309	1.3936	21.9230	1.9343
118111000	TOP	2184.535	8.7758	2507.201	456.868	4.14746	1.95632	.01152	42.5149	13.0274	1.4560	18.9683	2.1076

TABLE XVII (CONT'D)

Run Code	Column Section	Mass Rates: Liquid #/(ft^2 - min)	Mass Rates: Air #/(ft^2 - min)	Reynolds Number: Liquid	Reynolds Number: Air	$\delta_{\ell g}$	δ_ℓ	δ_g	Liquid Saturation %	X	Φ_ℓ	Φ_g	$\frac{\delta_{\ell g}}{\delta_\ell + \delta_g}$
118111000	MID	2184.535	8.7758	2507.201	456.868	3.94049	1.95632	.01460	42.5149	11.5747	1.4192	16.4272	1.9993
118111000	BTM	2184.535	8.7758	2507.201	456.868	4.54472	1.95632	.02032	42.5149	9.8118	1.5241	14.9548	2.2992
119111000	TOP	2184.535	12.2058	2448.439	637.251	4.52254	1.95837	.01964	38.6227	9.9836	1.5196	15.1716	2.2864
119111000	MID	2184.535	12.2058	2448.439	637.251	4.42985	1.95837	.02512	38.6227	8.8282	1.5039	13.2776	2.2333
119111000	BTM	2184.535	12.2058	2448.439	637.251	4.82963	1.95837	.03540	38.6227	7.4374	1.5703	11.6798	2.4223
120111000	TOP	2730.669	.0000	3256.831	.000	3.35243	3.02611	.00000	100.0000	999.9999	1.0525	999.9999	1.1078
120111000	MID	2730.669	.0000	3256.831	.000	2.89753	3.02611	.00000	100.0000	999.9999	.9785	999.9999	.9575
120111000	BTM	2730.669	.0000	3256.831	.000	2.99881	3.02611	.00000	100.0000	999.9999	.9954	999.9999	.9909
122111000	TOP	2730.669	3.8972	3284.134	201.026	4.30762	3.02526	.00287	61.9760	32.4657	1.1932	38.7402	1.4225
122111000	MID	2730.669	3.8972	3284.134	201.026	4.04531	3.02526	.00364	61.9760	28.8241	1.1563	33.3312	1.3355
122111000	BTM	2730.669	3.8972	3284.134	201.026	4.58496	3.02526	.00505	61.9760	24.4665	1.2310	30.1202	1.5130
123111000	TOP	2730.669	4.7216	3284.134	243.586	4.62946	3.02526	.00370	55.0898	28.5740	1.2370	35.3471	1.5283
123111000	MID	2730.669	4.7216	3284.134	243.586	4.51662	3.02526	.00474	55.0898	25.2619	1.2218	30.8667	1.4906
123111000	BTM	2730.669	4.7216	3284.134	243.586	5.04981	3.02526	.00671	55.0898	21.2242	1.2919	27.4213	1.6655
124111000	TOP	2730.669	7.2553	3344.209	374.774	5.09240	3.02343	.00717	50.5988	20.5235	1.2978	26.6356	1.6803
124111000	MID	2730.669	7.2553	3344.209	374.774	4.94322	3.02343	.00922	50.5988	18.1059	1.2786	23.1513	1.6299
124111000	BTM	2730.669	7.2553	3344.209	374.774	5.72305	3.02343	.01326	50.5988	15.0992	1.3758	20.7738	1.8846
125111000	TOP	2730.669	10.7246	3344.209	553.983	5.64544	3.02343	.01356	43.7125	14.9266	1.3664	20.3967	1.8588
125111000	MID	2730.669	10.7246	3344.209	553.983	5.40951	3.02343	.01759	43.7125	13.1074	1.3376	17.5325	1.7788
125111000	BTM	2730.669	10.7246	3344.209	553.983	6.33636	3.02343	.02577	43.7125	10.8305	1.4476	15.6790	2.0780
126111000	TOP	2730.669	14.4738	3303.918	748.702	6.10355	3.02465	.02202	40.4191	11.7183	1.4205	16.6463	2.0033
126111000	MID	2730.669	14.4738	3303.918	748.702	5.97668	3.02465	.02873	40.4191	10.2600	1.4056	14.4225	1.9573
126111000	BTM	2730.669	14.4738	3303.918	748.702	6.91584	3.02465	.04267	40.4191	8.4183	1.5121	12.7295	2.2546
127111000	TOP	734.455	.0000	938.385	.000	.28045	.23723	.00000	100.0000	999.9999	1.0872	999.9999	1.1822
127111000	MID	734.455	.0000	938.385	.000	.24212	.23723	.00000	100.0000	999.9999	1.0102	999.9999	1.0206
127111000	BTM	734.455	.0000	938.385	.000	.24693	.23723	.00000	100.0000	999.9999	1.0202	999.9999	1.0408
130111000	TOP	734.455	5.3371	787.162	280.047	.64615	.24217	.00230	54.4910	10.2500	1.6334	16.7427	2.6429
130111000	MID	734.455	5.3371	787.162	280.047	.57377	.24217	.00235	54.4910	10.1510	1.5392	15.6247	2.3464
130111000	BTM	734.455	5.3371	787.162	280.047	.63311	.24217	.00239	54.4910	10.0510	1.6168	16.2512	2.5886

TABLE XVII (CONT'D)

Run Code	Column Section	Mass Rates: Liquid #/(ft² - min)	Mass Rates: Air #/(ft² - min)	Reynolds Number: Liquid	Reynolds Number: Air	$\delta_{\ell g}$	δ_{ℓ}	δ_g	Liquid Saturation %	X	Φ_{ℓ}	Φ_g	$\frac{\delta_{\ell g}}{\delta_{\ell}+\delta_g}$
134111000	TOP	489.637	.0000	636.935	.000	.16586	.11084	.00000	100.0000	999.9999	1.2232	999.9999	1.4962
134111000	MID	489.637	.0000	636.935	.000	.12532	.11084	.00000	100.0000	999.9999	1.0632	999.9999	1.1305
134111000	BTM	489.637	.0000	636.935	.000	.11925	.11084	.00000	100.0000	999.9999	1.0372	999.9999	1.0758
135111000	TOP	489.637	.0000	673.581	.000	.10404	.10993	.00000	100.0000	999.9999	.9728	999.9999	.9464
135111000	MID	489.637	.0000	673.581	.000	.11580	.10993	.00000	100.0000	999.9999	1.0263	999.9999	1.0533
135111000	BTM	489.637	.0000	673.581	.000	.12618	.10993	.00000	100.0000	999.9999	1.0713	999.9999	1.1478
140111000	TOP	489.637	8.9300	538.569	467.230	.78399	.11392	.01712	28.4431	2.5794	2.6232	6.7666	5.9824
140111000	MID	489.637	8.9300	538.569	467.230	.78113	.11392	.01856	28.4431	2.4770	2.6184	6.4861	5.8956
140111000	BTM	489.637	8.9300	538.569	467.230	.78687	.11392	.02029	28.4431	2.3692	2.6280	6.2264	5.8624
143111000	TOP	244.818	.0000	332.239	.000	.04372	.03157	.00000	100.0000	999.9999	1.1767	999.9999	1.3848
143111000	MID	244.818	.0000	332.239	.000	.03960	.03157	.00000	100.0000	999.9999	1.1199	999.9999	1.2542
143111000	BTM	244.818	.0000	332.239	.000	.04453	.03157	.00000	100.0000	999.9999	1.1876	999.9999	1.4104
144112000	TOP	244.818	2.3192	318.467	118.963	.21382	.03192	.00289	28.7425	3.3225	2.5880	8.5989	6.1415
144112000	MID	244.818	2.3192	318.467	118.963	.11019	.03192	.00305	28.7425	3.2349	1.8578	6.0101	3.1506
144112000	BTM	244.818	2.3192	318.467	118.963	.15872	.03192	.00321	28.7425	3.1494	2.2297	7.0226	4.5164
150111000	TOP	97.927	.0000	132.895	.000	.00402	.00699	.00000	100.0000	999.9999	.7584	999.9999	.5752
150111000	MID	97.927	.0000	132.895	.000	.00401	.00699	.00000	100.0000	999.9999	.7574	999.9999	.5737
150111000	BTM	97.927	.0000	132.895	.000	.00791	.00699	.00000	100.0000	999.9999	1.0642	999.9999	1.1326
154111000	TOP	97.927	8.6192	124.170	443.351	.15243	.00721	.02532	14.0718	.5337	4.5958	2.4531	4.6836
154111000	MID	97.927	8.6192	124.170	443.351	.14454	.00721	.02686	14.0718	.5183	4.4753	2.3195	4.2411
154111000	BTM	97.927	8.6192	124.170	443.351	.11164	.00721	.02853	14.0718	.5028	3.9331	1.9778	3.1223
155111000	TOP	.000	17.2929	.000	912.655	.17256	.00000	.08837		.0000	999.9999	1.3973	1.9527
155111000	MID	.000	17.2929	.000	912.655	.16095	.00000	.09461	.0000	.0000	999.9999	1.3042	1.7011
155111000	BTM	.000	17.2929	.000	912.655	.13348	.00000	.10160	.0000	.0000	999.9999	1.1461	1.3137
156111000	TOP	.000	34.6671	.000	1864.900	.45402	.00000	.28562	.0000	.0000	999.9999	1.2607	1.5895
156111000	MID	.000	34.6671	.000	1864.900	.51687	.00000	.31324	.0000	.0000	999.9999	1.2845	1.6500
156111000	BTM	.000	34.6671	.000	1864.900	.56895	.00000	.34941	.0000	.0000	999.9999	1.2760	1.6282
157111000	TOP	.000	52.8243	.000	2858.691	.84606	.00000	.59854	.0000	.0000	999.9999	1.1889	1.4135
157111000	MID	.000	52.8243	.000	2858.691	.94298	.00000	.67875	.0000	.0000	999.9999	1.1786	1.3892

TABLE XVII (CONT'D)

Run Code	Column Section	Mass Rates: Liquid #/(ft^2 - min)	Mass Rates: Air #/(ft^2 - min)	Reynolds Number: Liquid	Reynolds Number: Air	$\delta_{\ell g}$	δ_ℓ	δ_g	Liquid Saturation %	X	Φ_ℓ	Φ_g	$\frac{\delta_{\ell g}}{\delta_\ell + \delta_g}$
157111000	BTM	.000	52.8243	.000	2858.691	.80153	.00000	.78264	.0000	.0000	999.9999	1.0119	1.0241
158111000	TOP	.000	69.8200	.000	3795.535	1.20794	.00000	.92121	.0000	.0000	999.9999	1.1460	1.3133
158111000	MID	.000	69.8200	.000	3795.535	1.28387	.00000	1.06333	.0000	.0000	999.9999	1.0997	1.2093
158111000	BTM	.000	69.8200	.000	3795.535	1.34587	.00000	1.26870	.0000	.0000	999.9999	1.0308	1.0625
159111000	TOP	.000	85.9709	.000	4673.529	1.54972	.00000	1.23792	.0000	.0000	999.9999	1.1188	1.2518
159111000	MID	.000	85.9709	.000	4673.529	1.65483	.00000	1.44677	.0000	.0000	999.9999	1.0694	1.1438
159111000	BTM	.000	85.9709	.000	4673.529	2.19207	.00000	1.80163	.0000	.0000	999.9999	1.1030	1.2167
160111000	TOP	.000	103.2608	.000	5530.178	2.07244	.00000	1.63520	.0000	.0000	999.9999	1.1257	1.2673
160111000	MID	.000	103.2608	.000	5530.178	1.95561	.00000	1.93832	.0000	.0000	999.9999	1.0044	1.0089
160111000	BTM	.000	103.2608	.000	5530.178	2.50382	.00000	2.43330	.0000	.0000	999.9999	1.0143	1.0289
161111000	TOP	.000	114.2911	.000	6227.164	2.17799	.00000	1.83694	.0000	.0000	999.9999	1.0897	1.1875
161111000	MID	.000	114.2911	.000	6227.164	2.22130	.00000	2.18198	.0000	.0000	999.9999	1.0097	1.0196
161111000	BTM	.000	114.2911	.000	6227.164	3.07786	.00000	2.80398	.0000	.0000	999.9999	1.0485	1.0994
162111000	TOP	71.562	.0000	5.245	.000	.04523	.04570	.00000	100.0000	999.9999	.9948	999.9999	.9896
162111000	MID	71.562	.0000	5.245	.000	.04511	.04570	.00000	100.0000	999.9999	.9935	999.9999	.9870
162111000	BTM	71.562	.0000	5.245	.000	.04453	.04570	.00000	100.0000	999.9999	.9871	999.9999	.9743
163111000	TOP	286.249	.0000	22.112	.000	.25985	.19799	.00000	100.0000	999.9999	1.1456	999.9999	1.3124
163111000	MID	286.249	.0000	22.112	.000	.16342	.19799	.00000	100.0000	999.9999	.9085	999.9999	.8254
163111000	BTM	286.249	.0000	22.112	.000	.19398	.19799	.00000	100.0000	999.9999	.9898	999.9999	.9797
164111000	TOP	465.155	.0000	38.132	.000	.34931	.33882	.00000	100.0000	999.9999	1.0153	999.9999	1.0309
164111000	MID	465.155	.0000	38.132	.000	.30378	.33882	.00000	100.0000	999.9999	.9468	999.9999	.8966
164111000	BTM	465.155	.0000	38.132	.000	.33353	.33882	.00000	100.0000	999.9999	.9921	999.9999	.9843
165111000	TOP	698.674	.0000	61.012	.000	.59308	.54953	.00000	100.0000	999.9999	1.0388	999.9999	1.0792
165111000	MID	698.674	.0000	61.012	.000	.52135	.54953	.00000	100.0000	999.9999	.9740	999.9999	.9487
165111000	BTM	698.674	.0000	61.012	.000	.49485	.54953	.00000	100.0000	999.9999	.9489	999.9999	.9005
166111000	TOP	1098.858	.0000	107.660	.000	1.09569	.97548	.00000	100.0000	999.9999	1.0598	999.9999	1.1232
166111000	MID	1098.858	.0000	107.660	.000	1.10286	.97548	.00000	100.0000	999.9999	1.0632	999.9999	1.1305
166111000	BTM	1098.858	.0000	107.660	.000	1.00950	.97548	.00000	100.0000	999.9999	1.0172	999.9999	1.0348
167111000	TOP	1557.422	.0000	156.402	.000	1.90490	1.64522	.00000	100.0000	999.9999	1.0760	999.9999	1.1578

TABLE XVII (CONT'D)

Run Code	Column Section	Mass Rates: Liquid #/(ft² - min)	Mass Rates: Air #/(ft² - min)	Reynolds Number: Liquid	Reynolds Number: Air	$\delta_{\ell g}$	δ_{ℓ}	δ_{g}	Liquid Saturation %	X	Φ_{ℓ}	Φ_{g}	$\frac{\delta_{\ell g}}{\delta_{\ell}+\delta_{g}}$
167111000	MID	1557.422	.0000	156.402	.000	1.73952	1.64522	.00000	100.0000	999.9999	1.0282	999.9999	1.0573
167111000	BTM	1557.422	.0000	156.402	.000	1.86064	1.64522	.00000	100.0000	999.9999	1.0634	999.9999	1.1309
168111000	TOP	107.343	.0000	9.624	.000	.23974	.05810	.00000	100.0000	999.9999	2.0312	999.9999	4.1260
168111000	MID	107.343	.0000	9.624	.000	.17094	.05810	.00000	100.0000	999.9999	1.7152	999.9999	2.9419
168111000	BTM	107.343	.0000	9.624	.000	.24841	.05810	.00000	100.0000	999.9999	2.0676	999.9999	4.2752
170111000	TOP	107.343	22.6713	9.711	1171.086	.68045	.05762	.06902	17.3652	.9137	3.4362	3.1398	5.3727
170111000	MID	107.343	22.6713	9.711	1171.086	.71784	.05762	.07284	17.3652	.8894	3.5294	3.1390	5.5017
170111000	BTM	107.343	22.6713	9.711	1171.086	.69408	.05762	.07718	17.3652	.8640	3.4704	2.9986	5.1483
171111000	TOP	107.343	33.5904	7.383	1770.207	1.09221	.07437	.24424	14.9700	.5518	3.8321	2.1146	3.4279
171111000	MID	107.343	33.5904	7.383	1770.207	.95305	.07437	.27688	14.9700	.5182	3.5797	1.8552	2.7132
171111000	BTM	107.343	33.5904	7.383	1770.207	1.03994	.07437	.31904	14.9700	.4828	3.7393	1.8054	2.6433
172111000	TOP	107.343	101.4614	7.383	5346.990	2.26607	.07437	1.31271	8.6826	.2380	5.5198	1.3138	1.6336
172111000	MID	107.343	101.4614	7.383	5346.990	2.64012	.07437	1.54094	8.6826	.2196	5.9580	1.3089	1.6344
172111000	BTM	107.343	101.4614	7.383	5346.990	2.91279	.07437	1.91453	8.6826	.1970	6.2581	1.2334	1.4645
173111000	TOP	698.674	9.0357	61.012	468.063	1.88214	.54953	.01754	35.9281	5.5972	1.8506	10.3586	3.3190
173111000	MID	698.674	9.0357	61.012	468.063	1.97676	.54953	.02076	35.9281	5.1445	1.8966	9.7573	3.4662
173111000	BTM	698.674	9.0357	61.012	468.063	2.14568	.54953	.02583	35.9281	4.6122	1.9760	9.1138	3.7292
174111000	TOP	698.674	33.2217	62.367	1718.494	3.18311	.54174	.14729	23.0538	1.9178	2.4239	4.6487	4.6196
174111000	MID	698.674	33.2217	62.367	1718.494	3.52485	.54174	.18128	23.0538	1.7287	2.5507	4.4095	4.8751
174111000	BTM	698.674	33.2217	62.367	1718.494	4.01953	.54174	.24465	23.0538	1.4880	2.7238	4.0533	5.1113
176111000	TOP	1557.422	11.9016	123.151	621.814	5.18303	1.83266	.01772	43.7125	10.1681	1.6817	17.0998	2.8010
176111000	MID	1557.422	11.9016	123.151	621.814	5.01849	1.83266	.02309	43.7125	8.9078	1.6548	14.7406	2.7042
176111000	BTM	1557.422	11.9016	123.151	621.814	5.09923	1.83266	.03313	43.7125	7.4368	1.6680	12.4051	2.7330
177111000	TOP	1557.422	39.8480	128.199	2075.954	7.25358	1.79795	.11681	34.4311	3.9232	2.0085	7.8800	3.7882
177111000	MID	1557.422	39.8480	128.199	2075.954	5.98067	1.79795	.14552	34.4311	3.5149	1.8238	6.4107	3.0773
177111000	BTM	1557.422	39.8480	128.199	2075.954	7.87946	1.79795	.19642	34.4311	3.0254	2.0934	6.3335	3.9508
178114000	TOP	1534.824	83.4870	107.037	4393.376	8.46577	1.90876	.43451	24.2514	2.0959	2.1059	4.4139	3.6127
178114000	MID	1534.824	83.4870	107.037	4393.376	9.19480	1.90876	.56515	24.2514	1.8377	2.1947	4.0335	3.7166
178114000	BTM	1534.824	83.4870	107.037	4393.376	12.04137	1.90876	.88643	24.2514	1.4674	2.5116	3.6856	4.3078

TABLE XVII (CONT'D)

Run Code	Column Section	Mass Rates: Liquid #/(ft² - min)	Mass Rates: Liquid #/(ft² - min)	Reynolds Number: Liquid	Reynolds Number: Air	$\delta_{\ell g}$	δ_{ℓ}	δ_{g}	Liquid Saturation %	X	Φ_{ℓ}	Φ_{g}	$\frac{\delta_{\ell g}}{\delta_{\ell}+\delta_{g}}$
179111000	TOP	698.674	89.7874	47.893	4728.346	4.93574	.64762	.75442	21.5568	.9265	2.7606	2.5578	3.5203
179111000	MID	698.674	89.7874	47.893	4728.346	5.32303	.64762	.95233	21.5568	.8246	2.8669	2.3642	3.3269
179111000	BTM	698.674	89.7874	47.893	4728.346	6.43779	.64762	1.36211	21.5568	.6895	3.1528	2.1740	3.2032
180111000	TOP	1996.213	28.6011	150.727	1498.594	7.04270	2.74582	.06746	43.7125	6.3796	1.6015	10.2171	2.5033
180111000	MID	1996.213	28.6011	150.727	1498.594	7.52501	2.74582	.08857	43.7125	5.5679	1.6554	9.2174	2.6548
180111000	BTM	1996.213	28.6011	150.727	1498.594	8.16732	2.74582	.13397	43.7125	4.5271	1.7246	7.8078	2.8360
181111000	TOP	286.249	7.7243	22.458	403.857	.92622	.19544	.01688	29.9401	3.4020	2.1769	7.4059	4.3621
181111000	MID	286.249	7.7243	22.458	403.857	.86285	.19544	.01895	29.9401	3.2112	2.1011	6.7473	4.0246
181111000	BTM	286.249	7.7243	22.458	403.857	.79339	.19544	.02145	29.9401	3.0184	2.0148	6.0816	3.6579
182111000	TOP	286.249	26.2564	22.634	1371.797	1.66603	.19416	.13857	21.8562	1.1836	2.9292	3.4673	5.0069
182111000	MID	286.249	26.2564	22.634	1371.797	1.54350	.19416	.16274	21.8562	1.0922	2.8194	3.0796	4.3245
182111000	BTM	286.249	26.2564	22.634	1371.797	1.46334	.19416	.19527	21.8562	.9971	2.7452	2.7374	3.7575
183111000	TOP	286.249	91.1417	21.137	4782.363	3.58034	.20564	.98386	16.1676	.4571	4.1725	1.9076	3.0099
183111000	MID	286.249	91.1417	21.137	4782.363	3.55501	.20564	1.21199	16.1676	.4119	4.1577	1.7126	2.5076
183111000	BTM	286.249	91.1417	21.137	4782.363	4.32603	.20564	1.62901	16.1676	.3553	4.5864	1.6296	2.3579
184114000	TOP	1996.213	68.5959	149.046	3596.758	9.73665	2.75916	.28639	27.5449	3.1038	1.8785	5.8307	3.1970
184114000	MID	1996.213	68.5959	149.046	3596.758	9.71045	2.75916	.37922	27.5449	2.6973	1.8759	5.0602	3.0940
184114000	BTM	1996.213	68.5959	149.046	3596.758	11.41241	2.75916	.58716	27.5449	2.1677	2.0337	4.4086	3.4104
185111000	TOP	465.155	17.7113	35.932	926.676	1.83792	.35437	.06373	34.4311	2.3579	2.2773	5.3698	4.3958
185111000	MID	465.155	17.7113	35.932	926.676	1.71708	.35437	.07532	34.4311	2.1689	2.2012	4.7744	3.9960
185111000	BTM	465.155	17.7113	35.932	926.676	1.64925	.35437	.09128	34.4311	1.9702	2.1573	4.2505	3.7007
186114000	TOP	465.155	41.0341	37.977	2139.273	2.80335	.33985	.25693	21.2574	1.1500	2.8720	3.3031	4.6973
186114000	MID	465.155	41.0341	37.977	2139.273	2.68487	.33985	.31467	21.2574	1.0392	2.8106	2.9210	4.1020
186114000	BTM	465.155	41.0341	37.977	2139.273	2.89828	.33985	.40866	21.2574	.9119	2.9202	2.6631	3.8720
187111000	TOP	1098.858	23.2041	91.960	1207.141	4.15338	1.06119	.06467	32.3353	4.0508	1.9783	8.0139	3.6890
187111000	MID	1098.858	23.2041	91.960	1207.141	4.74335	1.06119	.08216	32.3353	3.5937	2.1141	7.5977	4.1485
187111000	BTM	1098.858	23.2041	91.960	1207.141	4.75275	1.06119	.11571	32.3353	3.0283	2.1162	6.4087	4.0383
188111000	TOP	1098.858	55.0569	93.518	2861.352	6.16418	1.05140	.25636	26.6467	2.0251	2.4213	4.9035	4.7135
188111000	MID	1098.858	55.0569	93.518	2861.352	6.44806	1.05140	.32875	26.6467	1.7883	2.4764	4.4287	4.6719

TABLE XVII (CONT'D)

Run Code	Column Section	Mass Rates: Liquid #/(ft^2 - min)	Mass Rates: Liquid #/(ft^2 - min)	Reynolds Number: Liquid	Reynolds Number: Air	$\delta_{\ell g}$	δ_ℓ	δ_g	Liquid Saturation %	X	Φ_ℓ	Φ_g	$\frac{\delta_{\ell g}}{\delta_\ell+\delta_g}$
188111000	BTM	1098.858	55.0569	93.518	2861.352	8.14246	1.05140	.48868	26.6467	1.4667	2.7828	4.0819	5.2870
190111000	TOP	298.923	.0000	24.818	.000	.29402	.17673	.00000	100.0000	999.9999	1.2898	999.9999	1.6636
190111000	MID	298.923	.0000	24.818	.000	.28173	.17673	.00000	100.0000	999.9999	1.2625	999.9999	1.5940
190111000	BTM	298.923	.0000	24.818	.000	.29839	.17673	.00000	100.0000	999.9999	1.2993	999.9999	1.6883
191111000	TOP	486.012	.0000	40.351	.000	.39304	.31946	.00000	100.0000	999.9999	1.1091	999.9999	1.2303
191111000	MID	486.012	.0000	40.351	.000	.35241	.31946	.00000	100.0000	999.9999	1.0503	999.9999	1.1031
191111000	BTM	486.012	.0000	40.351	.000	.37856	.31946	.00000	100.0000	999.9999	1.0885	999.9999	1.1849
192111000	TOP	729.018	.0000	59.062	.000	.68958	.55054	.00000	100.0000	999.9999	1.1191	999.9999	1.2525
192111000	MID	729.018	.0000	59.062	.000	.64066	.55054	.00000	100.0000	999.9999	1.0787	999.9999	1.1636
192111000	BTM	729.018	.0000	59.062	.000	.63836	.55054	.00000	100.0000	999.9999	1.0768	999.9999	1.1595
193111000	TOP	1144.479	.0000	89.824	.000	1.41234	1.05061	.00000	100.0000	999.9999	1.1594	999.9999	1.3443
193111000	MID	1144.479	.0000	89.824	.000	1.21816	1.05061	.00000	100.0000	999.9999	1.0767	999.9999	1.1594
193111000	BTM	1144.479	.0000	89.824	.000	1.22228	1.05061	.00000	100.0000	999.9999	1.0786	999.9999	1.1634
194111000	TOP	1625.265	.0000	118.745	.000	2.35223	1.82992	.00000	100.0000	999.9999	1.1337	999.9999	1.2854
194111000	MID	1625.265	.0000	118.745	.000	2.04030	1.82992	.00000	100.0000	999.9999	1.0559	999.9999	1.1149
194111000	BTM	1625.265	.0000	118.745	.000	2.02889	1.82992	.00000	100.0000	999.9999	1.0529	999.9999	1.1087
195111000	TOP	2082.012	.0000	146.265	.000	3.66907	2.72602	.00000	100.0000	999.9999	1.1601	999.9999	1.3459
195111000	MID	2082.012	.0000	146.265	.000	3.13314	2.72602	.00000	100.0000	999.9999	1.0720	999.9999	1.1493
195111000	BTM	2082.012	.0000	146.265	.000	2.54849	2.72602	.00000	100.0000	999.9999	.9668	999.9999	.9348
196111000	TOP	1145.525	9.5679	94.327	488.041	2.67054	1.02440	.01843	47.3053	7.4548	1.6145	12.0365	2.5608
196111000	MID	1145.525	9.5679	94.327	488.041	2.44240	1.02440	.02251	47.3053	6.7453	1.5440	10.4154	2.3329
196111000	BTM	1145.525	9.5679	94.327	488.041	2.30411	1.02440	.02844	47.3053	6.0012	1.4997	9.0003	2.1884
197113080	TOP	1145.525	34.7569	95.107	1770.431	4.23660	1.01980	.15072	34.1317	2.6011	2.0382	5.3016	3.6193
197113080	MID	1145.525	34.7569	95.107	1770.431	3.92402	1.01980	.18929	34.1317	2.3210	1.9615	4.5529	3.2454
197113080	BTM	1145.525	34.7569	95.107	1770.431	4.85955	1.01980	.26162	34.1317	1.9743	2.1829	4.3098	3.7922
198114000	TOP	1145.525	83.0979	95.107	4232.792	6.23436	1.01980	.58255	25.4491	1.3230	2.4725	3.2713	3.8907
198114000	MID	1145.525	83.0979	95.107	4232.792	6.04180	1.01980	.73864	25.4491	1.1750	2.4340	2.8599	3.4358
198114000	BTM	1145.525	83.0979	95.107	4232.792	7.98879	1.01980	1.06582	25.4491	.9781	2.7988	2.7377	3.8303
199111000	TOP	298.923	9.7841	25.235	497.345	.66432	.17433	.01657	34.4311	3.2434	1.9520	6.3315	3.4798

TABLE XVII (CONT'D)

Run Code	Column Section	Mass Rates: Liquid #/(ft^2 - min)	Mass Rates: Air #/(ft^2 - min)	Reynolds Number: Liquid	Reynolds Number: Air	$\delta_{\ell g}$	δ_ℓ	δ_g	Liquid Saturation %	X	Φ_ℓ	Φ_g	$\frac{\delta_{\ell g}}{\delta_\ell+\delta_g}$
199111000	MID	298.923	9.7841	25.235	497.345	.66685	.17433	.01750	34.4311	3.1561	1.9557	6.1726	3.4761
199111000	BTM	298.923	9.7841	25.235	497.345	.62243	.17433	.01852	34.4311	3.0675	1.8895	5.7962	3.2273
200111000	TOP	298.923	24.7197	25.235	1256.548	.80820	.17433	.05994	30.5389	1.7053	2.1531	3.6718	3.4497
200111000	MID	298.923	24.7197	25.235	1256.548	.86045	.17433	.06248	30.5389	1.6704	2.2216	3.7110	3.6334
200111000	BTM	298.923	24.7197	25.235	1256.548	.85043	.17433	.06531	30.5389	1.6337	2.2086	3.6083	3.5486
201111000	TOP	298.923	40.5340	25.235	2061.272	1.53454	.17433	.24806	23.0538	.8383	2.9668	2.4871	3.6328
201111000	MID	298.923	40.5340	25.235	2061.272	1.38930	.17433	.27627	23.0538	.7943	2.8229	2.2424	3.0831
201111000	BTM	298.923	40.5340	25.235	2061.272	1.54031	.17433	.31212	23.0538	.7473	2.9724	2.2214	3.1663
202111000	TOP	74.730	8.5979	5.362	443.374	.04914	.04396	.01647	20.3592	1.6337	1.0572	1.7272	.8131
202111000	MID	74.730	8.5979	5.362	443.374	.20552	.04396	.01705	20.3592	1.6057	2.1620	3.4717	3.3682
202111000	BTM	74.730	8.5979	5.362	443.374	.19494	.04396	.01777	20.3592	1.5725	2.1057	3.3113	3.1573
203111000	TOP	74.730	20.8231	5.644	1069.582	.31373	.04186	.05989	18.5628	.8360	2.7374	2.2886	3.0830
203111000	MID	74.730	20.8231	5.644	1069.582	.40222	.04186	.06211	18.5628	.8209	3.0996	2.5446	3.8681
203111000	BTM	74.730	20.8231	5.644	1069.582	.41228	.04186	.06470	18.5628	.8043	3.1381	2.5241	3.8685
204111000	TOP	74.730	28.9865	5.602	1489.943	.53822	.04216	.13517	15.8682	.5585	3.5727	1.9954	3.0349
204111000	MID	74.730	28.9865	5.602	1489.943	.52584	.04216	.14290	15.8682	.5431	3.5314	1.9182	2.8413
204111000	BTM	74.730	28.9865	5.602	1489.943	.60838	.04216	.15200	15.8682	.5266	3.7984	2.0005	3.1332
205111000	TOP	74.730	38.2596	5.520	1967.970	.71878	.04276	.23923	13.4730	.4227	4.0997	1.7333	2.5488
205111000	MID	74.730	38.2596	5.520	1967.970	.72595	.04276	.25681	13.4730	.4080	4.1201	1.6812	2.4232
205111000	BTM	74.730	38.2596	5.520	1967.970	.68454	.04276	.27701	13.4730	.3929	4.0008	1.5719	2.1406
206111000	TOP	74.730	86.6419	5.324	4469.179	1.56893	.04426	.77277	10.1796	.2393	5.9534	1.4248	1.9202
206111000	MID	74.730	86.6419	5.324	4469.179	1.42847	.04426	.83702	10.1796	.2299	5.6807	1.3063	1.6208
206111000	BTM	74.730	86.6419	5.324	4469.179	1.47434	.04426	.91149	10.1796	.2203	5.7712	1.2718	1.5425
207111000	TOP	2082.012	13.0414	118.840	684.305	6.42678	3.00179	.01827	58.0838	12.8145	1.4632	18.7503	2.1280
207111000	MID	2082.012	13.0414	118.840	684.305	5.73279	3.00179	.02400	58.0838	11.1814	1.3819	15.4522	1.8946
207111000	BTM	2082.012	13.0414	118.840	684.305	6.39896	3.00179	.03506	58.0838	9.2520	1.4600	13.5084	2.1071
208112000	TOP	2082.012	46.7142	128.319	2437.145	8.89325	2.89315	.15057	41.6167	4.3833	1.7532	7.6851	2.9218
208112000	MID	2082.012	46.7142	128.319	2437.145	8.01718	2.89315	.19702	41.6167	3.8320	1.6646	6.3790	2.5944
208112000	BTM	2082.012	46.7142	128.319	2437.145	10.78091	2.89315	.30074	41.6167	3.1015	1.9303	5.9872	3.3754

TABLE XVII (CONT'D)

Run Code	Column Section	Mass Rates: Liquid #/(ft² - min)	Mass Rates: Air #/(ft² - min)	Reynolds Number: Liquid	Reynolds Number: Air	$\delta_{\ell g}$	δ_{ℓ}	δ_g	Liquid Saturation %	X	φ_{ℓ}	φ_g	$\frac{\delta_{\ell g}}{\delta_{\ell}+\delta_g}$
209114000	TOP	2082.012	66.3717	132.379	3455.294	9.97030	2.85137	.26673	35.0299	3.2695	1.8699	6.1138	3.1975
209114000	MID	2082.012	66.3717	132.379	3455.294	9.69292	2.85137	.35224	35.0299	2.8451	1.8437	5.2457	3.0256
209114000	BTM	2082.012	66.3717	132.379	3455.294	12.13781	2.85137	.54866	35.0299	2.2796	2.0632	4.7034	3.5699
210111000	TOP	1625.265	25.5560	106.715	1326.658	5.77370	1.93103	.06806	44.3113	5.3263	1.7291	9.2100	2.8881
210111000	MID	1625.265	25.5560	106.715	1326.658	5.42214	1.93103	.08824	44.3113	4.6779	1.6756	7.8387	2.6851
210111000	BTM	1625.265	25.5560	106.715	1326.658	5.89360	1.93103	.12640	44.3113	3.9085	1.7470	6.8282	2.8645
211113050	TOP	1625.265	59.0582	111.832	3054.966	7.25358	1.88537	.26610	34.4311	2.6617	1.9614	5.2209	3.3714
211113050	MID	1625.265	59.0582	111.832	3054.966	7.48458	1.88537	.34497	34.4311	2.3377	1.9924	4.6578	3.3557
211113050	BTM	1625.265	59.0582	111.832	3054.966	8.62174	1.88537	.51150	34.4311	1.9198	2.1384	4.1055	3.5970
212111000	TOP	729.018	20.9765	51.941	1082.473	2.13010	.60028	.06764	38.6227	2.9789	1.8837	5.6115	3.1891
212111000	MID	729.018	20.9765	51.941	1082.473	1.87821	.60028	.07756	38.6227	2.7819	1.7688	4.9208	2.7708
212111000	BTM	729.018	20.9765	51.941	1082.473	2.23165	.60028	.09137	38.6227	2.5630	1.9281	4.9419	3.2264
213112000	TOP	729.018	52.0057	49.484	2693.964	3.37452	.62077	.24718	33.5329	1.5847	2.3315	3.6948	3.8878
213112000	MID	729.018	52.0057	49.484	2693.964	3.04915	.62077	.28246	33.5329	1.4824	2.2162	3.2855	3.3757
213112000	BTM	729.018	52.0057	49.484	2693.964	3.39217	.62077	.33008	33.5329	1.3713	2.3376	3.2057	3.5674
214111000	TOP	486.012	8.4337	34.143	435.645	1.16193	.36237	.01716	42.5149	4.5950	1.7906	8.2280	3.0614
214111000	MID	486.012	8.4337	34.143	435.645	.91261	.36237	.01906	42.5149	4.3597	1.5869	6.9187	2.3925
214111000	BTM	486.012	8.4337	34.143	435.645	1.00652	.36237	.02130	42.5149	4.1244	1.6665	6.8738	2.6233
215111000	TOP	486.012	31.9754	35.380	1647.044	1.87132	.35262	.13806	31.1377	1.5981	2.3036	3.6815	3.8136
215111000	MID	486.012	31.9754	35.380	1647.044	1.70775	.35262	.15453	31.1377	1.5105	2.2006	3.3243	3.3672
215111000	BTM	486.012	31.9754	35.380	1647.044	1.76604	.35262	.17504	31.1377	1.4193	2.2379	3.1763	3.3468
216111000	TOP	486.012	89.1025	35.900	4583.190	3.80858	.34872	.77580	21.2574	.6704	3.3047	2.2156	3.3868
216111000	MID	486.012	89.1025	35.900	4583.190	3.48695	.34872	.91636	21.2574	.6168	3.1621	1.9506	2.7562
216111000	BTM	486.012	89.1025	35.900	4583.190	4.48676	.34872	1.14298	21.2574	.5523	3.5869	1.9812	3.0078
217121000	TOP	2082.012	.0000	171.302	.000	2.98552	2.73740	.00000	100.0000	999.9999	1.0443	999.9999	1.0906
217121000	MID	2082.012	.0000	171.302	.000	2.96270	2.73740	.00000	100.0000	999.9999	1.0403	999.9999	1.0823
217121000	BTM	2082.012	.0000	171.302	.000	3.06809	2.73740	.00000	100.0000	999.9999	1.0586	999.9999	1.1208
218121000	TOP	1625.265	.0000	138.397	.000	1.90993	1.83001	.00000	100.0000	999.9999	1.0216	999.9999	1.0436
218121000	MID	1625.265	.0000	138.397	.000	1.95508	1.83001	.00000	100.0000	999.9999	1.0336	999.9999	1.0683

TABLE XVII (CONT'D)

Run Code	Column Section	Mass Rates: Liquid #/(ft^2 - min)	Mass Rates: Air #/(ft^2 - min)	Reynolds Number: Liquid	Reynolds Number: Air	$\delta_{\ell g}$	δ_ℓ	δ_g	Liquid Saturation %	X	Φ_ℓ	Φ_g	$\frac{\delta_{\ell g}}{\delta_\ell+\delta_g}$
218121000	BTM	1625.265	.0000	138.397	.000	2.09323	1.83001	.00000	100.0000	999.9999	1.0694	999.9999	1.1438
219121000	TOP	1145.525	.0000	101.080	.000	1.09569	1.06371	.00000	100.0000	999.9999	1.0149	999.9999	1.0300
219121000	MID	1145.525	.0000	101.080	.000	1.14297	1.06371	.00000	100.0000	999.9999	1.0365	999.9999	1.0745
219121000	BTM	1145.525	.0000	101.080	.000	.93527	1.06371	.00000	100.0000	999.9999	.9376	999.9999	.8792
220121000	TOP	729.018	.0000	66.746	.000	.54985	.55027	.00000	100.0000	999.9999	.9996	999.9999	.9992
220121000	MID	729.018	.0000	66.746	.000	.55945	.55027	.00000	100.0000	999.9999	1.0083	999.9999	1.0166
220121000	BTM	729.018	.0000	66.746	.000	.52207	.55027	.00000	100.0000	999.9999	.9740	999.9999	.9487
221121000	TOP	486.012	.0000	46.235	.000	.32770	.31390	.00000	100.0000	999.9999	1.0217	999.9999	1.0439
221121000	MID	486.012	.0000	46.235	.000	.32735	.31390	.00000	100.0000	999.9999	1.0211	999.9999	1.0428
221121000	BTM	486.012	.0000	46.235	.000	.33006	.31390	.00000	100.0000	999.9999	1.0254	999.9999	1.0514
224121000	TOP	1145.525	9.6112	117.219	591.577	2.43584	.98477	.01867	46.7811	7.2611	1.5727	11.4199	2.4274
224121000	MID	1145.525	9.6112	117.219	591.577	2.57921	.98477	.02265	46.7811	6.5929	1.6183	10.6697	2.5601
224121000	BTM	1145.525	9.6112	117.219	591.577	2.32991	.98477	.02869	46.7811	5.8581	1.5381	9.0107	2.2989
225123040	TOP	1145.525	34.7569	117.219	2139.302	3.76699	.98477	.15396	30.0429	2.5290	1.9558	4.9463	3.3080
225123040	MID	1145.525	34.7569	117.219	2139.302	4.24756	.98477	.19192	30.0429	2.2651	2.0768	4.7044	3.6097
225123040	BTM	1145.525	34.7569	117.219	2139.302	4.73288	.98477	.26514	30.0429	1.9272	2.1922	4.2249	3.7865
226124000	TOP	1145.525	92.7404	115.281	5716.108	5.64619	.99308	.71621	20.6008	1.1775	2.3844	2.8077	3.3032
226124000	MID	1145.525	92.7404	115.281	5716.108	7.13438	.99308	.90505	20.6008	1.0474	2.6803	2.8076	3.7586
226124000	BTM	1145.525	92.7404	115.281	5716.108	8.27477	.99308	1.32586	20.6008	.8654	2.8865	2.4982	3.5683
227123080	TOP	729.018	19.7457	72.764	1218.733	1.89590	.52118	.87551	33.9055	2.6271	1.9072	5.0107	3.1773
227123080	MID	729.018	19.7457	72.764	1218.733	2.15581	.52118	.88953	33.9055	2.4126	2.0338	4.9068	3.5299
227123080	BTM	729.018	19.7457	72.764	1218.733	1.90621	.52118	.11020	33.9055	2.1747	1.9124	4.1590	3.0190
228123100	TOP	729.018	53.7434	73.365	3314.803	3.21268	.51854	.38037	21.4592	1.1675	2.4891	2.9062	3.5739
228123100	MID	729.018	53.7434	73.365	3314.803	3.85501	.51854	.46847	21.4592	1.0520	2.7265	2.8685	3.9057
228123100	BTM	729.018	53.7434	73.365	3314.803	4.19639	.51854	.63548	21.4592	.9033	2.8447	2.5697	3.6363
229121000	TOP	2082.012	13.3195	133.435	849.605	5.72888	3.05457	.01851	58.3690	12.8444	1.3694	17.5904	1.8642
229121000	MID	2082.012	13.3195	133.435	849.605	6.76616	3.05457	.02414	58.3690	11.2474	1.4883	16.7398	2.1977
229121000	BTM	2082.012	13.3195	133.435	849.605	6.72599	3.05457	.03604	58.3690	9.2052	1.4838	13.6595	2.1762
230124000	TOP	2082.012	47.7297	149.133	3022.624	8.09800	2.90354	.15435	39.0557	4.3372	1.6700	7.2432	2.6482

TABLE XVII (CONT'D)

Run Code	Column Section	Mass Rates: Liquid #/(ft² - min)	Mass Rates: Air #/(ft² - min)	Reynolds Number: Liquid	Reynolds Number: Air	$\delta_{\ell g}$	δ_{ℓ}	δ_g	Liquid Saturation %	X	Φ_{ℓ}	Φ_g	$\frac{\delta_{\ell g}}{\delta_{\ell}+\delta_g}$
230124000	MID	2082.012	47.7297	149.133	3022.624	9.52990	2.90354	.20104	39.0557	3.8003	1.8116	6.8849	3.0696
230124000	BTM	2082.012	47.7297	149.133	3022.624	10.96227	2.90354	.31068	39.0557	3.0570	1.9430	5.9400	3.4105
231122000	TOP	1625.265	25.7702	122.166	1626.377	5.12411	1.94202	.06988	42.4892	5.2714	1.6243	8.5627	2.5468
231122000	MID	1625.265	25.7702	122.166	1626.377	5.88704	1.94202	.08969	42.4892	4.6529	1.7410	8.1012	2.8975
231122000	BTM	1625.265	25.7702	122.166	1626.377	6.15411	1.94202	.13022	42.4892	3.8617	1.7801	6.8744	2.9697
232123030	TOP	1625.265	60.0368	127.683	3774.939	6.70763	1.90075	.27509	32.1888	2.6285	1.8785	4.9379	3.0827
232123030	MID	1625.265	60.0368	127.683	3774.939	8.09294	1.90075	.35340	32.1888	2.3191	2.0634	4.7853	3.5902
232123030	BTM	1625.265	60.0368	127.683	3774.939	9.37017	1.90075	.53256	32.1888	1.8891	2.2202	4.1945	3.8507
233124000	TOP	1625.265	92.9781	133.722	5827.947	7.83450	1.85949	.54780	26.1802	1.8423	2.0526	3.7817	3.2544
233124000	MID	1625.265	92.9781	133.722	5827.947	10.01888	1.85949	.70456	26.1802	1.6245	2.3211	3.7709	3.9074
233124000	BTM	1625.265	92.9781	133.722	5827.947	11.44415	1.85949	1.07492	26.1802	1.3152	2.4808	3.2628	3.8999
234121000	TOP	486.012	8.9329	41.098	558.658	1.05380	.34210	.01758	41.6309	4.4102	1.7550	7.7403	2.9296
234121000	MID	486.012	8.9329	41.098	558.658	1.11548	.34210	.01945	41.6309	4.1938	1.8057	7.5729	3.0852
234121000	BTM	486.012	8.9329	41.098	558.658	1.02821	.34210	.02174	41.6309	3.9661	1.7336	6.8758	2.8258
235122000	TOP	486.012	34.9920	42.272	2182.828	1.75445	.33505	.15389	29.6137	1.4755	2.2882	3.3764	3.5881
235122000	MID	486.012	34.9920	42.272	2182.828	1.87933	.33505	.17074	29.6137	1.4008	2.3683	3.3176	3.7155
235122000	BTM	486.012	34.9920	42.272	2182.828	1.78642	.33505	.19208	29.6137	1.3207	2.3090	3.0496	3.3888
236122000	TOP	486.012	93.6178	43.516	5826.809	3.18927	.32800	.80687	19.7424	.6375	3.1182	1.9881	2.8102
236122000	MID	486.012	93.6178	43.516	5826.809	3.59603	.32800	.92793	19.7424	.5945	3.3110	1.9685	2.8632
236122000	BTM	486.012	93.6178	43.516	5826.809	3.47052	.32800	1.10047	19.7424	.5459	3.2528	1.7758	2.4295
237121000	TOP	298.923	18.4874	28.000	1146.641	.90884	.17433	.06419	28.3261	1.6479	2.2832	3.7626	3.8101
237121000	MID	298.923	18.4874	28.000	1146.641	.90556	.17433	.06987	28.3261	1.5795	2.2791	3.5999	3.7081
237121000	BTM	298.923	18.4874	28.000	1146.641	.78552	.17433	.07634	28.3261	1.5111	2.1226	3.2076	3.1335
238121000	TOP	298.923	45.7182	28.549	2831.615	1.41663	.17162	.25676	23.1759	.8175	2.8729	2.3488	3.3068
238121000	MID	298.923	45.7182	28.549	2831.615	1.47713	.17162	.27955	23.1759	.7835	2.9337	2.2986	3.2739
238121000	BTM	298.923	45.7182	28.549	2831.615	1.38405	.17162	.30672	23.1759	.7480	2.8397	2.1242	2.8933
239121000	TOP	74.730	8.1567	6.691	507.677	.20411	.03895	.01701	21.8884	1.5131	2.2891	3.4639	3.6473
239121000	MID	74.730	8.1567	6.691	507.677	.20259	.03895	.01783	21.8884	1.4778	2.2806	3.3703	3.5677
239121000	BTM	74.730	8.1567	6.691	507.677	.20995	.03895	.01875	21.8884	1.4411	2.3217	3.3459	3.6384

TABLE XVII (CONT'D)

Run Code	Column Section	Mass Rates: Liquid #/(ft² - min)	Mass Rates: Air #/(ft² - min)	Reynolds Number: Liquid	Reynolds Number: Air	$\delta_{\ell g}$	δ_{ℓ}	δ_{g}	Liquid Saturation %	X	Φ_{ℓ}	Φ_{g}	$\frac{\delta_{\ell g}}{\delta_{\ell}+\delta_{g}}$
240121000	TOP	74.730	16.8051	6.842	1044.490	.34534	.03813	.06321	18.8841	.7766	3.0092	2.3372	3.4072
240121000	MID	74.730	16.8051	6.842	1044.490	.33840	.03813	.06699	18.8841	.7544	2.9788	2.2474	3.2187
240121000	BTM	74.730	16.8051	6.842	1044.490	.32404	.03813	.07122	18.8841	.7317	2.9149	2.1329	2.9629
241121000	TOP	74.730	30.4005	6.791	1890.818	.47445	.03840	.14197	15.4506	.5201	3.5146	1.8280	2.6301
241121000	MID	74.730	30.4005	6.791	1890.818	.45710	.03840	.14919	15.4506	.5073	3.4498	1.7503	2.4365
241121000	BTM	74.730	30.4005	6.791	1890.818	.46574	.03840	.15720	15.4506	.4942	3.4822	1.7212	2.3809
242121000	TOP	74.730	93.5737	6.408	5844.598	1.53023	.04057	.98231	5.1502	.2032	6.1410	1.2481	1.4959
242121000	MID	74.730	93.5737	6.408	5844.598	1.67042	.04057	1.07593	5.1502	.1941	6.4161	1.2460	1.4961
242121000	BTM	74.730	93.5737	6.408	5844.598	1.69744	.04057	1.19540	5.1502	.1842	6.4678	1.1916	1.3733
243121000	TOP	149.461	5.2746	14.796	325.784	.31446	.07502	.00837	29.6137	2.9939	2.0472	6.1294	3.7707
243121000	MID	149.461	5.2746	14.796	325.784	.30273	.07502	.00885	29.6137	2.9115	2.0087	5.8484	3.6091
243121000	BTM	149.461	5.2746	14.796	325.784	.25732	.07502	.00936	29.6137	2.8298	1.8519	5.2408	3.0490
244121000	TOP	224.192	6.1704	22.750	379.897	.44629	.11636	.00812	33.4763	3.7835	1.9584	7.4097	3.5849
244121000	MID	224.192	6.1704	22.750	379.897	.45431	.11636	.00853	33.4763	3.6927	1.9759	7.2965	3.6375
244121000	BTM	224.192	6.1704	22.750	379.897	.44431	.11636	.00898	33.4763	3.5989	1.9540	7.0327	3.5447
245121000	TOP	286.249	.0000	296.842	.000	.09449	.04762	.00000	100.0000	999.9999	1.4085	999.9999	1.9839
245121000	MID	286.249	.0000	296.842	.000	.09474	.04762	.00000	100.0000	999.9999	1.4104	999.9999	1.9893
245121000	BTM	286.249	.0000	296.842	.000	.09352	.04762	.00000	100.0000	999.9999	1.4013	999.9999	1.9637
246121000	TOP	572.498	.0000	606.591	.000	.19400	.16280	.00000	100.0000	999.9999	1.0916	999.9999	1.1916
246121000	MID	572.498	.0000	606.591	.000	.19350	.16280	.00000	100.0000	999.9999	1.0902	999.9999	1.1885
246121000	BTM	572.498	.0000	606.591	.000	.19101	.16280	.00000	100.0000	999.9999	1.0831	999.9999	1.1732
248121000	TOP	698.674	.0000	756.731	.000	.26638	.23462	.00000	100.0000	999.9999	1.0655	999.9999	1.1353
248121000	MID	698.674	.0000	756.731	.000	.26569	.23462	.00000	100.0000	999.9999	1.0641	999.9999	1.1323
248121000	BTM	698.674	.0000	756.731	.000	.26227	.23462	.00000	100.0000	999.9999	1.0572	999.9999	1.1178
249121000	TOP	1097.917	.0000	1205.219	.000	.57297	.55025	.00000	100.0000	999.9999	1.0204	999.9999	1.0412
249121000	MID	1097.917	.0000	1205.219	.000	.57148	.55025	.00000	100.0000	999.9999	1.0191	999.9999	1.0385
249121000	BTM	1097.917	.0000	1205.219	.000	.56908	.55025	.00000	100.0000	999.9999	1.0169	999.9999	1.0342
250121000	TOP	1557.422	.0000	1733.052	.000	1.06554	1.07711	.00000	100.0000	999.9999	.9946	999.9999	.9892
250121000	MID	1557.422	.0000	1733.052	.000	1.06276	1.07711	.00000	100.0000	999.9999	.9933	999.9999	.9866

TABLE XVII (CONT'D)

Run Code	Column Section	Mass Rates: Liquid #/(ft² - min)	Mass Rates: Air #/(ft² - min)	Reynolds Number: Liquid	Reynolds Number: Air	$\delta_{\ell g}$	δ_{ℓ}	δ_g	Liquid Saturation %	X	φ_{ℓ}	φ_g	$\frac{\delta_{\ell g}}{\delta_{\ell}+\delta_g}$
250121000	BTM	1557.422	.0000	1733.052	.000	1.04908	1.07711	.00000	100.0000	999.9999	.9869	999.9999	.9739
251121000	TOP	1996.213	.0000	2237.673	.000	1.65359	1.74407	.00000	100.0000	999.9999	.9737	999.9999	.9481
251121000	MID	1996.213	.0000	2237.673	.000	1.64928	1.74407	.00000	100.0000	999.9999	.9724	999.9999	.9456
251121000	BTM	1996.213	.0000	2237.673	.000	1.63301	1.74407	.00000	100.0000	999.9999	.9676	999.9999	.9363
252121000	TOP	.000	94.2972	.000	6210.281	1.32354	.00000	1.56981	.0000	.0000	999.9999	.9182	.8431
252121000	MID	.000	94.2972	.000	6210.281	1.82026	.00000	1.83199	.0000	.0000	999.9999	.9967	.9935
252121000	BTM	.000	94.2972	.000	6210.281	1.98918	.00000	2.27928	.0000	.0000	999.9999	.9341	.8727
256121000	TOP	71.562	92.6536	78.556	5986.569	1.52505	.00533	1.08997	4.7210	.0699	16.9116	1.1828	1.3923
256121000	MID	71.562	92.6536	78.556	5986.569	1.68041	.00533	1.21219	4.7210	.0663	17.7521	1.1773	1.3801
256121000	BTM	71.562	92.6536	78.556	5986.569	1.66829	.00533	1.37284	4.7210	.0623	17.6880	1.1023	1.2105
257124000	TOP	1996.213	11.3980	2384.657	730.008	3.60535	1.73868	.01823	36.9098	9.7638	1.4400	14.0599	2.0520
257124000	MID	1996.213	11.3980	2384.657	730.008	4.43743	1.73868	.02296	36.9098	8.7003	1.5975	13.8993	2.5189
257124000	BTM	1996.213	11.3980	2384.657	730.008	4.22834	1.73868	.03191	36.9098	7.3809	1.5594	11.5103	2.3880
258124000	TOP	1996.213	44.4141	2420.249	2840.440	5.46422	1.73747	.17620	24.0343	3.1401	1.7733	5.5687	2.8553
258124000	MID	1996.213	44.4141	2420.249	2840.440	6.28629	1.73747	.22326	24.0343	2.7896	1.9021	5.3062	3.2060
258124000	BTM	1996.213	44.4141	2420.249	2840.440	7.58675	1.73747	.32608	24.0343	2.3083	2.0896	4.8234	3.6765
259124000	TOP	1996.213	67.0877	2437.225	4287.373	5.91624	1.73691	.34023	15.8798	2.2594	1.8455	4.1699	2.8482
259124000	MID	1996.213	67.0877	2437.225	4287.373	7.80481	1.73691	.43087	15.8798	2.0077	2.1197	4.2560	3.6003
259124000	BTM	1996.213	67.0877	2437.225	4287.373	8.68939	1.73691	.63371	15.8798	1.6555	2.2366	3.7029	3.6654
261123000	TOP	286.249	39.2545	357.000	2503.182	1.02547	.04534	.26101	7.7253	.4167	4.7557	1.9821	3.3473
261123000	MID	286.249	39.2545	357.000	2503.182	1.11950	.04534	.28812	7.7253	.3966	4.9689	1.9711	3.3571
261123000	BTM	286.249	39.2545	357.000	2503.182	1.09498	.04534	.32269	7.7253	.3748	4.9142	1.8420	2.9751
262124000	TOP	1557.422	26.3518	2040.529	1671.932	3.16177	1.06675	.06568	27.0386	4.0299	1.7216	6.9378	2.7919
262124000	MID	1557.422	26.3518	2040.529	1671.932	3.73120	1.06675	.07553	27.0386	3.7581	1.8702	7.0284	3.2664
262124000	BTM	1557.422	26.3518	2040.529	1671.932	3.69049	1.06675	.09009	27.0386	3.4409	1.8599	6.4001	3.1901
263124000	TOP	1557.422	53.0515	2040.529	3365.935	4.63914	1.06675	.27222	11.1587	1.9795	2.0853	4.1281	3.4646
263124000	MID	1557.422	53.0515	2040.529	3365.935	5.47825	1.06675	.34004	11.1587	1.7711	2.2661	4.0137	3.8941
263124000	BTM	1557.422	53.0515	2040.529	3365.935	6.29353	1.06675	.47848	11.1587	1.4931	2.4289	3.6267	4.0728
264124000	TOP	1557.422	92.5809	1860.483	5929.496	5.64997	1.07240	.63896	12.4463	1.2955	2.2953	2.9736	3.3014

TABLE XVII (CONT'D)

Run Code	Column Section	Mass Rates: Liquid #/(ft^2 - min)	Mass Rates: Air #/(ft^2 - min)	Reynolds Number: Liquid	Reynolds Number: Air	$\delta_{\ell g}$	δ_ℓ	δ_g	Liquid Saturation %	X	φ_ℓ	φ_g	$\frac{\delta_{\ell g}}{\delta_\ell+\delta_g}$
264124000	MID	1557.422	92.5809	1860.483	5929.496	7.48907	1.07240	.80031	12.4463	1.1575	2.6426	3.0590	3.9990
264124000	BTM	1557.422	92.5809	1860.483	5929.496	8.17958	1.07240	1.14464	12.4463	.9679	2.7617	2.6731	3.6893
265121000	TOP	465.155	8.1031	567.919	517.850	.71581	.10866	.01713	23.1759	2.5179	2.5665	6.4625	5.6897
265121000	MID	465.155	8.1031	567.919	517.850	.76822	.10866	.01884	23.1759	2.4013	2.6588	6.3847	6.0245
265121000	BTM	465.155	8.1031	567.919	517.850	.78372	.10866	.02102	23.1759	2.2736	2.6855	6.1060	6.0430
266123080	TOP	465.155	28.5860	580.126	1822.876	1.13954	.10827	.14197	15.4506	.8732	3.2441	2.8330	4.5535
266123080	MID	465.155	28.5860	580.126	1822.876	1.22334	.10827	.15770	15.4506	.8285	3.3613	2.7851	4.5992
266123080	BTM	465.155	28.5860	580.126	1822.876	1.15832	.10827	.17766	15.4506	.7806	3.2707	2.5533	4.0508
267123040	TOP	465.155	92.9788	580.126	5929.078	2.44986	.10827	.92861	4.7210	.3414	4.7567	1.6242	2.3626
267123040	MID	465.155	92.9788	580.126	5929.078	2.82839	.10827	1.06359	4.7210	.3190	5.1110	1.6307	2.4135
267123040	BTM	465.155	92.9788	580.126	5929.078	2.81635	.10827	1.25907	4.7210	.2932	5.1001	1.4956	2.0597
268121000	TOP	1098.858	9.2246	1402.031	586.961	1.55901	.54429	.01754	39.0557	5.5704	1.6924	9.4276	2.7748
268121000	MID	1098.858	9.2246	1402.031	586.961	1.84000	.54429	.02022	39.0557	5.1878	1.8386	9.5385	3.2594
268121000	BTM	1098.858	9.2246	1402.031	586.961	1.74858	.54429	.02411	39.0557	4.7504	1.7923	8.5145	3.0762
269123060	TOP	1098.858	33.3768	1409.410	2122.229	2.58823	.54407	.15042	18.0257	1.9017	2.1810	4.1479	3.7267
269123060	MID	1098.858	33.3768	1409.410	2122.229	3.04677	.54407	.17899	18.0257	1.7434	2.3664	4.1257	4.2136
269123060	BTM	1098.858	33.3768	1409.410	2122.229	3.08710	.54407	.22555	18.0257	1.5531	2.3820	3.6995	4.0111
270124000	TOP	1098.858	93.1627	1393.278	5932.205	4.46206	.54455	.76513	8.5836	.8436	2.8625	2.4148	3.4069
270124000	MID	1098.858	93.1627	1393.278	5932.205	5.46704	.54455	.93599	8.5836	.7627	3.1685	2.4167	3.6925
270124000	BTM	1098.858	93.1627	1393.278	5932.205	7.22253	.54455	1.30575	8.5836	.6457	3.6418	2.3518	3.9034
271122000	TOP	698.674	17.6287	899.918	1120.577	1.39937	.22958	.06216	23.1759	1.9217	2.4688	4.7446	4.7965
271122000	MID	698.674	17.6287	899.918	1120.577	1.51015	.22958	.07122	23.1759	1.7953	2.5647	4.6046	5.0203
271122000	BTM	698.674	17.6287	899.918	1120.577	1.43693	.22958	.08363	23.1759	1.6568	2.5017	4.1449	4.5876
272123060	TOP	698.674	42.7984	909.532	2717.363	1.97207	.22930	.25516	13.3047	.9479	2.9326	2.7800	4.0706
272123060	MID	698.674	42.7984	909.532	2717.363	2.26673	.22930	.29355	13.3047	.8838	3.1440	2.7788	4.3353
272123060	BTM	698.674	42.7984	909.532	2717.363	2.41827	.22930	.35163	13.3047	.8075	3.2474	2.6224	4.1626
273131000	TOP	.000	93.0483	.000	2028.375	4.59053	.00000	4.06478	.0000	.0000	99.9999	1.0627	1.1293
273131000	MID	.000	93.0483	.000	2028.375	6.23173	.00000	5.05031	.0000	.0000	99.9999	1.1108	1.2339
273131000	BTM	.000	93.0483	.000	2028.375	8.71919	.00000	7.54797	.0000	.0000	99.9999	1.0747	1.1551

TABLE XVII (CONT'D)

Run Code	Column Section	Mass Rates: Liquid #/(ft² - min)	Mass Rates: Air #/(ft² - min)	Reynolds Number: Liquid	Reynolds Number: Air	$\delta_{\ell g}$	δ_ℓ	δ_g	Liquid Saturation %	X	Φ_ℓ	Φ_g	$\frac{\delta_{\ell g}}{\delta_\ell+\delta_g}$
274131000	TOP	1996.213	.0000	760.608	.000	8.16747	10.22304	.00000	100.0000	999.9999	.8938	9.9999	.7989
274131000	MID	1996.213	.0000	760.608	.000	8.77280	10.22304	.00000	100.0000	999.9999	.9263	9.9999	.8581
274131000	BTM	1996.213	.0000	760.608	.000	9.05581	10.22304	.00000	100.0000	999.9999	.9411	9.9999	.8858
275131000	TOP	1557.422	.0000	594.548	.000	5.42822	6.39873	.00000	100.0000	999.9999	.9210	9.9999	.8483
275131000	MID	1557.422	.0000	594.548	.000	5.86524	6.39873	.00000	100.0000	999.9999	.9574	9.9999	.9166
275131000	BTM	1557.422	.0000	594.548	.000	5.93824	6.39873	.00000	100.0000	999.9999	.9633	9.9999	.9280
276131000	TOP	1097.917	.0000	419.131	.000	3.11620	3.34764	.00000	100.0000	999.9999	.9648	9.9999	.9308
276131000	MID	1097.917	.0000	419.131	.000	3.35873	3.34764	.00000	100.0000	999.9999	1.0016	9.9999	1.0033
276131000	BTM	1097.917	.0000	419.131	.000	3.21654	3.34764	.00000	100.0000	999.9999	.9802	9.9999	.9608
277131000	TOP	698.674	.0000	270.585	.000	1.41234	1.48201	.00000	100.0000	999.9999	.9762	9.9999	.9529
277131000	MID	698.674	.0000	270.585	.000	1.49889	1.48201	.00000	100.0000	999.9999	1.0056	9.9999	1.0113
277131000	BTM	698.674	.0000	270.585	.000	1.53404	1.48201	.00000	100.0000	999.9999	1.0174	9.9999	1.0351
278131000	TOP	286.249	.0000	112.490	.000	.44481	.33287	.00000	100.0000	999.9999	1.1559	9.9999	1.3362
278131000	MID	286.249	.0000	112.490	.000	.37447	.33287	.00000	100.0000	999.9999	1.0606	9.9999	1.1249
278131000	BTM	286.249	.0000	112.490	.000	.37509	.33287	.00000	100.0000	999.9999	1.0615	9.9999	1.1268
281133000	TOP	286.249	23.9488	102.629	511.245	4.08027	.34670	.40572	24.7826	.9244	3.4305	3.1712	5.4227
281133000	MID	286.249	23.9488	102.629	511.245	4.85081	.34670	.51316	24.7826	.8219	3.7404	3.0745	5.6413
281133000	BTM	286.249	23.9488	102.629	511.245	5.61059	.34670	.74326	24.7826	.6829	4.0227	2.7474	5.1474
282134000	TOP	286.249	40.3335	103.369	860.383	5.07785	.34557	.89805	19.5652	.6203	3.8332	2.3778	4.0830
282134000	MID	286.249	40.3335	103.369	860.383	6.01617	.34557	1.14147	19.5652	.5502	4.1724	2.2957	4.0457
282134000	BTM	286.249	40.3335	103.369	860.383	7.36934	.34557	1.69461	19.5652	.4515	4.6178	2.0853	3.6120
283134000	TOP	286.249	59.6898	103.837	1272.347	6.20115	.34487	1.57333	17.8260	.4681	4.2404	1.9853	3.2327
283134000	MID	286.249	59.6898	103.837	1272.347	7.26186	.34487	1.99422	17.8260	.4158	4.5887	1.9082	3.1045
283134000	BTM	286.249	59.6898	103.837	1272.347	9.76180	.34487	3.01058	17.8260	.3384	5.3203	1.8006	2.9092
284134000	TOP	286.249	88.1987	104.025	1880.042	7.42877	.34458	2.73142	16.9565	.3551	4.6431	1.6491	2.4150
284134000	MID	286.249	88.1987	104.025	1880.042	9.66433	.34458	3.48077	16.9565	.3146	5.2958	1.6662	2.5263
284134000	BTM	286.249	88.1987	104.025	1880.042	12.99930	.34458	5.46617	16.9565	.2510	6.1420	1.5421	2.2371
285131000	TOP	71.562	20.0662	26.560	426.789	1.96536	.04991	.40301	16.9565	.3519	6.2750	2.2083	4.3392
285131000	MID	71.562	20.0662	26.560	426.789	2.23501	.04991	.47259	16.9565	.3249	6.6916	2.1746	4.2775

TABLE XVII (CONT'D)

Run Code	Column Section	Mass Rates: Liquid #/(ft² - min)	Mass Rates: Air #/(ft² - min)	Reynolds Number: Liquid	Reynolds Number: Air	$\delta_{\ell g}$	δ_{ℓ}	δ_g	Liquid Saturation %	X	Φ_{ℓ}	Φ_g	$\frac{\delta_{\ell g}}{\delta_{\ell}+\delta_g}$
285131000	BTM	71.562	20.0662	26.560	426.789	2.52325	.04991	.58617	16.9565	.2918	7.1100	2.0747	3.9668
286131000	TOP	71.562	50.3215	25.657	1074.236	4.37521	.05125	1.49777	8.2608	.1849	9.2392	1.7091	2.8244
286131000	MID	71.562	50.3215	25.657	1074.236	4.76380	.05125	1.86344	8.2608	.1658	9.6408	1.5988	2.4880
286131000	BTM	71.562	50.3215	25.657	1074.236	6.33039	.05125	2.64205	8.2608	.1392	11.1135	1.5479	2.3504
288133000	TOP	1097.917	15.4061	425.205	326.238	6.28674	3.33952	.11600	54.7826	5.3653	1.3720	7.3615	1.8193
288133000	MID	1097.917	15.4061	425.205	326.238	9.32779	3.33952	.14893	54.7826	4.7352	1.6712	7.9139	2.6739
288133000	BTM	1097.917	15.4061	425.205	326.238	11.53106	3.33952	.24017	54.7826	3.7288	1.8582	6.9290	3.2212
289133000	TOP	698.674	29.7798	280.617	628.319	6.71651	1.46926	.41771	26.5217	1.8754	2.1380	4.0098	3.5593
289133000	MID	698.674	29.7798	280.617	628.319	8.20208	1.46926	.54174	26.5217	1.6468	2.3627	3.8910	4.0785
289133000	BTM	698.674	29.7798	280.617	628.319	9.82442	1.46926	.84541	26.5217	1.3183	2.5858	3.4089	4.2443
290133000	TOP	698.674	50.1804	211.362	1088.777	8.23951	1.58191	.86260	30.0000	1.3542	2.2822	3.0906	3.3706
290133000	MID	698.674	50.1804	211.362	1088.777	10.72375	1.58191	1.11862	30.0000	1.1891	2.6036	3.0962	3.9709
290133000	BTM	698.674	50.1804	211.362	1088.777	13.55097	1.58191	1.80573	30.0000	.9359	2.9268	2.7394	4.0001
291133000	TOP	465.155	11.6273	150.607	250.809	4.06242	.78278	.11268	42.6086	2.6357	2.2780	6.0043	4.5366
291133000	MID	465.155	11.6273	150.607	250.809	4.67280	.78278	.14256	42.6086	2.3432	2.4432	5.7250	5.0497
291133000	BTM	465.155	11.6273	150.607	250.809	5.23298	.78278	.20402	42.6086	1.9587	2.5855	5.0644	5.3029
292133000	TOP	465.155	44.5852	157.343	957.436	6.80757	.77063	8.72132	24.3478	.9400	2.9721	2.7938	4.1439
292133000	MID	465.155	44.5852	157.343	957.436	8.34300	.77063	1.13452	24.3478	.8241	3.2903	2.7117	4.3791
292133000	BTM	465.155	44.5852	157.343	957.436	9.81495	.77063	1.77555	24.3478	.6588	3.5687	2.3511	3.8547
293133000	TOP	465.155	65.1467	162.132	1394.835	7.71227	.76260	1.53674	24.3478	.7044	3.1801	2.2402	3.3541
293133000	MID	465.155	65.1467	162.132	1394.835	9.69652	.76260	1.97791	24.3478	.6209	3.5658	2.2141	3.5382
293133000	BTM	465.155	65.1467	162.132	1394.835	12.78407	.76260	3.14360	24.3478	.4925	4.0943	2.0166	3.2727
294132000	TOP	71.562	11.8150	10.064	253.908	1.64871	.11236	.14130	16.9565	.8917	3.8305	3.4157	6.4993
294132000	MID	71.562	11.8150	10.064	253.908	3.64868	.11236	.16938	16.9565	.8144	5.6984	4.6412	12.9502
294132000	BTM	71.562	11.8150	10.064	253.908	4.24040	.11236	.23737	16.9565	.6880	6.1431	4.2265	12.1245
295132000	TOP	71.562	11.8150	10.064	253.908	1.90002	.11236	.15067	16.9565	.8635	4.1121	3.5510	7.2233
295132000	MID	71.562	11.8150	10.064	253.908	4.04973	.11236	.18737	16.9565	.7743	6.0034	4.6489	13.5108
295132000	BTM	71.562	11.8150	10.064	253.908	2.70635	.11236	.25835	16.9565	.6594	4.9077	3.2365	7.3003
296131000	TOP	286.249	17.7414	47.808	376.238	5.32435	.52763	.19133	30.0000	1.6605	3.1766	5.2751	7.4055

TABLE XVII (CONT'D)

Run Code	Column Section	Mass Rates: Liquid #/(ft² - min)	Mass Rates: Air #/(ft² - min)	Reynolds Number: Liquid	Reynolds Number: Air	$\delta_{\ell g}$	δ_{ℓ}	δ_g	Liquid Saturation %	X	Φ_{ℓ}	Φ_g	$\frac{\delta_{\ell g}}{\delta_{\ell}+\delta_g}$
296131000	MID	286.249	17.7414	47.808	376.238	6.81358	.52763	.24707	30.0000	1.4613	3.5935	5.2514	8.7950
296131000	BTM	286.249	17.7414	47.808	376.238	8.05810	.52763	.38404	30.0000	1.1721	3.9079	4.5806	8.8387
297133000	TOP	698.674	32.8466	130.258	690.517	9.01805	1.86609	.41877	35.6521	2.1109	2.1983	4.6405	3.9468
297133000	MID	698.674	32.8466	130.258	690.517	1.22394	1.86609	.55417	35.6521	1.8350	2.3661	4.3419	4.3167
297133000	BTM	698.674	32.8466	130.258	690.517	1.22394	1.86609	.89159	35.6521	1.4467	2.5610	3.7050	4.4383
301131000	TOP	71.562	6.6539	23.321	143.423	2.53877	.05520	.05916	7.8260	.9659	6.7814	6.5503	22.1972
301131000	MID	71.562	6.6539	23.321	143.423	2.89205	.05520	.07307	7.8260	.8691	7.2379	6.2908	22.5441
301131000	BTM	71.562	6.6539	23.321	143.423	2.68142	.05520	.09644	7.8260	.7565	6.9693	5.2727	17.6814
302131000	TOP	286.249	12.3928	98.913	265.534	4.15938	.35263	.11646	22.1739	1.7400	3.4344	5.9761	8.8668
302131000	MID	286.249	12.3928	98.913	265.534	5.82702	.35263	.14959	22.1739	1.5353	4.0650	6.2411	11.6024
302131000	BTM	286.249	12.3928	98.913	265.534	5.79717	.35263	.22349	22.1739	1.2561	4.0545	5.0930	10.0623
303131000	TOP	286.249	44.0001	107.233	935.154	6.31544	.33993	.87871	15.2173	.6219	4.3102	2.6808	5.1823
303131000	MID	286.249	44.0001	107.233	935.154	8.40349	.33993	1.14173	15.2173	.5456	4.9720	2.7129	5.6716
303131000	BTM	286.249	44.0001	107.233	935.154	9.67621	.33993	1.80468	15.2173	.4340	5.3352	2.3155	4.5118
304133000	TOP	698.674	15.1941	270.585	321.749	5.85450	1.48201	.11411	24.7826	3.6037	1.9875	7.1626	3.6679
304133000	MID	698.674	15.1941	270.585	321.749	9.14698	1.48201	.14593	24.7826	3.1867	2.4843	7.9170	5.6187
304133000	BTM	698.674	15.1941	270.585	321.749	11.44986	1.48201	.23598	24.7826	2.5060	2.7795	6.9656	6.6646
305133000	TOP	698.674	33.1685	277.283	700.835	7.83552	1.47340	.41117	29.5652	1.8929	2.3060	4.3653	4.1577
305133000	MID	698.674	33.1685	277.283	700.835	11.62420	1.47340	.53946	29.5652	1.6526	2.8088	4.6419	5.7749
305133000	BTM	698.674	33.1685	277.283	700.835	13.05423	1.47340	.89354	29.5652	1.2841	2.9765	3.8222	5.5152
306131000	TOP	465.155	29.7428	185.524	627.996	7.16420	.72935	.41024	13.9130	1.3333	3.1341	4.1788	6.2865
306131000	MID	465.155	29.7428	185.524	627.996	8.89911	.72935	.54252	13.9130	1.1594	3.4930	4.0500	6.9968
306131000	BTM	465.155	29.7428	185.524	627.996	9.52207	.72935	.86189	13.9130	.9198	3.6132	3.3238	5.9840
307132000	TOP	465.155	13.7023	192.218	288.266	5.78719	.72132	.11511	20.8695	2.5032	2.8324	7.0903	6.9188
307132000	MID	465.155	13.7023	192.218	288.266	7.67616	.72132	.15078	20.8695	2.1871	3.2621	7.1349	8.8017
307132000	BTM	465.155	13.7023	192.218	288.266	8.46370	.72132	.23988	20.8695	1.7340	3.4254	5.9398	8.8052

XIII. APPENDIX V - TABULATION OF HYDROCARBON DATA

The following pages make up three tables of data on hydrocarbon systems. These tables of data and calculated results were made available through the courtesy of the Humble Oil and Refining Company in whose laboratories the data were obtained.

Table XVIII includes the physical properties of the hydrocarbons and the packing materials used in the two-phase investigation.

Table XIX is a description of the two-phase runs obtained, and includes an index to the run numbers associated with the various systems in addition to a description of the flow patterns observed during the runs.

Table XX is a tabulation of the data and the calculated results of the hydrocarbon experiments.

TABLE XVIII

PROPERTIES OF HYDROCARBONS AND PACKING MATERIALS

Catalyst
Size 1/8" x 1/8" cylinders
Porosity = 0.357 (effective)
= 0.683 (including voids in pellets)
Bulk density = 1.145 gm/cc

Glass Beads
Size 3 mm spheres
Porosity = 0.364 (Runs 608), 0.375 (Runs 9-13), 0.371 (Runs 14-21)
Bulk density = 1.56 gm/cc
Bead density = 2.48 gm/cc

Kerosene (I) (before $\Delta P/L$ runs)
Density = 0.8164 gm/cc @ 80°F
Viscosity = 1.766 CP @ 80°F
Surface tension = 26.7 dynes/cm @ 25°C
Distillation Data

IBP	365°F
2%	372
4	382
5	386
6	390
8	395
10	400
20	415
30	426
40	436
50	446
60	455
70	468
80	482
90	500
95	516

Kerosene (I) (after $\Delta P/L$ runs)
Density = 0.8093 gm/cc @ 80°F
Viscosity = 1.780 CP @ 80°F
Surface Tension = 26.8 dynes/cm @ 25°C
Distillation Data

IBP	380°F
2%	386
4	390
5	395
6	397
8	402
10	406

(Continued)

TABLE XVIII (CONT'D)

Kerosene (I) (Continued)

Distillation Data (Continued)

20	415
30	426
40	436
50	446
60	454
70	467
80	481
90	500
95	516

Kerosene (II) (before $\Delta P/L$ runs)

Density = 0.8247 gm/cc @ 80°F

Viscosity = 1.851 CP @ 80°F

Surface Tension = 27.0 dynes/cm @ 25°C

Distillation Data

IBP	352°F	
2%	376	
4	391	
5	397	
6	400	
8	406	
10	412	
20	427	
30	438	Dry Point = 545°F
40	445	Recovery 98.0%
50	452	Loss 1.0%
60	462	Residue 1.0%
70	473	
80	483	
90	504	
95	526	
FBP	548	

Kerosene (II) (after $\Delta P/L$ runs)

Density = 0.8261 gm/cc @ 80°F

Viscosity = 1.993 CP @ 80°F

Surface Tension = 27.0 dynes/cm @ 25°C

Distillation Data

IBP	384°F
2%	396
4	402
5	406
6	408
8	414
10	418
20	428

(Continued)

TABLE XVIII (CONT'D)

Kerosene (II) (Continued)

Distillation Data (Continued)

30	436	Dry Point = Cloudy
40	444	Recovery 98.0%
50	452	Loss 1.0%
60	462	Residue 1.0%
70	471	
80	484	
90	504	
95	522	
FBP	549	

Lube Oil

Density = 0.8533 gm/cc @ 80°F
Viscosity = 38.84 CP @ 80°F (before $\Delta P/L$ runs)
40.98 CP @ 80°F (after $\Delta P/L$ runs)
Surface Tension = 30.6 dynes/cm @ 25.0°C

n-Hexane

Density = 0.6607 gm/cc @ 80°F
Viscosity = 0.329 CP @ 80°F
Surface Tension = 18.1 dynes/cm @ 25°C

Natural Gas

Molecular Weight = 17 gm/gm mole (average)
Density = 0.0432 #/Ft^3 @ 80°F and 1 atm
Viscosity = 0.0122 CP @ 80°F

Carbon Dioxide

Molecular Weight = 44.01 gm/gm mole
Density = 0.112 #/Ft^3 @ 80°F and 1 atm
Viscosity = 0.0153 CP @ 80°F

TABLE XIX

DESCRIPTION OF TWO-PHASE HYDROCARBON RUNS

Run No.	Figure No.	Date	Liquid	Gas	Superficial Liquid Velocity (FPS)	Packing	Packing Depth (In.)	Flow Description
1	1	8-9-57	Kerosene(I)	Nat.Gas	0.00270	1/8" Catalyst Pellets	95 5/8	Both Phases Continuous (No Bubbling)
2	1	8-12-57	Kerosene(I)	Nat.Gas	0.00540	1/8" Catalyst Pellets	95 5/8	No Bubbling in Range of V_G=0.2 FPS Bubbling at V_G> 0.15 FPS
3	3	8-13-57	Kerosene(I)	Nat.Gas	0.01673	1/8" Catalyst Pellets	95 5/8	Foaming Pressure Surges at V_G > 0.1 FPS
4	3	8-14-57	Kerosene(I)	Nat.Gas	0.02698	1/8" Catalyst Pellets	95 5/8	Foaming Pressure Surges at V_G > 0.1 FPS
5	3	8-15-57	Kerosene(I)	Nat.Gas	0.04317	1/8" Catalyst Pellets	95 5/8	Foaming.
6	1	8-19-57	Kerosene(I)	Nat.Gas	0.00270	3mm. Glass Beads	76	Both Phases Continuous (No Bubbling)
7	4,5	8-20-57	Kerosene(I)	Nat.Gas	0.02698	3mm. Glass Beads	76	Foaming. Pressure Surges at V_G > 0.1 FPS
8	2	8-22-57	Hexane	Carbon Dioxide	0.0267	3mm. Glass Beads	76	Both Phases Continuous at Low Gas Velocities. Increasing Instability of Flow Pattern with Increasing Gas Rates. Pressure Surges at V_G > 0.25 FPS.
9	5,6	7-8-58	Kerosene(II)	Nat.Gas	0.02698	3mm. Glass Beads	93	Slight Foaming. Pressure Surges at V_G > 0.25 FPS.

TABLE XIX (CONT'D)

Run No.	Figure No.	Date	Liquid	Gas	Superficial Liquid Velocity (FPS)	Packing	Packing Depth (In.)	Flow Description
10	6	7-11-58	Kerosene(II)	Nat.Gas	0.02698	3mm. Glass Beads	93	Foaming and Pressure Surges.
11	1	7-11-58	Kerosene(II)	Nat.Gas	0.00270	3mm. Glass Beads	93	Both Phases Continuous (No Bubbling or Pressure Surges)
12	6	7-16-58	Kerosene(II)	Nat.Gas	0.02698	3mm. Glass Beads	93	Foaming and Pressure Surges. (Gas Entered Column Dry)
13	6	7-23-58	Kerosene(II)	Nat.Gas	0.02698	3mm. Glass Beads	93	Foaming and Pressure Surges. (Gas Entered Column Wet)
14	4	8-7-58	Kerosene(II)	Nat.Gas	0.08094	3mm. Glass Beads	49 1/4	Intense Foaming Slight Pressure Surges at $V_G > 0.35$ FPS
15	2	8-12-58	Lube Oil	Nat.Gas	0.00270	3mm. Glass Beads	49 1/4	Bubbling, No Pressure Surges
16	4	8-13-58	Lube Oil	Nat.Gas	0.01349	3mm. Glass Beads	49 1/4	Bubbling, Slight Pressure Surges at $V_G > 0.15$ FPS.
17	2	8-15-58	Carbon Dioxide	Nat.Gas	0.00270	3mm. Glass Beads	49 1/4	Bubbling, No Pressure Surges.
18	4	8-20-58	Kerosene(II)	Nat.Gas	0.08094	3mm. Glass Beads	49 1/4	Foaming (Check Points for Run #14).
19	6	8-21-58	Kerosene(II)	Nat.Gas	0.02698	3mm. Glass Beads	49 1/4	Slight Foaming Pressure Surges. (Check Points for Run #'s 7,9,10,12,13).
20	6	8-21-58	Kerosene(II)	Nat.Gas	0.02698	3mm. Glass Beads	77 1/2	Same as Above.
21	6	8-21-58	Kerosene(II)	Nat.Gas	0.02698	3mm. Glass	77 1/2	Same as Above. (Monometer Trap Size at Top of Column was changed from 1000 cc. to 250 cc., the size used in 1957 runs.)

TABLE XX

TABULATION OF HYDROCARBON DATA AND CALCULATED RESULTS

Liquid Rate (cc./min.)	Average Gas Rate (Ft^3/Min)	Superficial Liquid Velocity (Ft/Sec)	Superficial Gas Velocity (Ft/Sec)	Two-Phase Pressure Drop (PSI/Ft)	% Liquid Saturation	X	ϕ_G	ϕ_L
(Run No. 1)								
100	0.113	0.00270	0.0863	0.0080	41.0	2.101	1.985	0.9449
100	0.190	0.00270	0.145	0.0173	41.0	1.556	2.162	1.390
100	0.261	0.00270	0.199	0.0277	42.2	1.297	2.282	1.758
100	0.428	0.00270	0.327	0.0586	40.4	0.9601	2.455	2.557
100	0.611	0.00270	0.467	0.0943	39.3	0.7625	2.474	3.243
100	0.794	0.00270	0.607	0.151	39.0	0.6358	2.610	4.105
(Run No. 2)								
200	0.05[illegible]7	0.00540	0.0418	0.0111	51.2	4.341	3.381	0.7790
200	0.111	0.00540	0.0848	0.0185	50.1	2.987	3.004	1.005
200	0.185	0.00540	0.141	0.160	47.1	2.254	6.666	2.958
200	0.255	0.00540	0.195	0.191	45.5	1.870	6.043	3.231
200	0.415	0.00540	0.317	0.259	44.6	1.390	5.147	3.763
200	0.574	0.00540	0.439	0.308	44.4	1.126	4.622	4.104
200	0.756	0.00540	0.578	0.333	44.3	0.9312	3.974	4.267
200	0.113	0.00540	0.0863	0.0154	49.7	2.958	2.714	0.9176
200	0.269	0.00540	0.206	0.0740	45.1	1.814	3.648	2.011
200	0.262	0.00540	0.200	0.179	45.1	1.840	5.758	3.128
200	0.777	0.00540	0.588	0.321	43.0	0.9219	3.863	4.189
(Run No. 3)								
620	0.0075	0.01673	0.0057	0.314	63.9	21.94	49.53	2.257
620	0.040	0.01673	0.0306	0.801	43.7	9.336	33.66	3.606
620	0.090	0.01673	0.0688	1.122	-	6.075	25.93	4.267
620	0.171	0.01673	0.131	0.493	43.4	4.283	12.11	2.828
620	0.155	0.01673	0.118	1.171	43.4	4.502	19.63	4.359
620	0.239	0.01673	0.183	0.518	43.7	3.533	10.72	2.899
620	0.217	0.01673	0.166	1.165	43.7	3.692	16.05	4.347
620	0.377	0.01673	0.288	0.764	46.6	2.666	9.387	3.521
620	0.374	0.01673	0.286	0.820	46.8	2.675	9.759	3.648
620	0.531	0.01673	0.406	0.752	47.5	2.138	7.466	3.493
620	0.526	0.01673	0.402	0.814	47.5	2.146	7.800	3.635
620	0.700	0.01673	0.535	0.764	47.6	1.769	6.227	3.521
620	0.694	0.01673	0.530	0.820	47.6	1.774	6.476	3.648
(Run No. 4)								
1000	0.0074	0.02698	0.0057	0.345	78.0	28.85	51.91	1.799
1000	0.047	0.02698	0.0359	0.758	54.0	11.30	30.15	2.667
1000	0.090	0.02698	0.0688	1.153	-	7.987	26.28	3.289
1000	0.146	0.02698	0.112	1.504	-	6.061	22.77	3.758
1000	0.150	0.02698	0.115	1.233	-	6.000	20.41	3.401
1000	0.201	0.02698	0.154	1.627	-	5.037	19.68	3.908
1000	0.221	0.02698	0.169	0.863	-	4.834	13.76	2.846
1000	0.362	0.02698	0.277	0.851	42.3	3.581	10.12	2.826
1000	0.332	0.02698	0.254	1.553	42.3	3.712	14.17	3.818
1000	0.505	0.02698	0.386	1.116	50.7	2.868	9.283	3.236
1000	0.496	0.02698	0.379	1.251	50.7	2.892	9.909	3.426
1000	0.670	0.02698	0.512	1.112	51.0	2.362	7.630	3.231
1000	0.666	0.02698	0.509	1.171	51.0	2.67	7.847	3.315
(Run No. 5)								
1600	0.0079	0.04317	0.0060	0.339	87.0	37.78	50.11	1.341
1600	0.0487	0.04317	0.0372	0.740	60.2	14.75	29.23	1.981
1600	0.0897	0.04317	0.0685	1.147	-	10.66	26.29	2.466
1600	0.146	0.04317	0.112	1.603	-	8.078	23.55	2.916

TABLE XX (CONT'D)

Liquid Rate (cc./min.)	Average Gas Rate (FT^3/Min)	Superficial Liquid Velocity (Ft/Sec)	Superficial Gas Velocity (Ft/Sec)	Two-Phase Pressure Drop (PSI/Ft)	% Liquid Saturation	X	ϕ_G	ϕ_L
(Run No. 6)								
100	0.117	0.0027	0.0894	0.0093	35.5	2.034	2.042	1.004
100	0.234	0.0027	0.179	0.0155	34.1	1.384	1.793	1.296
100	0.359	0.0027	0.274	0.0310	33.9	1.077	1.975	1.833
100	0.490	0.0027	0.374	0.0543	33.7	0.8882	2.154	2.425
100	0.648	0.0027	0.495	0.0853	34.1	0.7397	2.249	3.040
(Run No. 7)								
1000	0.0071	0.02698	0.0054	0.341	76.9	29.52	52.23	1.769
1000	0.0472	0.02698	0.0361	0.814	54.6	11.24	30.71	2.733
1000	0.0926	0.02698	0.0707	1.163	-	7.868	25.71	3.266
1000	0.155	0.02698	0.118	1.357	-	5.919	20.89	3.528
1000	0.154	0.02698	0.118	1.435	-	5.919	21.48	3.629
1000	0.233	0.02693	0.178	0.776	-	4.711	12.57	2.669
1000	0.214	0.02698	0.163	1.551	-	4.910	18.52	3.772
1000	0.378	0.02698	0.289	0.892	42.7	3.513	10.05	2.861
1000	0.352	0.02698	0.269	1.528	42.7	3.621	13.56	3.744
1000	0.523	0.02698	0.400	1.070	49.4	2.837	8.890	3.134
1000	0.513	0.02698	0.392	1.233	49.4	2.862	9.595	3.365
1000	0.692	0.02698	0.529	1.078	48.8	2.347	7.382	3.145
1000	0.683	0.02698	0.522	1.194	48.8	2.360	7.813	3.311
(Run No. 8)								
998	0.0443	0.02693	0.0338	0.0271	73.0	5.460	5.075	0.9296
997	0.0896	0.02690	0.0684	0.0543	68.6	3.700	4.869	1.316
995	0.149	0.02685	0.113	0.0931	62.8	2.752	4.742	1.723
993	0.212	0.02679	0.162	0.132	67.1	2.197	4.507	2.052
988	0.338	0.02666	0.258	0.209	61.5	1.605	4.142	2.582
988	0.338	0.02666	0.258	0.225	61.5	1.602	4.293	2.679
984	0.462	0.02655	0.353	0.263	58.6	1.277	3.699	2.896
984	0.462	0.02655	0.353	0.279	58.6	1.277	3.809	2.983
980	0.594	0.02644	0.454	0.334	52.9	1.051	3.429	3.263
980	0.594	0.02644	0.454	0.349	52.9	1.051	3.506	3.336
		$V_{AVG.}$=0.0267						
(Run No. 9)								
1000	0.00883	0.02698	0.00675	0.222	72.1	26.92	40.11	1.490
1000	0.0529	0.02698	0.0404	0.418	64.5	10.81	22.11	2.045
1000	0.1009	0.02698	0.0771	0.697	57.7	7.669	20.25	2.640
1000	0.1681	0.02698	0.128	0.843	54.1	5.773	16.76	2.904
1000	0.2356	0.02698	0.180	0.887	53.7	4.746	14.14	2.979
1000	0.3829	0.02698	0.293	0.932	50.4	3.521	10.75	3.053
1000	0.3792	0.02698	0.290	1.001	50.4	3.537	11.19	3.164
1000	0.5434	0.02698	0.415	0.976	49.9	2.807	8.770	3.124
1000	0.5401	0.02698	0.413	1.014	49.9	2.812	8.951	3.184
1000	0.7155	0.02698	0.547	0.976	50.1	2.319	7.246	3.124
1000	0.7118	0.02698	0.544	1.014	50.1	2.324	7.401	3.184
1000	1.722	0.02698	1.316	1.230	47.9	1.162	4.077	3.507
1000	1.713	0.02698	1.309	1.274	47.9	1.164	4.157	3.569
(Run No. 10)								
1000	0.0942	0.02698	0.0720	1.008	54.6	7.930	25.18	3.175
1000	0.2330	0.02698	0.178	1.065	50.7	4.761	15.54	3.263
1000	0.2295	0.02698	0.175	1.185	50.7	4.794	16.50	3.442
1000	1.046	0.02698	0.700	1.103	45.9	1.748	5.807	3.321
1000	1.041	0.02698	0.795	1.144	45.9	1.769	5.986	3.382

TABLE XX (CONT'D)

Liquid Rate (cc./min.)	Average Gas Rate (Ft^3/Min)	Superficial Liquid Velocity (Ft/Sec)	Superficial Gas Velocity (Ft/Sec)	Two-Phase Pressure Drop (PSI/Ft)	% Liquid Saturation	X	ϕ_G	ϕ_L
(Run No. 11)								
100	0.2023	0.0027	0.155	0.0139	40.8	1.530	1.960	1.281
100	0.2794	0.0027	0.213	0.0228	39.3	1.273	2.088	1.641
100	0.4558	0.0027	0.348	0.0475	38.6	0.9447	2.237	2.368
100	0.6471	0.0027	0.494	0.0805	38.5	0.7519	2.318	3.082
100	0.8343	0.0027	0.637	0.1223	39.4	0.6311	2.399	3.800
100	0.9624	0.0027	0.735	0.1546	38.8	0.5697	2.434	4.272
100	1.734	0.0027	1.325	0.3286	36.6	0.3590	2.236	6.229
(Run No. 12)								
1000	0.6864	0.02698	0.524	1.185	-	2.371	8.161	3.442
1000	0.6713	0.02698	0.513	1.372	-	2.388	8.847	3.704
1000	0.2296	0.02698	0.175	1.401	-	4.778	17.89	3.743
1000	0.2246	0.02698	0.172	1.610	-	4.805	19.28	4.012
1000	0.0856	0.02698	0.0654	1.195	-	8.332	28.81	3.457
1000	0.2379	0.02698	0.182	1.261	-	4.678	16.61	3.551
1000	0.2275	0.02698	0.174	1.679	-	4.767	19.53	4.098
1000	0.0936	0.02698	0.0715	1.204	-	7.955	27.60	3.470
(Run No. 13)								
1000	0.6869	0.02698	0.525	1.191	-	2.364	8.159	3.451
1000	0.6748	0.02698	0.516	1.344	-	2.379	8.723	3.666
1000	0.2254	0.02698	0.172	1.153	-	4.845	16.45	3.396
1000	0.2119	0.02698	0.162	1.724	-	4.969	20.93	4.152
1000	0.0951	0.02698	0.0726	1.179	-	7.880	27.06	3.434
(Run No. 14)								
3000	0.0228	0.08094	0.0174	0.646	-	33.46	41.50	1.241
3000	0.0715	0.08094	0.0546	1.041	-	18.48	29.12	1.57
3000	0.1068	0.08094	0.0816	1.329	-	14.89	26.50	1.78
3000	0.1716	0.08094	0.131	1.784	-	11.42	23.54	2.06
3000	0.2311	0.08094	0.177	2.095	-	9.57	21.37	2.23
3000	0.3601	0.08094	0.275	2.466	-	7.27	17.62	2.42
3000	0.5011	0.08094	0.383	2.681	-	5.84	14.77	2.53
3000	0.4991	0.08094	0.381	2.753	-	5.86	15.00	2.56
3000	0.6552	0.08094	0.501	2.825	-	4.84	12.57	2.59
3000	0.6509	0.08094	0.497	2.945	-	4.86	12.87	2.65
3000	0.7263	0.08094	0.555	2.873	-	4.50	11.78	2.61
3000	0.7198	0.08094	0.550	2.945	-	4.51	11.95	2.65
3000	1.498	0.08094	1.144	3.040	-	2.77	7.46	2.69
3000	1.480	0.08094	1.131	3.280	-	2.80	7.22	2.80
(Run No. 15)								
100	0.00677	0.00270	0.00517	0.311	-	41.23	53.12	1.29
100	0.0533	0.00270	0.0407	0.383	-	14.44	20.64	1.43
100	0.1092	0.00270	0.0834	0.431	-	9.88	14.98	1.52
100	0.1842	0.00270	0.141	0.467	-	7.40	11.68	1.58
100	0.2609	0.00270	0.199	0.491	-	6.07	9.82	1.62
100	0.3949	0.00270	0.302	0.539	-	4.72	8.00	1.70
100	0.5943	0.00270	0.454	0.599	-	3.63	6.49	1.79
100	0.7845	0.00270	0.599	0.670	-	3.00	5.68	1.89
100	1.140	0.00270	0.871	0.790	-	2.29	4.69	2.05
100	2.103	0.00270	1.606	1.155	-	1.39	3.45	2.48

TABLE XX (CONT'D)

Liquid Rate (cc./min.)	Average Gas Rate (Ft3/Min)	Superficial Liquid Velocity (Ft/Sec)	Superficial Gas Velocity (Ft/Sec)	Two-Phase Pressure Drop (PSI/Ft)	% Liquid Saturation	X	ϕ_G	ϕ_L
(Run No. 16)								
500	0.00580	0.01349	0.00443	1.532	-	99.76	127.37	1.28
500	0.0451	0.01349	0.0349	2.119	-	34.88	52.37	1.50
500	0.0945	0.01349	0.0722	2.119	-	23.72	35.63	1.50
500	0.1624	0.01349	0.124	2.179	-	19.58	26.77	1.52
500	0.2248	0.01349	0.172	2.131	-	14.56	21.92	1.51
500	0.2233	0.01349	0.171	2.226	-	14.60	22.46	1.54
500	0.3684	0.01349	0.281	2.167	-	10.79	16.39	1.52
500	0.3650	0.01349	0.279	2.310	-	10.82	16.96	1.57
500	0.5160	0.01349	0.394	2.274	-	8.65	13.46	1.55
500	0.5114	0.01349	0.391	2.412	-	8.68	13.90	1.60
500	0.6821	0.01349	0.521	2.346	-	7.14	11.28	1.58
500	0.6776	0.01349	0.518	2.454	-	7.15	11.55	1.62
500	0.9017	0.01349	0.689	2.490	-	5.82	9.47	1.63
500	0.8959	0.01349	0.684	2.597	-	5.83	9.70	1.66
500	1.489	0.01349	1.137	2.777	-	3.91	6.73	1.72
500	1.482	0.01349	1.132	2.861	-	3.92	6.84	1.74
(Run No. 17)								
100	0.00558	0.00270	0.00426	0.302	-	40.41	51.26	1.27
100	0.0352	0.00270	0.0269	0.383	-	15.65	22.39	1.43
100	0.0708	0.00270	0.0541	0.431	-	10.69	16.24	1.52
100	0.1247	0.00270	0.0953	0.455	-	7.71	12.02	1.56
100	0.1670	0.00270	0.128	0.491	-	6.43	10.42	1.62
100	0.2740	0.00270	0.209	0.551	-	4.68	8.03	1.71
100	0.3840	0.00270	0.293	0.613	-	3.69	6.69	1.81
100	0.5020	0.00270	0.384	0.682	-	3.02	5.77	1.91
100	0.6661	0.00270	0.509	0.766	-	2.43	4.91	2.02
100	1.017	0.00270	0.777	0.982	-	1.70	3.89	2.29
100	1.378	0.00270	1.053	1.209	-	1.29	3.27	2.54
(Run No. 18)								
3000	0.1777	0.08094	0.136	1.760	-	11.17	22.89	2.05
3000	0.1653	0.08094	0.126	1.772	-	11.67	23.99	2.05
3000	0.3607	0.08094	0.276	2.394	-	7.26	17.35	2.39
(Run No. 19)								
1000	0.2412	0.02698	0.184	1.233	-	4.70	16.17	3.43
1000	0.2351	0.02698	0.180	1.514	-	4.74	18.09	3.81
1000	0.3980	0.02698	0.304	1.083	-	3.47	11.20	3.22
1000	0.3828	0.02698	0.292	1.538	-	3.54	13.60	3.84
(Run No. 20)								
1000	0.2343	0.02698	0.179	0.932	-	4.76	14.25	2.99
1000	0.2221	0.02698	0.170	1.400	-	4.87	17.88	3.66
1000	0.3965	0.02698	0.303	0.970	-	3.46	10.55	3.05
1000	0.3651	0.02698	0.279	1.483	-	3.60	13.59	3.77
(Run No. 21)								
1000	0.2301	0.02698	0.176	1.130	-	4.79	15.80	3.29
1000	0.2231	0.02698	0.170	1.411	-	4.87	17.94	3.67
1000	0.3866	0.02698	0.295	1.038	-	3.51	11.09	3.15
1000	0.3666	0.02698	0.280	1.525	-	3.57	13.73	3.82

XIV. BIBLIOGRAPHY

1. Bain, W. A., Jr., and Hougen, O. A. Trans. Am. Inst. Chem. Engrs., 40, (1944), 29.

2. Baker, T., Chilton, T. H., and Vernon, H. C. Trans. Am. Inst. Chem. Engrs., 31, (1935), 296.

3. Bergelin, O. P. Chem. Eng., 56, (1949), 104.

4. Bertetti, J. W. Trans. Am. Inst. Chem. Engrs., 38, (1942), 1023.

5. Brownell, L. E., and Katz, D. L. Chem. Eng. Prog., 43, (October, 1947), 537.

6. Brownell, L. E., and Katz, D. L. Chem. Eng. Prog., 43, (November, 1947), 601.

7. Brownell, L. E., and Katz, D. L. Chem. Eng. Prog., 43, (December, 1947), 703.

8. Brownell, L. E., Dombrowski, H. S., and Dickey, C. A. Chem. Eng. Prog., 46, (1950), 415.

9. Brownell, L. E., Gami, D. C., Miller, R. A., and Nekarvis, W. F. Am. Inst. Chem. Engrs. Journal, 2, (1956), 79.

10. Chenoweth, J. M., and Martin, M. W. Petroleum Refiner, 34, (October, 1955), 151.

11. Elgin, J. C., and Weiss, F. B. Ind. Eng. Chem., 31, (1939), 435.

12. Elgin, J. C., and Jesser, B. W. Trans. Am. Inst. Chem. Engrs., 39, (1942), 277.

13. Ergun, S., and Orning, A. A. Ind. Eng. Chem., 41, (1949), 1179.

14. Ergun, S. Chem. Eng. Prog., 48, (1952), 89.

15. Furnas, C. C., and Bellinger, F. Trans. Am. Inst. Chem. Engrs., 34, (1938), 251.

16. Galegar, W. C., Stoval, W. B., and Huntington, R. L. Petroleum Refiner, 33, (November, 1954), 208.

17. Hassler, G. L., Raymond, R. R., and Leeman, E. H. Trans. Am. Inst. Mining Met. Engrs., 118, (1936), 116.

18. Hassler, G. G., Brunner, D., and Deahl, T. J. Trans. Am. Inst. Mining Met. Engrs., 155, (1944), 155.

19. Hill, S. Chem. Eng. Sci., 1, (1952), 247.

20. Hodgman, C. D. (ed.). Handbook of Chemistry and Physics, 34th ed. Cleveland: Chemical Rubber Publishing Company, (1952), 1885.

21. Leva, M., and Grummer, M. Chem. Eng. Prog., 43, (1947), 549.

22. Leva, M. Chem. Eng., 64, (January, 1957), 204; (February, 1957), 263; (March, 1957), 261.

23. Leverett, M. C. Trans. Am. Inst. Mech. Engrs., 132, (1939), 149.

24. Lockhart, R. W., and Martinelli, R. C. Chem. Eng. Prog., 45, (January, 1949), 39.

25. Martin, J. J. Chem. Eng. Prog., 47, (February, 1951), 91.

26. Martinelli, R. C., Boelter, L. M. K., Taylor, T. H. M., Thomsen, E. G., and Morrin, E. H. Trans. Am. Soc. Mech. Engrs., 66, (1944), 139.

27. Martinelli, R. C., Putnam, J. A., and Lockhart, R. W. Trans. Am. Inst. Chem. Engrs., 41, (1945), 681.

28. Morcom, A. R. Trans. Inst. Chem. Engrs., London, 24, (1946), 30.

29. Perry, J. H. (ed.). Chemical Engineers' Handbook, 3rd ed. New York: McGraw-Hill Book Company, (1950), 370.

30. Perry, J. H. (ed.). Chemical Engineers' Handbook, 3rd ed. New York: McGraw-Hill Book Company, (1950), 374.

31. Piret, E. L., Mann, C. A., and Wall, T., Jr. Ind. Eng. Chem., 32, (1940), 861.

32. Schoenborn, E. M., and Dougherty, W. J. Trans. Am. Inst. Chem. Engrs., 40, (1944), 51.

33. White, A. M. Trans. Am. Inst. Chem. Engrs., 31, (1935), 390.

34. Wyckoff, R. D., and Votset, H. G. Physics, 7, (1936), 325.